Marine Biodiversity (2023) 53:42
https://doi.org/10.1007/s12526-022-01334-9

SENCKENBERG

ORIGINAL PAPER

Hyperdiversity of the genus *Halgerda* Bergh, 1880 (Nudibranchia: Discodorididae) with descriptions of fourteen new species

Samantha A. Donohoo[1,2] · Shaina G. Villalobos[1,3] · Joshua M. Hallas[1,4,5] · Terrence M. Gosliner[1]

Received: 19 July 2022 / Revised: 10 November 2022 / Accepted: 20 December 2022

Abstract

The Indo-Pacific genus *Halgerda* Bergh, 1880a is one of the most diverse and better-studied genera within the nudibranch family Discodorididae. Previous studies have been predominantly based on morphology; however, the addition of molecular data has led to new species descriptions as well as unresolved species complexes. Here, we broaden the available molecular data within *Halgerda* by utilizing two mitochondrial and two nuclear genes in coordination with morphology to describe 14 new *Halgerda* species. Bayesian inference, maximum likelihood, and species delimitation analyses were used to clarify previously established relationships and evaluate the new species positions within *Halgerda*. Based on our results *Halgerda elegans* Bergh, 1905 is synonymized with *Halgerda willeyi* Eliot, 1904 and new descriptions for *Halgerda mango* sp. nov., *Halgerda berberiani* sp. nov., *Halgerda biqiea* sp. nov., *Halgerda paulayi* sp. nov., *Halgerda labyrinthus* sp. nov., *Halgerda anosy* sp. nov., *Halgerda mesophotica* sp. nov., *Halgerda profunda* sp. nov., *Halgerda takipsilim* sp. nov., *Halgerda scripta* sp. nov., *Halgerda hervei* sp. nov., *Halgerda maaikeae* sp. nov., *Halgerda pattiae* sp. nov., and *Halgerda radamaensis* sp. nov. are provided here. We also provide an updated morphological description for juvenile specimens of *Halgerda dalanghita* Fahey & Gosliner, 1999a; expand upon the two unresolved species complexes previously identified in Tibiriçá et al. (2018); and identify a new mesophotic clade in the Central Pacific.

Keywords Mollusca · Biodiversity · Phylogenetics · Species delimitation · Central and Western Pacific Ocean · Indian Ocean

Introduction

The nudibranch genus *Halgerda* Bergh, 1880a is one of 29 recognized genera in the family Discodorididae Bergh, 1891 and has been extensively studied using morphology (Rudman 1978; Carlson and Hoff 1993, 2000; Gosliner and Fahey 1998; Fahey and Gosliner 1999a, b, 2000, 2001a, b; Fahey and Healy 2003; Fahey and Carroll 2007). Currently, there are 42 recognized species of *Halgerda* (MolluscaBase 2021), which are predominantly found in tropical and subtropical regions on shallow reefs (Eliot 1904; Rudman 1978; Gosliner 1987; Fahey and Gosliner 2001b; Tibiriçá et al. 2018). Additional species have also been found in temperate regions (Carlson and Hoff 2000; Fahey and Gosliner 2001a) and the deep-sea including the mesophotic zone (Carlson and Hoff 2000; Tibiriçá et al. 2018) and the twilight zone (Fahey and Gosliner 2000). Furthermore, numerous undescribed species of *Halgerda* have been identified and range from the Indo-Pacific to the western Indian Ocean, including the Red Sea (Ono 2004; Debelius and Kuiter 2007; Yonow

Communicated by C. Chen

This article is registered in ZooBank under http://zoobank.org/C7A7FCC8-D9F2-4A96-8D99-285FC2BB9997

✉ Samantha A. Donohoo
Sdonohoo@calacademy.org

[1] Department of Invertebrate Zoology and Geology, California Academy of Sciences, San Francisco, CA 94118, USA

[2] Department of Biology, San Francisco State University, San Francisco, CA 94132, USA

[3] Department of Biology, University of West Florida, Pensacola, FL 32514, USA

[4] Wildlife Genetics Research Unit, Wildlife Health Laboratory, CA, Department of Fish and Wildlife, Sacramento, CA 95814, USA

[5] Mammalian Ecology and Conservation Unit, Veterinary Genetics Laboratory, School of Veterinary Medicine, University of California, Davis, CA 95616, USA

2008; Hervé 2010; Humann and Deloach 2010; Gosliner et al. 2008, 2015, 2018).

The genus *Halgerda* is characterized by having a semi-firm, gelatinous body with ridges, tubercles, and no caryophyllidia; a low, smooth rhinophoral and branchial sheath; an unarmed penis and vagina; and a smooth labial cuticle and smooth, hamate inner and middle radular teeth with denticulated outer teeth (Bergh 1880a; Fahey and Gosliner 2001a). Differentiation between *Halgerda* species usually includes external morphology (i.e., dorsum coloration, presence of tubercles, number of branchial leaves), but due to variability in coloration as seen in *Halgerda dichromis* Fahey & Gosliner, 1999a and the *Halgerda wasinensis* Eliot, 1904 species complex, internal differences in the reproductive system (i.e., size and shape of the penis, vagina, and bursa copulatrix) and the radular teeth (i.e., number of small inner teeth and the shape of the outermost teeth) prove helpful in species identifications.

The first morphological phylogeny for *Halgerda* was proposed in 1999 and utilized 22 species and 48 morphological characters (Fahey and Gosliner 1999b). In 2001, Fahey and Gosliner revised their morphological phylogeny by including an additional morphological character and increasing the representation to 35 species of *Halgerda*. Since then, two molecular phylogenies have been published for *Halgerda*. In the first, Fahey (2003) combined morphology with the mitochondrial gene cytochrome oxidase I (COI) from 17 specimens representing 13 species from the central and western Pacific Ocean and Western Australia. In the second molecular study, Tibiriçá et al. (2018) sequenced three genes (COI, 16S, and histone 3 (H3)) from 32 specimens including six new species of *Halgerda* collected in the western Indian Ocean. Both molecular phylogenies show similar well-supported groupings; however, Tibiriçá et al. (2018) also found two species complexes with strong geographical separation: the *H. wasinensis* complex from the western Indian Ocean and the *Halgerda carlsoni* Rudman, 1978 complex predominantly from the Pacific Ocean and Western Australia. Here, we provide an updated phylogenetic analysis of the genus *Halgerda* with additional representatives from the western Indian Ocean, the Red Sea, and the central and western Pacific Ocean.

Materials and methods

Taxon sampling

Ninety-nine *Halgerda* specimens representing 11 of 14 new species described here and 25 of 42 previously described species collected from the Central and Western Pacific Ocean and the Indian Ocean (Fig. 1) were sequenced for this study. Some specimens including the holotypes of *Halgerda berberiani* Donohoo & Gosliner sp. nov., *Halgerda hervei* Donohoo & Gosliner sp. nov., *Halgerda labyrinthus* Donohoo & Gosliner sp. nov., and *Halgerda radamaensis* Donohoo and Gosliner sp. nov. were not sequenced due to DNA degradation from prior fixation in formalin or Bouin's solution. Some *Halgerda* specimens initially sequenced by Fahey (2003) were resequenced to achieve longer cytochrome oxidase I (COI) fragments as well as the other genes studied here. Therefore, a total of 128 specimens, 70 newly sequenced, 12 originally from Fahey (2003), and 46 with two or more genes already published and available on Genbank, were used in the molecular analyses. Sampled specimens with the current proposed taxonomy, museum voucher numbers, locality, and GenBank accession numbers are listed in Table 1. Outgroup comparisons included Goniodorididae, Doridiidae, and several members of Discodorididae based on molecular phylogenetic analysis by Hallas et al. (2017) and Donohoo and Gosliner (2020). Voucher specimens, holotypes, and paratypes are deposited in the collections at the California Academy of Sciences (CASIZ), the National Museum of Philippines (NMP), the National Museum of Natural History (MNHN), the Iziko Museum South African Museum (SAMC), and the Florida Museum of Natural History (UF).

DNA extraction, amplification, and sequencing

DNA extractions were performed on a small tissue sample from each specimen's foot or mantle using the Qiagen Dneasy Blood and Tissue Kit (Qiagen, Valencia, CA, USA) spin column extraction method. Fragments from two mitochondrial (16S and COI) genes and two nuclear (28S and H3) genes were utilized to estimate our *Halgerda* phylogeny based upon previous sequencing success for members of Discodorididae including *Asteronotus* Ehrenberg, 1831; *Carminodoris* Bergh, 1889; *Diaulula* Bergh, 1878; *Halgerda*, *Hoplodoris* Bergh, 1880b; *Jorunna* Bergh, 1876; *Sclerodoris* Eliot, 1904; and *Thordisa* Bergh, 1877 (Fahey 2003; Giribet et al. 2006; Göbbeler and Klussmann-Kolb 2010; Lindsay et al. 2016; Hallas et al. 2017; Tibiriçá et al. 2018; Donohoo and Gosliner 2020; Neuhaus et al. 2021). Each polymerase chain reaction (PCR) used gene-specific primers (Table 2) and contained the following: 2.5 µL of 10×PCR buffer, 0.5 µL dNTPs (10 mM stock), 0.5 µL of each primer (10 µM stock), 0.25 µL DreamTaq™ Hot Start DNA Polymerase (5U/µL, Thermo Fisher), 5 µL betaine, 2 µL bovine serum albumin (BSA), 2–4 µL of template DNA, and then filled to a final volume of 25 µL with Millipore-H_2O. An additional 1 µL of dimethyl sulfoxide (DMSO) was added to both 28S PCR amplifications to account for secondary structure and nucleotide repeats. The PCR gene-specific protocols were run on a BioRad MyCycler Thermocycler (Bio-Rad Laboratories) at the California Academy of Sciences Center for Comparative Genomics (CCG). PCR protocols are as

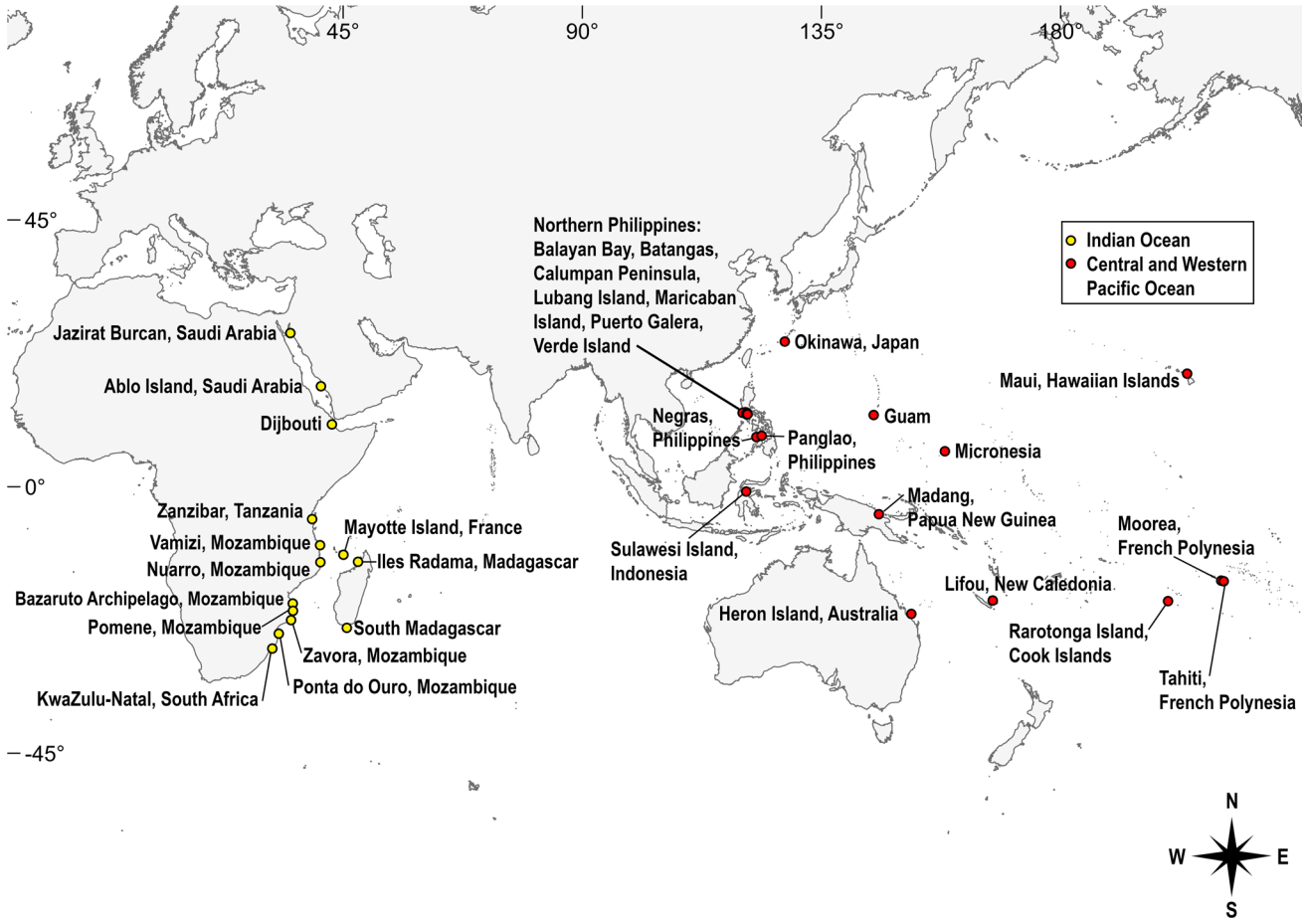

Fig. 1 Localities of all specimens of *Halgerda* sequenced and dissected for this study. Map created using QGIS (QGIS 2022)

follows: for 16S and COI, an initial denaturing for 3 min at 94 °C, followed by 40 cycles of denaturing for 30 s at 94 °C, annealing for 30 s at 46–50 °C, and extension for 45 s at 72 °C with a final extension period of 10 min at 72 °C and for H3, an initial denaturing for 3 min at 94 °C, followed by 35 cycles of denaturing for 30 s at 94 °C, annealing for 30 s at 45–54 °C, and extension for 1 min at 72 °C with a final extension period of 10 min at 72 °C. Both fragments of 28S were initially denatured for 4 min at 95 °C, followed by 40 cycles of denaturing for 30 s at 94 °C, annealing for 30 s at 52.5 °C, and extension for 2.5 min at 72 °C with a final extension period of 5 min at 72 °C. Amplified DNA was stained with ethidium bromide and examined using gel electrophoresis on a 1% TBE agarose gel. Successfully amplified products were cleaned using an ExoSAP-IT protocol (USB Scientific) before being sequenced at either ELIM Biopharmaceuticals (Hayward, CA, USA) or on an ABI3130 Genetic Analyzer in the CCG, which followed fluorescently labeled dye terminator protocols used by Donohoo and Gosliner (2020).

Phylogenetic analyses

Successfully sequenced fragments were assembled, trimmed to remove primers, and edited using Geneious v11.1.5 (Kearse et al. 2012) and Mesquite v3.61 (Maddison and Maddison 2018). Each gene was aligned with MAFFT (Katoh et al. 2009) using the algorithm E-INS-I. Regions of ambiguous data were identified using the least stringent settings and then removed from the 16S and 28S alignments using GBlocks 0.91b (Talavera and Castresana 2007). Bayesian inference (BI) and maximum likelihood (ML) analyses were used to estimate the evolutionary relationships within *Halgerda*. Best-fit evolution model partition definitions for BI and ML analyses were determined for the individual genes 16S and 28S and each codon position within COI and H3 within the final four-gene concatenated dataset (16S + 28S + COI + H3) using PartitionFinder2 (Lanfear et al. 2016). The concatenated dataset was partitioned by gene and codon position for both the BI and ML analyses (Table 2). Bayesian inference was performed

Table 1 Specimens successfully sequenced and/or dissected for this study, including current proposed taxonomy, museum voucher numbers, locality, and GenBank accession numbers. Dashes indicate missing sequences. Pound (#) symbol indicates specimens dissected. Asterisk (*) symbol indicates specimen sequences acquired from GenBank (Fahey 2003; Pola and Gosliner 2010; Hallas and Gosliner 2015; Hallas et al. 2017; Tibiriçá et al. 2018; Donohoo and Gosliner 2020)

Species	Voucher	Locality	GenBank Accession Numbers			
			16S	28S	COI	H3
Goniodorididae						
Ancula gibbosa	CASIZ 182028*	Cape Elizabeth, Maine, USA	KP340291	KP340356	KP340388	KP340413
Doridiidae						
Aphelodoris sp. 1	CASIZ 176920*	Oudekraal, South Africa	MF958293	MF958379	MF958424	–
Discodorididae						
Asteronotus cespitosus	CASIZ 177226*	Balayan Bay, Philippines	KP871680	MN728188	KP871633	KP871656
Asteronotus hepaticus	CASIZ 191310*	Madang, Papua New Guinea	MN722442	MN728202	MN720295	MN720326
Asteronotus namuro	CASIZ 192297*	Tigerhead Island, Saudi Arabia	MN722445	MN728205	MN720298	MN720329
Atagema notacristata	CASIZ 167980*	Isla Uva, Panama	KP871681	MT452661	KP871634	KP871657
Carminodoris flammea	CASIZ 177628*	Calumpan Peninsula, Philippines	MN722433	MN728190	MN720285	MN720311
Diaulula odonoghuei	UF 511380	Calvert Island, Canada	MW220875	MW220114	MW223019	MW414939
Diaulula sandiegensis	CASIZ 181321*	Scott Creek, California, USA	MN722435	MN728193	MN720287	MN720317
Discodoris boholiensis	CASIZ 204802*	Puerto Galera, Philippines	MN722451	MN728210	MN720304	MN720335
Discodoris cebuensis	CASIZ 190761*	Rasch Passage, Papua New Guinea	MN722440	MN728200	MN720293	MN720322
Geitodoris heathi	CASIZ 181314*	Carmel Point, California, USA	KP871690	MN728192	KP871642	KP871666
Hoplodoris desmoparypha	CASIZ 70066*	Okinawa, Japan	MN722431	MN728185	MN720283	MN720309
Hoplodoris rosans	CASIZ 182921*	Calumpan Peninsula, Philippines	MN722438	MN728197	MN720290	MN720320
Paradoris liturata	CASIZ 182756	Maricaban Strait, Philippines	MW220951	MW220191	MW223084	MW415015
Peltodoris nobilis	CASIZ 182223*	Pillar Point, California, USA	HM162593	MN728194	HM162684	HM162499
Platydoris sanguinea	CASIZ 177762*	Maricaban Island, Philippines	MF958285	MF958372	MF958416	MN720312
Rostanga byga	CASIZ 181157	Devonshire Parish, Bermuda	MW220952	MW220192	MW223085	MW415016
Rostanga pulchra	CASIZ 174490A	Cape Arago, Oregon, USA	MW220953	MW220193	MW223086	MW415017
Sclerodoris sp.	CASIZ 182866*	Balayan Bay, Philippines	MN722437	MN728196	MN720289	MN720319
Sclerodoris sp.	CASIZ 191525*	Madang, Papua New Guinea	MN722444	MN728204	MN720297	MN720328
Sclerodoris tuberculata	CASIZ 190788*	Madang, Papua New Guinea	MF958286	MF958373	MF958417	MN720323
Taringa sp.	CASIZ 172039*	Galápagos Is., Ecuador	MN722432	MN728186	MN720284	MN720310
Taringa telopia	CASIZ 182933*	Bocas Del Toro, Panama	KP871700	MN728198	MN720291	KP871675
Thordisa albomacula A	CASIZ 181136*	Kwajalein Atoll, Marshall Islands	MN722434	MN728191	MN720286	MN720314
Thordisa albomacula B	CASIZ 181345*	Kwajalein Atoll, Marshall Islands	MT452885	MT452656	MT454621	MT454625
Thordisa albomacula C	CASIZ 179586*	Kwajalein Atoll, Marshall Islands	MT452889	MT452660	MT454623	MT454629
Thordisa bimaculata	CASIZ 184516*	Naples, California, USA	MN722439	MN728199	MN720292	MN720321
Thordisa nielseni	CASIZ 173057	Islas Marietas, Mexico	MW220954	MW220194	MW223087	MW415018

Table 1 (continued)

Species	Voucher	Locality	GenBank Accession Numbers			
			16S	28S	COI	H3
Halgerda albocristata	UF 301541	Sulawesi Island, Indonesia	MW220876	MW220115	MW223020	MW414940
H. anosy sp. nov.	CASIZ 194036	South Madagascar	MW220896	MW220135	MW223034	MW414960
H. anosy sp. nov.	CASIZ 194045	South Madagascar	MW220897	MW220136	MW223035	MW414961
H. anosy sp. nov.	CASIZ 194046	South Madagascar	MW220898	MW220137	MW223036	MW414962
H. anosy sp. nov.	CASIZ 194054[#]	South Madagascar	MW220899	MW220138	MW223037	MW414963
H. anosy sp. nov.	CASIZ 194616A	South Madagascar	MW220900	MW220139	MW223038	MW414964
H. anosy sp. nov.	CASIZ 194616B[#]	South Madagascar	–	–	–	–
H. aurantiomaculata	GB	Lifou, New Caledonia	MW220878	MW220117	AY128132	MW414942
H. aurantiomaculata	GB	Heron Island, Australia	MW220877	MW220116	AY128131	MW414941
H. aurantiomaculata	UF 392571	Rarotonga Island, Cook Islands	MW220879	MW220118	MW223021	MW414943
H. aurantiomaculata	UF 437371	Heron Island, Australia	MW220880	MW220119	MW223022	MW414944
H. batangas	CASIZ 175332	Panglao, Philippines	MW220885	MW220124	MW223023	MW414949
H. batangas	CASIZ 177451	Batangas, Philippines	MW220886	MW220125	MW223024	MW414950
H. batangas	CASIZ 191615A	Madang, Papua New Guinea	MW220887	MW220126	MW223025	MW414951
H. batangas (formerly *H. carlsoni*)	GB	Lifou, New Caledonia	MW220884	MW220123	AY128136	MW414948
H. batangas	GB	Okinawa, Japan	MW220882	MW220121	AY128134	MW414946
H. batangas	GB	Negros, Philippines	MW220883	MW220122	AY128135	MW414947
H. batangas	GB	Heron Island, Australia	MW220881	MW220120	AY128133	MW414945
H. batangas	UF 426890	Federated States of Micronesia	MW220888	MW220127	MW223026	MW414952
H. batangas	UF 445572	Okinawa, Japan	MW220889	MW220128	MW223027	MW414953
H. batangas	UF 493087	Puerto Galera, Philippines	MW220890	MW220129	MW223028	MW414954
H. berberiani sp. nov.	UF 456643[#]	Moorea, French Polynesia	–	–	–	–
H. berberiani sp. nov.	MNHN-IM-2000-27156	Tahiti, French Polynesia	–	–	–	–
H. biqiea sp. nov.	CASIZ 192299[#]	Ablo Island, Saudi Arabia	MW220891	MW220130	MW223029	MW414955
H. biqiea sp. nov.	UF 455832[#]	Djibouti	MW220892	MW220131	MW223030	MW414956
H. brunneomaculata	UF 457854	Tahiti, French Polynesia	MW220893	MW220132	MW223031	MW414957
H. carlsoni	CASIZ 177575	Maricaban Island, Philippines	KP871691	MN728189	KP871643	KP871667
H. carlsoni	CASIZ 191239	Madang, Papua New Guinea	MW220894	MW220133	MW223032	MW414958
H. carlsoni	UF 310724	Sulawesi Island, Indonesia	MW220895	MW220134	MW223033	MW414959
H. dalanghita	CASIZ 190743	Madang, Papua New Guinea	MW220901	MW220140	MW223039	MW414965
H. dalanghita	CASIZ 200578	Maricaban Island, Philippines	MW220902	MW220141	MW223040	MW414966
H. dalanghita	CASIZ 204807[#]	Puerto Galera, Philippines	MW220903	MW220142	MW223041	MW414967
H. dalanghita	CASIZ 231295[#]	Calumpan Peninsula, Philippines	MW220904	MW220143	MW223042	MW414968
H. diaphana	UF 351996	Okinawa, Japan	MW220905	MW220144	MW223043	MW414969
H. diaphana	UF 445660	Irimote Island, Japan	MW220906	MW220145	MW223044	MW414970
H. dichromis	CASIZ 231104	KwaZulu-Natal, South Africa	MW220907	MW220146	MW223045	MW414971
H. dichromis	CASIZ 231307	KwaZulu-Natal, South Africa	MW220908	MW220147	MW223046	MW414972
H. dichromis	MHN-VF1*	KwaZulu-Natal, South Africa	MH578116	–	MH578088	MH578152

Table 1 (continued)

Species	Voucher	Locality	GenBank Accession Numbers			
			16S	28S	COI	H3
H. dichromis	MHN-VF2*	KwaZulu-Natal, South Africa	MH578117	–	MH578089	MH578151
H. dichromis	MHN-VF3*	KwaZulu-Natal, South Africa	MH578118	–	MH578090	MH578139
H. cf. *formosa*	MHN-YT1682*	Ponta do Ouro, Mozambique	–	–	MH578087	MH578150
H. guahan	UF 305119B	Guam	MW220910	MW220149	MW223048	MW414974
H. guahan	UF 305119C	Guam	MW220911	MW220150	MW223049	MW414975
H. gunnesi	GB	Rottnest Island, Western Australia	MW220912	MW220151	AY128138	MW414976
H. hervei sp. nov.	CASIZ 186494#	New Caledonia	–	–	–	–
H. indotessellata	CASIZ 180324	Maricaban Island, Philippines	MW220913	MW220152	MW223050	MW414977
H. indotessellata	CASIZ 204806	Verde Island, Philippines	MW220914	MW220153	MW223051	MW414978
H. indotessellata	CASIZ 227557	Zanzibar, Tanzania	MW220915	MW220154	MW223052	MW414979
H. jennyae	MB28-005031*	Zavora, Mozambique	–	–	MH578104	MH578138
H. labyrinthus sp. nov.	CASIZ 070068	Okinawa, Japan	–	–	–	–
H. labyrinthus sp. nov.	CASIZ 070174	Okinawa, Japan	–	–	–	–
H. labyrinthus sp. nov.	CASIZ 160949#	Okinawa, Japan	MW220916	MW220155	AY128143	MW414980
H. leopardalis	MB28-004933*	Zavora, Mozambique	MH578114	–	MH578080	MH578161
H. maaikeae sp. nov.	CASIZ 231070#	KwaZulu-Natal, South Africa	MW220917	MW220156	MW223053	MW414981
H. maaikeae sp. nov.	SAMC-A094639 / CASIZ 231106#	KwaZulu-Natal, South Africa	MW220918	MW220157	MW223054	MW414982
H. malesso	GB	Guam	MW220919	MW220158	AY128139	MW414983
H. malesso	UF 289547	Guam	MW220920	MW220159	MW223055	MW414984
H. mango sp. nov.	NMP 041323/CASIZ 181264#	Maricaban Island, Philippines	MF958289	MF958376	MF958420	MN720316
H. mango sp. nov.	CASIZ 204808#	Puerto Galera, Philippines	MW220921	MW220160	MW223056	MW414985
H. mango sp. nov.	CASIZ 217210#	Maricaban Island, Philippines	MW220922	MW220161	MW223057	MW414986
H. meringuecitrea	CASIZ 231100	KwaZulu-Natal, South Africa	MW220923	MW220162	MW223058	MW414987
H. meringuecitrea	MB28-004716*	Zavora, Mozambique	MH578112	–	MH578106	MH578154
H. meringuecitrea	MB28-004802*	Zavora, Mozambique	MH578113	–	MH578107	MH578131
H. mesophotica sp. nov.	NMP 041324/ CASIZ 193832#	Balayan Bay, Philippines	MW220924	MW220163	MW223059	MW414988
H. mozambiquensis	MB28-004661*	Zavora, Mozambique	–	–	MH578110	MH578157
H. nuarrensis	MB28-004874*	Nuarro, Mozambique	MH578115	–	MH578102	MH578132
H. okinawa	GB	Okinawa, Japan	MW220925	MW220164	AY128140	MW414989
H. pattiae sp. nov.	UF 422800#	Mayotte Island, Comoros Archipelago	MW220926	MW220165	MW223060	MW414990
H. paulayi sp. nov.	CASIZ 192298#	Ablo Island, Saudi Arabia	MW220927	MW220166	MW223061	MW414991
H. paulayi sp. nov.	UF 476040#	Jazirat Burcan, Saudi Arabia	MW220928	MW220167	MW223062	MW414992
H. paulayi sp. nov.	UF 476041#	Jazirat Burcan, Saudi Arabia	MW220929	MW220168	MW223063	MW414993
H. profunda sp. nov.	NMP 041325/CASIZ 201240#	Lubang Islands, Philippines	MW220930	MW220169	MW223064	MW414994
H. radamaensis sp. nov.	CASIZ 173456#	Iles Radama, Madagascar	–	–	–	–
H. radamaensis sp. nov.	CASIZ 234753	Iles Radama, Madagascar	–	–	–	–

Table 1 (continued)

Species	Voucher	Locality	GenBank Accession Numbers			
			16S	28S	COI	H3
H. scripta sp. nov.	NMP 041326/CASIZ 204788#	Verde Island, Philippines	MW220934	MW220173	MW223068	MW414998
H. scripta sp. nov.	CASIZ 193823#	Maricaban Island, Philippines	MW220931	MW220170	MW223065	MW414995
H. scripta sp. nov.	CASIZ 201239	Lubang Islands, Philippines	MW220932	MW220171	MW223066	MW414996
H. scripta sp. nov.	CASIZ 204787	Verde Island, Philippines	MW220933	MW220172	MW223067	MW414997
H. scripta sp. nov.	CASIZ 204789	Verde Island, Philippines	MW220935	MW220174	MW223069	MW414999
H. takipsilim sp. nov.	NMP 041327/CASIZ 204791#	Verde Island, Philippines	MW220937	MW220176	MW223071	MW415001
H. takipsilim sp. nov.	CASIZ 201241	Lubang Islands, Philippines	MW220936	MW220175	MW223070	MW415000
H. terramtuentis	CASIZ 171214	Maui, Hawaiian Island	OM780016	MW220177	MW223072	MW415002
H. tessellata	CASIZ 181590	Panglao, Philippines	MW220940	MW220179	MW223073	MW415004
H. tessellata	CASIZ 191088	Madang, Papua New Guinea	OM780017	MW220180	MW223074	MW415005
H. tessellata	CASIZ 191590	Madang, Papua New Guinea	OM780018	MW220181	MW223075	MW415006
H. tessellata	CASIZ 191618	Madang, Papua New Guinea	MW220943	MW220182	MW223076	MW415007
H. tessellata	GB	Lifou, New Caledonia	MW220939	MW220178	AY128141	MW415003
H. theobroma	GB	Rottnest Island, Western Australia	–	MW220183	AY128142	–
H. toliara	MB28-004783*	Vamizi, Mozambique	–	–	MH578081	MH578158
H. toliara	MB28-004800*	Zavora, Mozambique	–	–	MH578082	MH578159
H. aff. *wasinensis*	MB28-005079*	Ponta do Ouro, Mozambique	MH578121	–	MH578085	MH578149
H. wasinensis	CASIZ 176983	Bazaruto Archipelago, Mozambique	MW220944	MW220184	MW223077	MW415008
H. wasinensis	CASIZ 227568	Zanzibar, Tanzania	MW220945	MW220185	MW223078	MW415009
H. wasinensis	CASIZ 227601	Zanzibar, Tanzania	MW220946	MW220186	MW223079	MW415010
H. wasinensis	MB28-004918*	Pomene, Mozambique	MH578129	–	MH578091	MH578140
H. wasinensis	MB28-004972*	Zavora, Mozambique	MH578120	–	MH578100	MH578142
H. wasinensis	MB28-005002*	Vamizi, Mozambique	MH578122	–	MH578094	MH578143
H. wasinensis	MB28-005068*	Zavora, Mozambique	MH578127	–	MH578093	MH578144
H. wasinensis	MHN-YT1381*	Pomene, Mozambique	MH578126	–	MH578096	MH578146
H. wasinensis	MHN-YT1383*	Pomene, Mozambique	MH578128	–	MH578098	MH578147
H. wasinensis	MHN-YT1464*	Zavora, Mozambique	MH578124	–	MH578097	MH578148
H. wasinensis	MHN-YT1478c*	Zavora, Mozambique	MH578125	–	MH578099	MH578134
H. willeyi	CASIZ 083676A#	Calumpan Peninsula, Philippines	–	–	–	–
H. willeyi	CASIZ 177248	Maricaban Island, Philippines	MW220947	MW220187	MW223080	MW415011
H. willeyi	CASIZ 191259	Madang, Papua New Guinea	MW220909	MW220148	MW223047	MW414973
H. willeyi	CASIZ 191495	Madang, Papua New Guinea	MW220948	MW220188	MW223081	MW415012
H. willeyi	CASIZ 201944	Maricaban Island, Philippines	MW220949	MW220189	MW223082	MW415013
H. willeyi	CASIZ 204790	Verde Island, Philippines	MW220950	MW220190	MW223083	MW415014

Table 2 Primers for DNA amplification and substitution models for Bayesian inference analysis

Primer	Sequence	Citation	Substitution model	Length	
16S			GTR + I + G	433	
AR	5′-CGCCTGTTTATCAAAAACAT-3′	Palumbi et al. (1991)			
BR	5′-CCGGTCTGAACTCAGATCACGT-3′	Palumbi et al. (1991)			
28S			GTR + I + G	750	
D2	5′-CTTGGTCCGTGTTTCAAGACGG-3′	Dayrat et al. (2001) (modified)			
C1'	5′-ACCCGCTGAATTTAAGCAT-3′	Dayrat et al. (2001)			
C2'	5′-GAAAGAACTTTGAAGAGAGAGTTCA-3′	Dayrat et al. (2001) (modified)			
C2	5′-TGAACTCTCTCTTCAAAGTTCTTTTC-3′	Dayrat et al. (2001)			
Primer	**Sequence**	**Citation**	**Substitution Model**	**Length**	**Codon position**
COI			GTR + I + G	220	P3
HCO21 98	5′-TAAACTTCAGGGAGACCAAAAAATCA-3′	Folmer et al. (1994)	SYM + I + G	219	P1
LCO1490	5′-GGTCAACAAATCATAAAGATATTGG-3′	Folmer et al. (1994)	GTR + I + G	219	P2
H3			GTR + G	110	P1
AF	5′-ATGGCTCGTACCAAGCAGACVGC-3′	Colgan et al. (1998)	JC + I	110	P2
AR	5′-ATATCCTTRGGCATRATRGTGAC-3′	Colgan et al. (1998)	GTR + G	110	P3

in MrBayes v3.2.6 (Ronquist and Huelsenbeck 2003), and the dataset was run for 5×10^7 generations. Markov chains were sampled every 1000 generations, and the standard 25% burn-in was calculated before checking the convergence of the two chains using TRACER v1.7.1 (Drummond and Rambaut 2007). A 50% majority rule consensus tree of calculated posterior probabilities (pp) was created from the remaining tree estimates. Maximum likelihood was performed using randomized accelerated maximum likelihood (RAxML) v8.2.12 (Stamatakis 2014). Non-parametric bootstrap values (bs) were estimated from 5×10^4 fast bootstrap runs set with the evolution model GTR + GAMMA + I. Final trees were collapsed (pp ≥ 0.95) in TreeGraph 2 v2.15.0 (Stöver and Müller 2010) before final editing in FigTree v1.4.4 (Rambaut 2018) and Adobe Photoshop 2022 (San Jose, CA, USA). Tree branches were considered supported when posterior probability values were ≥ 0.95 and bootstrap values were ≥ 70 (Alfaro et al. 2003).

Species delimitation analyses

Species were delimited using four different approaches: (i) Automatic Barcode Gap Discovery (ABGD) method (Puillandre et al. 2012), (ii) Assemble Species by Automatic Partitioning (ASAP) method (Puillandre et al. 2021), (iii) Bayesian Poisson Tree Process (bPTP) by Zhang et al. 2013), and (iv) General Mixed Yule Coalescent (GMYC) model (Pons et al. 2006; Fujisawa and Barraclough 2013). The ABGD method uses genetic pairwise distances to detect breaks between intraspecific and interspecific variation. An ingroup COI alignment and an ingroup 16S alignment were created in Mesquite v3.51 and uploaded to the ABGD Web-based interface (https://bioinfo.mnhn.fr/abi/public/abgd/abgdweb.html). We tested Jukes-Cantor (JC69), Kimura (K80), and Simple Distances as well as different gap widths to evaluate which settings were congruent with our own phylogenetic and morphological analyses (Kekkonen et al. 2015; Tibiriçá et al. 2018). The following parameters were applied for the COI ingroup: Kimura80 (K80) P.min = 0.001, P.max = 0.2, Steps = 10, NB = 20 with a relative gap width × = 1.3. The 16S ingroup used similar parameters; however, the relative gap width × was set to 1.0.

The ASAP method also uses genetic pairwise distances; however, it does not require any prior species hypotheses, and it also provides a score for each suggested partition. The previously used COI and 16S ingroup alignments were uploaded to the ASAP Web-based interface (https://bioinfo.mnhn.fr/abi/public/asap/asapweb.html) and tested with the following settings: Jukes-Cantor (JC69), Kimura (K80), and Simple Distances. Bayesian PTP uses a previously inputted phylogenetic tree to model the number of substitutions between branchings and uses Bayesian MCMC methods to identify groups descended from a single ancestor. This test was performed using the 16S + COI concatenated BI tree on the bPTP server (https://species.h-its.org/) with the following parameters: 500,000 generations, 100 thinning, 0.1 burn-in, and 123 seeds. Convergence was checked using the ML convergence plot generated by the bPTP server.

The GMYC model is a likelihood-based method that assumes species-independent evolution, which results in differences between branching rates (i.e., diversification between species) that can then be delimited using a Yule

model (Fujisawa and Barraclough 2013). We used BEAST package v 1.10.4 (Drummond et al. 2012) to estimate a COI ultrametric tree using the following priors defined in BEAUTi v1.10.4: GTR + GAMMA + I, yule speciation process, uncorrelated lognormal relaxed clock, and 10 million generations MCMC chain length sampled every 1000 steps. The resulting log files were checked for convergence using TRACER v1.7.1 (Drummond and Rambaut 2007). The first 10% of trees (burn-in) were removed using TreeAnnotator v1.10.4, and a maximum clade credibility tree was built from the remaining tree estimates. The R package Species Limits by Threshold Statistics (SPLITS, v1.0–20, Fujisawa and Barraclough 2013) was used to perform the GMYC approach using the "single threshold" model (Pons et al. 2006).

Morphological study

At least one specimen from each of the fourteen new species of *Halgerda*, as well as representatives of *H. dalanghita* and *H. willeyi*, was examined morphologically. Specimens that were dissected are indicated in Table 1 with a # symbol and noted as such in their respective Material Examined section in each species description. External features were examined and described utilizing photographs of living animals and when necessarily preserved specimens. Using a Nikon SMZ-U dissection microscope, each specimen was dissected along the center of the foot, and the buccal mass and reproductive system were removed for further study. The arrangement of the reproductive organs and the shape of the buccal mass were hand-drawn using a camera lucida drawing attachment on a Nikon SMZ-U dissection microscope. After being illustrated, the buccal mass was dissolved in 10% sodium hydroxide (NaOH) for 12–24 h, and then the labial cuticle and radula were rinsed with deionized water and mounted on glass coverslips for examination by scanning electron microscope (SEM). The SEM samples were coated with gold/palladium using a Cressington 108 Auto vacuum sputter coater before micrographs were taken using a Hitachi SU3500 scanning electron microscope at the California Academy of Sciences. Specimens and the corresponding dissected structures were deposited at the California Academy of Sciences Department of Invertebrate Zoology (CASIZ) collection, the Florida Museum of Natural History (UF), and the National Museum of Philippines (NMP).

Results

Phylogenetic analyses

Three hundred and eight new sequences from 80 specimens were deposited on GenBank with the following accession numbers: 16S (MW220875–MW220954, OM780016–OM780018), 28S (MW220114–MW220194), COI (MW223019–MW223087), and H3 (MW414939–MW415018). The final four-gene concatenated dataset was 2171 bp in length after removing 98 bp of ambiguous data. The single gene alignments without ambiguous data contained 433 bp for 16S, 750 bp for 28S, 658 bp for COI, and 330 bp for H3. The BI and ML analyses resulted in similar topologies; however, BI analysis generally resulted in better support values than the ML analysis (Fig. 2). A second Bayesian phylogenetic tree estimated from the four-gene concatenated dataset including the ambiguous data is provided in Supplementary Fig. S1. A third Bayesian tree estimated from the four-gene concatenated dataset without collapsed nodes is provided in Supplementary Figure S2. In this study, the position of *Halgerda* within Discodorididae remains unresolved, and a comprehensive phylogenetic study of the entire family of Discodorididae is needed to better evaluate the position of *Halgerda* with the other 28 recognized genera in the family.

Our analyses support the monophyly of *Halgerda* (pp = 1; bs = 100), which contains seven well-supported subclades (indicated and labeled with black bars in Fig. 2) and an ungrouped specimen of *Halgerda leopardalis* Tibiriçá, Pola & Cervera, 2018. The first subclade composed of *H. dalanghita* and *Halgerda mango* Donohoo & Gosliner sp. nov. and the second subclade composed of two translucent white species *Halgerda meringuecitrea* Tibiriçá, Pola & Cervera, 2018 and *Halgerda pattiae* Donohoo & Gosliner sp. nov. are both well-supported (pp = 1; bs = 99, pp = 1; bs = 90, respectively). The third subclade including *Halgerda brunneomaculata* Carlson & Hoff, 1993; *Halgerda biqiea* Donohoo & Gosliner sp. nov.; *Halgerda albocristata* Gosliner & Fahey, 1998; and *Halgerda toliara* Fahey & Gosliner, 1999a is also well-supported (pp = 1; bs = 98); however, the two specimens of *H. toliara* group together with the one specimen of *H. albocristata* are unresolved.

The fourth subclade containing *Halgerda mozambiquensis* Tibiriçá, Pola & Cervera, 2018; *Halgerda maaikeae* Donohoo & Gosliner sp. nov.; *Halgerda indotessellata* Tibiriçá, Pola & Cervera, 2018; and *Halgerda tessellata* (Bergh, 1880b) is well-supported (pp = 1; bs = 100) but includes a polytomy between the first two species and a subclade of *H. indotessellata* that forms a second polytomy with a clade of *H. tessellata*. The fifth subclade (i.e., the mesophotic subclade) composed of *Halgerda scripta* Donohoo & Gosliner sp. nov.; *Halgerda okinawa* Carlson & Hoff, 2000; *Halgerda mesophotica* Donohoo & Gosliner sp. nov.; *Halgerda profunda* Donohoo & Gosliner sp. nov.; and *Halgerda takipsilim* Donohoo & Gosliner sp. nov. is well-supported (pp = 1; bs = 100).

The sixth clade which forms the *H. carlsoni* species complex is partially unresolved with a large polytomy and includes the following nine species: *Halgerda theobroma* Fahey & Gosliner, 2001b; *Halgerda labyrinthus* Donohoo & Gosliner sp. nov.;

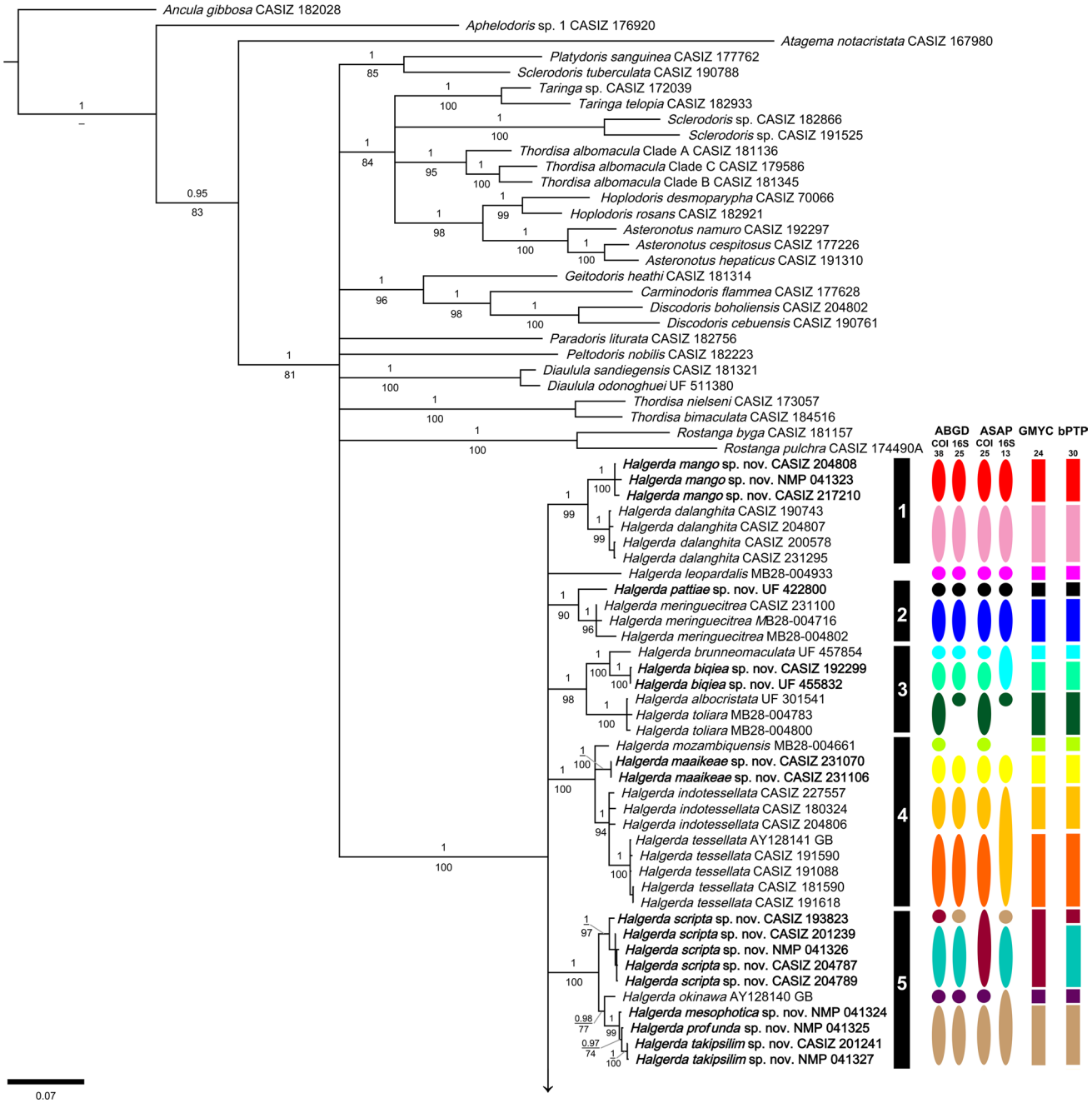

Fig. 2 Bayesian phylogenetic tree of *Halgerda* Bergh, 1800a estimated from the four gene (16S + 28S + COI + H3) concatenated data. Numbers above branches refer to BI posterior probabilities (pp), while numbers below branches refer to ML non-parametric bootstrapping values (bs). Relationships not recovered during ML analysis are indicated by dashes. To the right are the results of the COI and 16S ABGD analysis, the COI and 16S ASAP analysis, the COI GMYC analysis, and the 16S + COI bPTP analysis

Halgerda batangas Carlson & Hoff, 2000; *Halgerda terramtuentis* Bertsch & S. Johnson, 1982; *Halgerda malesso* Carlson & Hoff, 1993; *Halgerda diaphana* Fahey & Gosliner, 1999b; *H. carlsoni*; *Halgerda nuarrensis* Tibiriçá, Pola & Cervera, 2018; and *Halgerda aurantiomaculata* (Allan, 1932). Within this clade, the first two species are basal to a polytomy composed of ungrouped specimens of *H. batangas*, a well-supported (pp = 1, bs = 95) group of two *H. batangas* specimens, and a well-supported (pp = 1, bs = 52) clade composed of a second polytomy of the rest of the species previously listed. The seventh subclade is also well-supported (pp = 1; bs = 0.91) and further divides into two major clades. The first major clade is unresolved, but

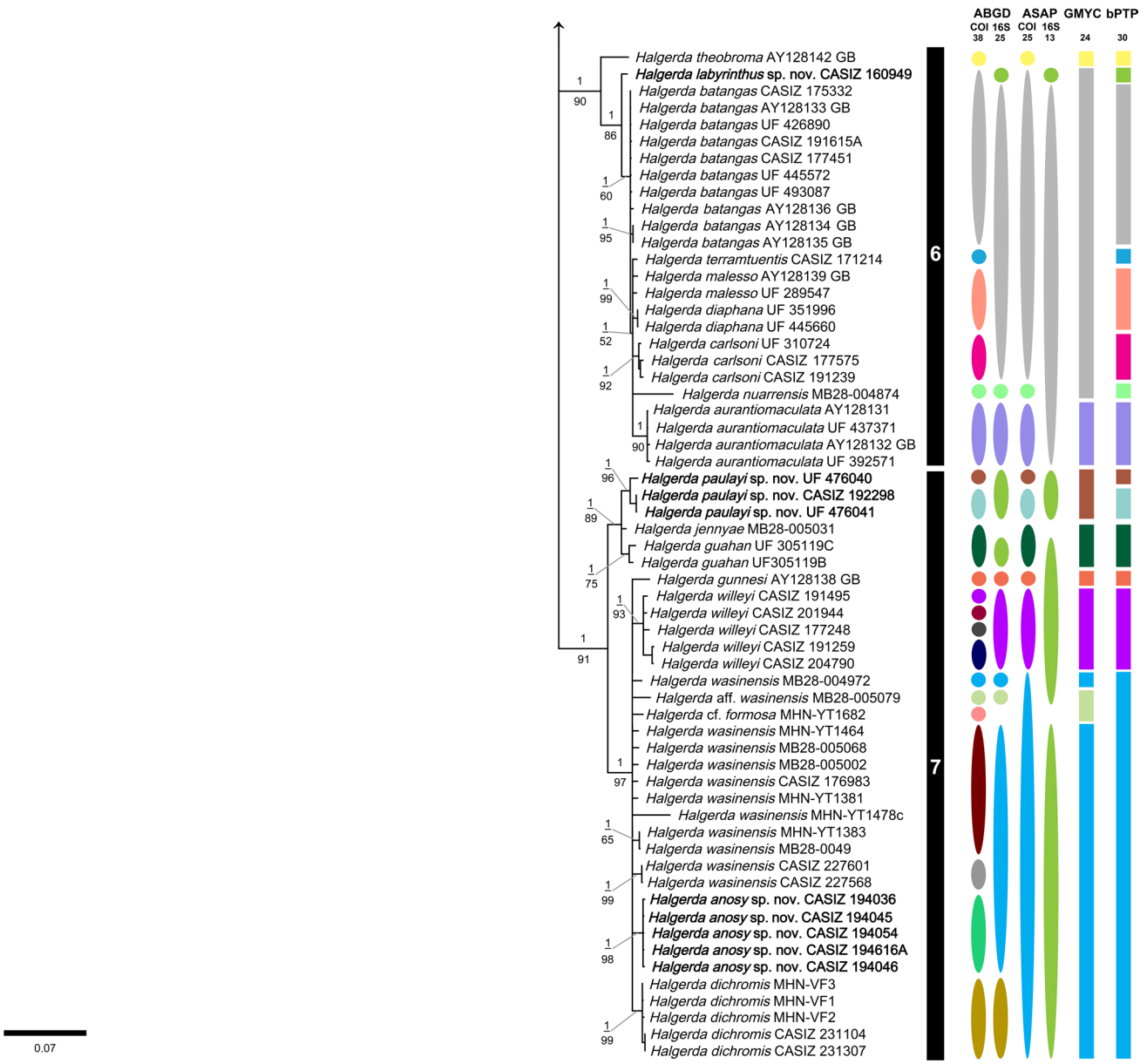

Fig. 2 (continued)

well-supported (pp = 1; bs = 89) and composed of *Halgerda paulayi* Donohoo & Gosliner sp. nov.; a single specimen of *Halgerda jennyae* Tibiriçá, Pola & Cervera, 2018; and *Halgerda guahan* Carlson & Hoff, 1993. The second major clade is also unresolved and composed of *Halgerda gunnesi* Fahey & Gosliner, 2001b well-supported clade of *H. willeyi*, and members of the *H. wasinensis* species complex including ungrouped specimens of *Halgerda* cf. *formosa* Bergh, 1880a; *Halgerda* aff. *wasinensis* Eliot, 1904 and *H. wasinensis*; and well-supported clades of *H. wasinensis*; *Halgerda anosy* Donohoo & Gosliner sp. nov.; and *H. dichromis*.

Species delimitation

The COI ABGD analysis recovered six partitions (Supplementary Table S1). Eighteen groups were retrieved with a prior maximal distance *p*-distance of 0.02, 21 groups with 0.01, 34 groups with 0.006, 38 groups with 0.003, 41 groups with 0.002, and 47 groups with 0.001. The partitions with 18–21 groups were clearly under-divided as all 24 specimens from eight morphologically distinct species including *H. labyrinthus* sp. nov., *H. batangas*, *H. terramtuentis*, *H. malesso*, *H. diaphana*, *H. carlsoni*, *H. nuarrensis*, and *H. aurantiomaculata*

were grouped together as a single taxonomic unit. The partition with 18 groups also recovered *H. okinawa*, *H. mesophotica* sp. nov., *H. profunda* sp. nov., and *H. takipsilim* sp. nov. as one taxonomic unit; *H. paulayi* sp. nov., *H. guahan*, and *H. jennyae* as one unit; and *H. gunnesi*, *H. willeyi*, *H.* cf. *formosa*, *H.* aff. *wasinensis*, *H. wasinensis*, *H. dichromis*, and *H. anosy* sp. nov. as one single large taxonomic unit. The partition with 21 groups recovered similar units as the 18 groups partition; however, it does recover *H. gunnesi*, *H. willeyi*, and *H. okinawa* as distinct individual units.

The partitions with 34–47 groups also recover *H. mesophotica* sp. nov., *H. profunda* sp. nov., and *H. takipsilim* sp. nov. as one taxonomic unit as well as over-dividing several *Halgerda* species including *H. willeyi*, *H. paulayi* sp. nov., *H. batangas*, and the *H. wasinensis* species complex; however, the partition with 34 groups also fails to separate out *H. diaphana*, *H. malesso* and *H. labyrinthus* sp. nov. from the *H. batangas* clade. The partitions with 41–47 groups successfully separate out the aforementioned species from *H. batangas*, but also over-divides the three specimens of *H. carlsoni* and one specimen of *H. scripta* sp. nov. The partition with 47 groups also over-divides several specimens of *H. batangas*. Therefore, the partition with 38 groups is the most congruent with the Bayesian and maximum likelihood analyses. This partition also over-divides *H. willeyi*, *H. paulayi* sp. nov., *H. scripta* sp. nov., and the *H. wasinensis* species complex as well as fails to recover *H. labyrinthus* sp. nov. separately from *H. batangas*; however, the latter may be attributed to the low genetic differences between the two species (maximum *p*-distance = 1.4%).

The 16S ABGD analysis recovered four partitions (Supplementary Table S2). One group was retrieved with a prior maximal distance *p*-distance of 0.006, 25 groups with 0.003, 52 groups with 0.002, and 52 groups with 0.001. The partition with one group recovers all *Halgerda* specimens together, while the partitions with 52 groups recover most specimens as individual taxonomic units. Therefore, the partition with 25 groups is the most likely as it successfully recovers some species; however, it fails to delimit species in several clades. The following species were also not recovered *H. theobroma*, *H. jennyae*, *H. toliara*, *H.* cf. *formosa*, and *H. mozambiquensis* due to a lack of sequencing. Most of the species in the *H. carlsoni* species complex including *H. carlsoni*, *H. batangas*, *H. terramtuentis*, *H. malesso*, and *H. diaphana* were recovered together as one large taxonomic unit. *Halgerda meringuecitrea* is over-divided into two groups, while *H. anosy* sp. nov. groups together with the majority of the *H. wasinensis* species complex excluding *H. dichromis* and *H.* aff. *wasinensis* which are recovered as separate units. All specimens of *H. labyrinthus* sp. nov., *H. paulayi* sp. nov., and *H. guahan* are recovered as one unit, and one specimen of *H. scripta* sp. nov. is recovered in a unit with *H. mesophotica* sp. nov., *H. profunda* sp. nov., and *H. takipsilim* sp. nov.

The COI ASAP analysis (Supplementary Figure S3) using Kimura80 recovered 19 groups (ASAP score = 1.50); however, all species in the *H. carlsoni* species complex in the first clade were grouped together as one large taxonomic unit. Additionally, the seventh clade was split into two taxonomic units. One unit included *H. paulayi* sp. nov., *H. jennyae*, and *H. guahan*, and the second included all specimens of the *H. wasinensis* species complex, *H. dichromis*, *H. anosy* sp. nov., *H.* cf. *formosa*, and *H. willeyi*. The partition with 25 groups (ASAP score = 8.50) recovers similar groups, but also successfully separates *H. nuarrensis*, *H. aurantiomaculata*, and *H. willeyi* from the previously mentioned large taxonomic units. It also separates *H. paulayi* sp. nov. from *H. jennyae* and *H. guahan*, but over-partitions this species into two groups.

The 16S ASAP analysis (Supplementary Figure S4) using Kimura80 recovered 13 groups (ASAP score = 2.50) which are similar to the COI ASAP analysis; however, *H. theobroma*, *H. toliara*, *H. jennyae*, *H.* cf. *formosa*, and *H. mozambiquensis* are not recovered due to a lack of sequencing. Additionally, in this partition, *H. biqiea* sp. nov. is recovered with *H. brunneomaculata*, and H. *labyrinthus* sp. nov., *H. willeyi*, *H. paulayi* sp. nov., and *H. guahan* are recovered with the *H. wasinensis* complex including *H.* aff. *wasinensis*, *H. anosy* sp. nov., and *H. dichromis* in one large taxonomic unit.

The COI + 16S bPTP analysis was mostly congruent with the COI ABGD results. However, the bPTP analysis does successfully recover *H. labyrinthus* sp. nov. separately from *H. batangas*, while grouping all five specimens of *H. willeyi* together into one unit, and grouping all specimens of *H.* cf. *formosa*, *H.* aff. *wasinensis*, *H. wasinensis*, *H. dichromis*, and *H. anosy* sp. nov. into one single large taxonomic unit.

The COI GYMC recovers 24 groups similar to the COI ASAP with 25 groups with a few differences. The entire *H. carlsoni* species complex including *H. nuarrensis* but excluding *H. aurantiomaculata* is recovered as one large taxonomic unit. All three specimens of *H. paulayi* sp. nov. are recovered together in one unit rather than two. The majority of the *H. wasinensis* species complex is recovered as one large taxonomic unit; however, *H.* aff. *wasinensis* and *H.* cf. *formosa* are recovered together in one unit outside the *H. wasinensis* species complex.

Species descriptions

Order Nudibranchia Cuvier, 1817
Family Discodorididae Bergh, 1891
Genus *Halgerda* Bergh, 1880a
Type species *Halgerda formosa* Bergh, 1880a, by monotypy

Halgerda dalanghita Fahey & Gosliner, 1999a
(Fig. 3a–c and 4)

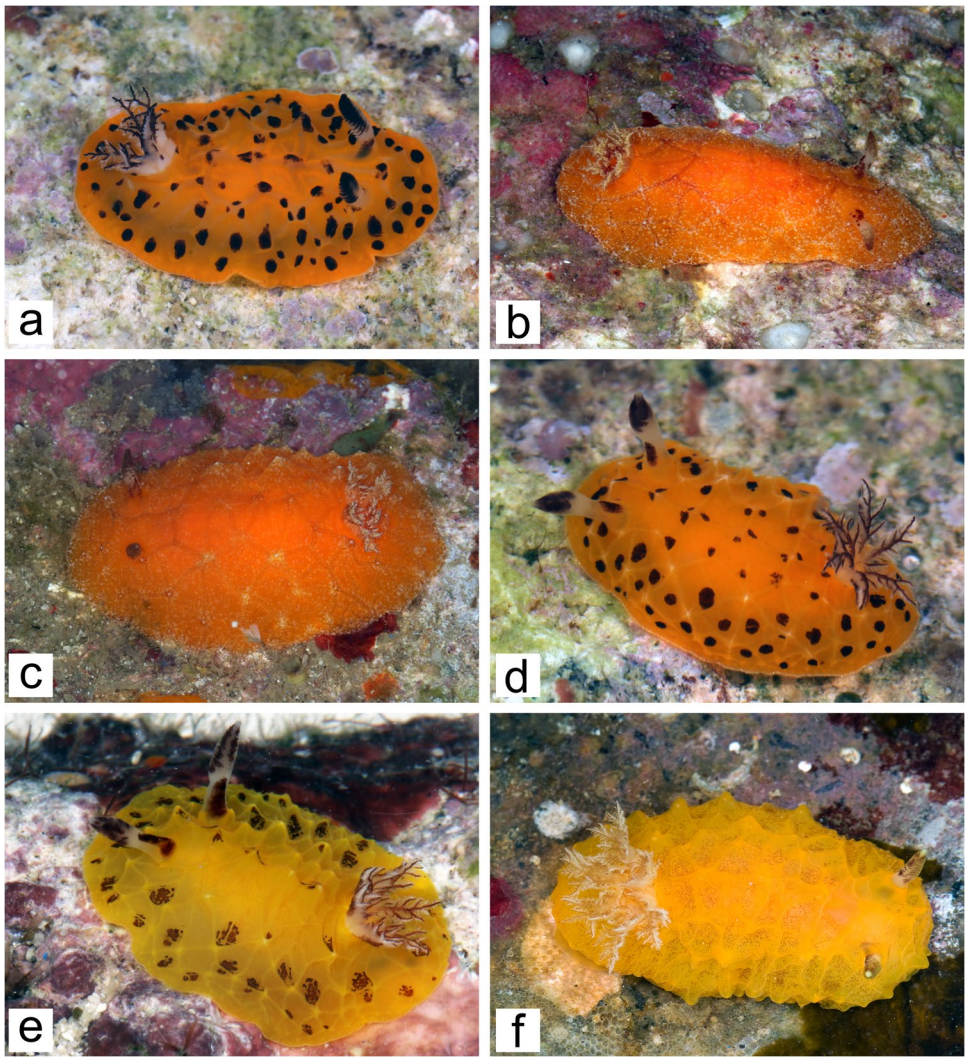

Fig. 3 Living specimens: **a–c** *Halgerda dalanghita* Fahey & Gosliner, 1999a; **a** juvenile, CASIZ 204807, Puerto Galera, Philippines, photo by T.M. Gosliner; **b** CASIZ 200578, Maricaban Island, Philippines, photo by T.M. Gosliner; **c** CASIZ 231295, Maricaban Island, Philippines, photo by T.M. Gosliner; **d–f** *Halgerda mango* sp. nov.; **d** juvenile, CASIZ 204808, Puerto Galera, Philippines, photo by T.M. Gosliner; **e** juvenile, CASIZ 217210, Maricaban Island, Philippines, photo by T.M. Gosliner; **f** holotype, NMP 041323, Maricaban Island, Philippines, photo by T.M. Gosliner

Halgerda dalanghita Fahey & Gosliner, 1999a: 373–374, Figs. 3b, 4a, 5, and 6; Fahey and Gosliner (2000): 496–497, Figs. 14c, 16d, 18; Ono (2004): 139, top photograph; Debelius and Kuiter (2007): 227, bottom photograph; Gosliner et al. (2008): 176, third photograph; Gosliner et al. (2015): 184, bottom right photograph; Gosliner et al. (2018): 105, middle right photograph; Strömvoll and Jones (2019): 46, middle left photograph; Tibiriçá et al. (2018): 1404–1406, Figs. 7e, f and 9a, b. *Halgerda* sp. 1 Gosliner et al. (2018): 105, bottom left photograph. *Halgerda* sp. 4 Gosliner et al. (2018): 106, middle left photograph.

Sclerodoris sp. Gosliner (1987): 68, top photograph.

Material examined: One adult specimen, CASIZ 200758, sequenced, 20 mm preserved, locality: Devil's Point (13° 39′ 03.0″ N 120° 50′ 28.6″ E), Maricaban Island, Batangas Province, Luzon, Philippines, 30.78 m depth, 04 May 2014, collected by T.M. Gosliner. One adult specimen, CASIZ 231295, dissected and sequenced, 25 mm preserved, locality: Peri's Point (13° 42′ 0.0″ N 120° 55′ 12.0″ E), Batangas Bay, Calumpan Peninsula, Batangas Province, Luzon, Philippines, 15 September 2019, collected by Peri Paleracio. One juvenile specimen, CASIZ 190743, sequenced, 6 mm preserved, locality: Madang, Papua New Guinea, 09 Dec 2012, collected by Papua New Guinea Biodiversity Expedition 2012. One juvenile specimen, CASIZ 204807, dissected and sequenced, 8 mm preserved, locality: Puerto Galera (13° 31′ 11.6″ N 120° 57′ 37.4″ E), Oriental Mindoro Province, Mindoro, Philippines, 3–15 m depth, 12 April 2015, collected by T.M. Gosliner.

Type locality: Bethlehem, Maricaban Island, Batangas Province, Luzon, Philippines.

External anatomy (Fig. 3a–c): Adult preserved animals 20–25 mm in length (Fig. 3b, c). Similar to adult description described in Fahey and Gosliner (1999a, Fig. 4a). Juvenile coloration described here. In small juvenile CASIZ 204807 dorsum color uniform orange with small to large, random black spots (Fig. 3a). Ridges thicker, less angled with no tubercles. Thin, semi-opaque white mantle band lines mantle edge. Mantle underside orange with numerous medium to large dark

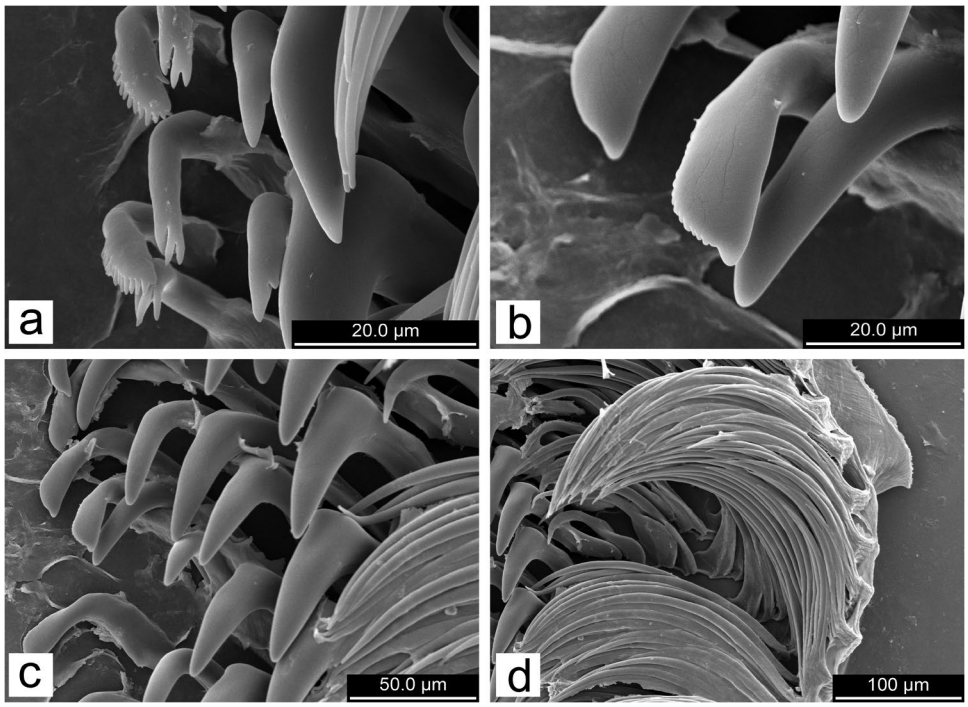

Fig. 4 *Halgerda dalanghita* Fahey & Gosliner, 1999a, scanning electron micrographs of radula: **a** Juvenile, CASIZ 204807, inner lateral teeth; **b–c** Adult CASIZ 231295; **b** inner lateral teeth; **c** mid-lateral teeth; **d** outer lateral teeth

brown/black spots. Gill surrounds elevated anus with six bipinnate branchial leaves. Gill branches translucent white with dorsal black stripes and occasional black spots. Opaque white glands present within gill rachis. Gill pocket smooth with similar dorsum coloration. Rhinophores tapered and perfoliate, with 11 lamellae. Rhinophoral sheath and lamellae translucent white with black subapical and posterior near base splotches. Foot is broad, anteriorly notched, orange with numerous small to medium dark brown/black spots. Oral tentacles digitiform.

Internal anatomy (Fig. 4a–d): Buccal mass unpigmented. Similar to Fahey and Gosliner (1999a) original description. Labial cuticle smooth. Radula composed of both smooth hamate and extremely elongate teeth. Radular formula 42×19.0.19 in CASIZ 231295 and 30×20.0.20 in small juvenile CASIZ 204807. In CASIZ 231295 innermost lateral tooth (Fig. 4b) small, paddle shaped, with broad base and approximately 14 greatly reduced denticles. Middle lateral teeth 2–5 hamate, gradually increase in size and elongation (Fig. 4c). Outer lateral teeth (Fig. 4d) thin, extremely elongate, with fine tips. Outermost tooth is reduced version of outer laterals. Juvenile inner teeth denticulation (Fig. 4a) more pronounced in CASIZ 204807 with 12–13 elongate denticles (first inner tooth), 3 elongate denticles (second inner tooth), and occasionally one reduced denticle on third inner tooth.

Reproductive system: Not illustrated. Similar to reproductive system drawn and described in Fahey and Gosliner (1999a, Fig. 3b).

Geographical distribution: Known from South Africa (Gosliner 1987; Fahey and Gosliner 1999a; Gosliner et al. 2008; Strömvoll and Jones 2019), Mozambique (Tibiriçá et al. 2018), Japan (Ono 2004; Gosliner et al. 2008), the Philippines (Fahey and Gosliner 1999a; Gosliner et al. 2008), Papua New Guinea (Fahey and Gosliner 1999a; Gosliner et al. 2008), Fiji (Fahey 2000), the Marshall Islands (Debelius and Kuiter 2007), the Solomon Islands, and Hawaii (Gosliner et al. 2008).

Ecology: Found on orange sponges in shallow water between 3 and 15 m and on coral rubble at 20 m.

Remarks: Our molecular and species delimitation analyses reveal that specimens previously thought to be a new species (*Halgerda* sp. 4, Gosliner et al. 2018) are juveniles of the previously described species *Halgerda dalanghita*. Here, we have provided a second description for juvenile *H. dalanghita* and make morphological comparisons with adult *H. dalanghita* originally described by Fahey and Gosliner (1999a) and a juvenile *H. dalanghita* from Mozambique identified in Tibiriçá et al. (2018, Fig. 7e). Externally, the dorsum color is a uniform orange similar to that found in adult specimens; however, there are many small to large, random black spots across the entire mantle (Fig. 3a) that are similar to the Mozambique juvenile rather than the numerous minute brown and white spots seen in adult specimens (Fahey and Gosliner 1999a, Fig. 4a; present study Fig. 3b, c). The dorsum ridging is thicker and less angled in the juvenile specimen studied here, but both adults and juveniles lack tubercles at the ridge junctions. Furthermore, both adults and juveniles have numerous small to medium brown/light brown spots on the mantle underside and along the foot. In both the juvenile studied here and the Mozambique juvenile, the rhinophores and gill plume have darker, less diffused pigment than in adults; however, there are a similar number of bipinnate gill branches with opaque white glands visible in the rachises. Internally, there are fewer rows in

both juvenile radulae, and the first few inner teeth have more pronounced denticles than the adult specimens (Fig. 4a). The middle and outer teeth are similar in shape in both adults and juveniles and accurately counting the thin, extremely elongate, fine tipped outer teeth is difficult.

In summary, as individuals of *H. dalanghita* grow, the dorsum ridging becomes narrower and more pronounced; the black spots along the mantle, rhinophores, and gills begin to diffuse and fade; and the denticles along the inner laterals of the radular teeth become reduced. The intraspecific variation between the four specimens (two adults and two juveniles studied here) collected from Papua New Guinea and three different locations in the Philippines have a range of 0.5–1.7% in the COI gene, which further supports our description of juvenile *H. dalanghita*.

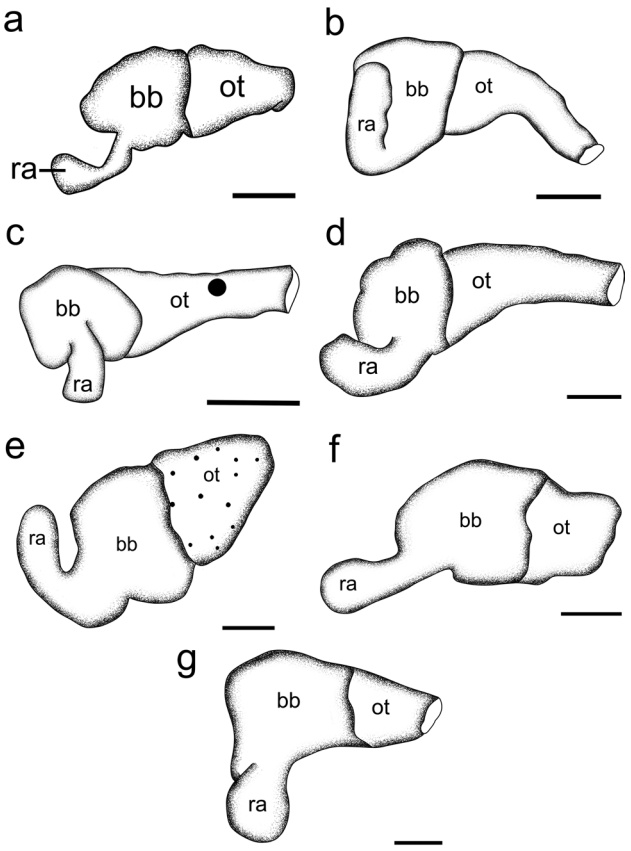

Fig. 5 Buccal masses: **a** *Halgerda mango* sp. nov., holotype, NMP 041323, scale bar = 0.5 mm; **b** *Halgerda berberiani* sp. nov., holotype, UF 456643, scale bar = 1 mm; **c** *Halgerda biqiea* sp. nov., holotype, UF 455832, scale bar = 0.5 mm; **d** *Halgerda willeyi* Eliot, 1904, CASIZ 083676A, scale bar = 1 mm; **e** *Halgerda paulayi* sp. nov., holotype, CASIZ 192298, scale bar = 1 mm; **f** *Halgerda labyrinthus* sp. nov., paratype, CASIZ 160949, scale bar = 0.25 mm; **g** *Halgerda anosy* sp. nov., holotype, CASIZ 194054, scale bar = 1 mm. Abbreviations: bb, buccal bulb; ot, oral tube; ra, radular sac

Halgerda mango Donohoo & Gosliner sp. nov.
https://zoobank.org/B34FCF5A-5165-4F1C-99E5-6C7BD089BFC5
(Figs. 3d, f, 5a, 6 and 7a)

Halgerda sp. 2 Gosliner et al. (2018): 105, bottom right photograph. *Halgerda* sp. 3 Gosliner et al. (2018): 106, top left photograph.

Material examined: Holotype: One Specimen, NMP 041323, formerly CASIZ 181264, dissected and sequenced, 20 mm preserved, type locality: Devil's Point (13° 39′ 3.31″ N 120° 50′ 28.03″ E), Maricaban Island, Batangas Province, Luzon, Philippines, 24 May 2009, collected by Peri Paleracio. Other material examined: One juvenile specimen, CASIZ 204808, dissected and sequenced, 7 mm preserved, locality: Puerto Galera (13° 31′ 30.4″ N 120° 56′ 47.1″ E), Oriental Mindoro Province, Mindoro, Philippines, 6–23 m depth, 16 April 2015, collected by P.J. Aristorenas. One juvenile specimen, CASIZ 217210, dissected and sequenced, 15 mm preserved, locality: Sepok Wall (13° 41′ 24.0″ N 120° 49′ 48.0″ E), Maricaban Island, Batangas Province, Luzon, Philippines, 6–23 m depth, 15 April 2016, collected by Peri Paleracio.

Type locality: Devil's Point, Maricaban Island, Batangas Province, Luzon, Philippines

Etymology: This species is named mango after the similar vibrant yellow-orange coloration found in the Carabao or Philippine mango, a glorious treat that has sustained many expeditions to the Philippines.

External morphology (Fig. 3d–f): Adult preserved animals approximately 20 mm in length (Fig. 3f). Body oval, rigid, and gelatinous. Dorsum color uniform lemon yellow with minute, light brown flecking across entire mantle. Ridging arranged in reticulated pattern with highly elevated tips at ridge junctions. Thin, semi-opaque white mantle band lines mantle edge. Mantle underside lemon yellow with occasional large brown spots. Gill surrounds elevated anus with six bipinnate sometimes tripinnate branchial leaves. Gill branches translucent white with light brown dorsal lining. Opaque white glands within pinnate portions of gill rachis. Gill pocket smooth with similar dorsum coloration. Rhinophores tapered and perfoliate with 16 lamellae. Rhinophoral sheath and lamellae translucent white with diffused brown subapical pigment and posterior near base splotches. Foot is broad, anteriorly notched, lemon yellow with occasional medium dark brown spots. Oral tentacles digitiform.

Juvenile coloration varies with size. In small juvenile CASIZ 204808 dorsum color uniform orange with small to large, random black spots (Fig. 3d). Ridging and ridge tips less pronounced with occasional white coloration. Thin, semi-opaque white mantle band similar to adult. Mantle underside similar to dorsum coloration with ring of small to large brown and dark brown spots. Gill branches translucent white with dark brown lining. Fewer opaque

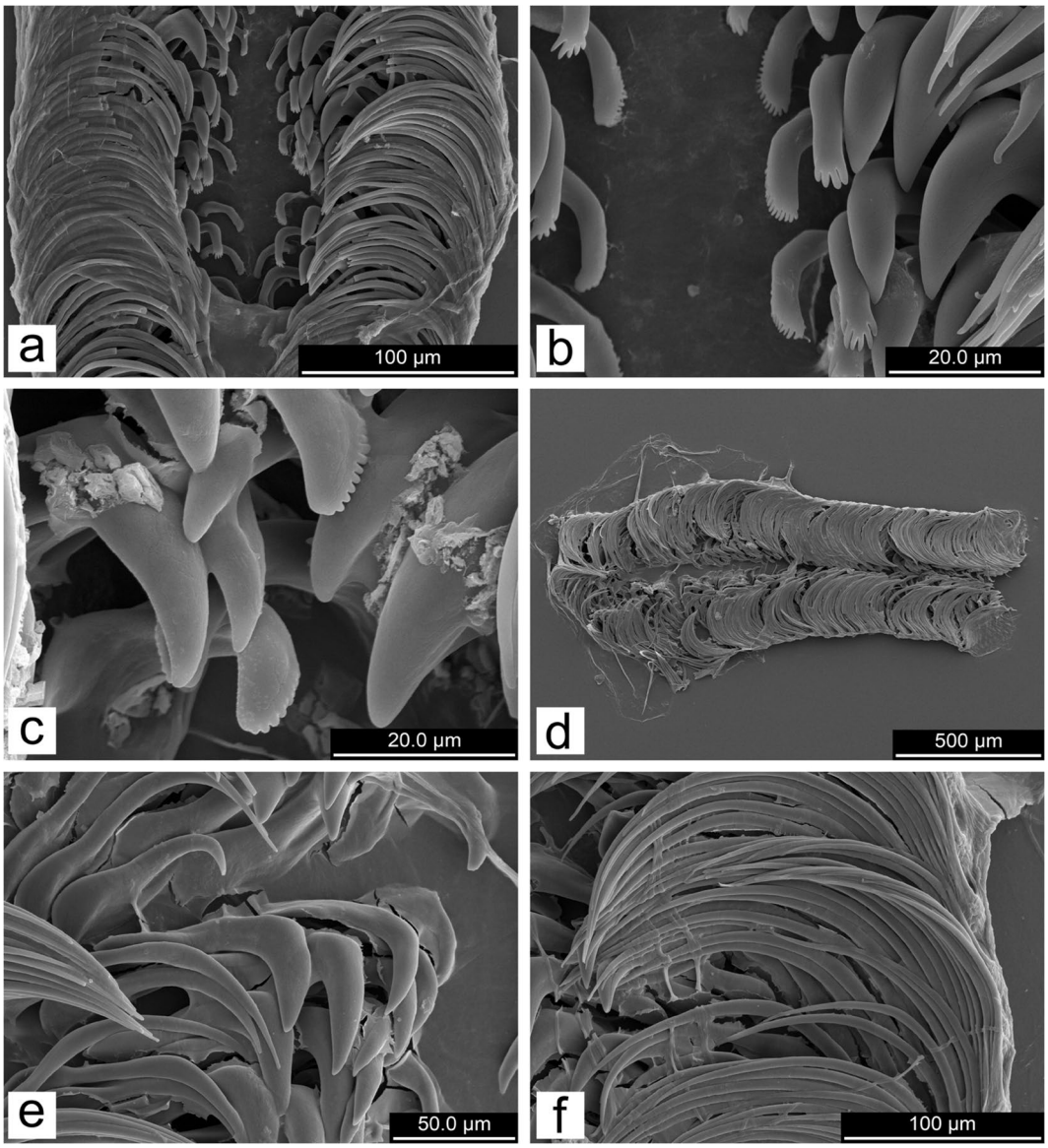

Fig. 6 *Halgerda mango* sp. nov., scanning electron micrographs of radula: **a**–**b** juvenile, CASIZ 204808, radula half row; **b** inner lateral teeth; **c** juvenile, CASIZ 217,210, inner lateral teeth; **d**–**f** holotype, adult, NMP 041323; **d** entire radula; **e** inner and mid-lateral teeth; **f** outer teeth

white glands within gill rachis. Gill pocket smooth with similar dorsum coloration. Rhinophores tapered and perfoliate with 12 lamellae. Rhinophoral sheath and lamellae translucent white with dark brown subapical and posterior near base splotches. Foot is broad, anteriorly notched, orange with ring of small dark brown/black spots. Oral tentacles digitiform. In a larger juvenile CASIZ 217210 dorsum color uniform pale yellow with random diffused brown spots (Fig. 3e). Ridging and ridge tips more pronounced with less white coloration. Thin, semi-opaque white mantle band less pronounced. Mantle underside pale yellow with ring of large dark brown spots. Gill branches translucent white with brown lining. More opaque white glands present within gill rachis. Rhinophores tapered and perfoliate with 14 lamellae. Rhinophoral sheath and lamellae translucent white with more diffused dark brown subapical pigment and posterior near base splotches. Foot is broad, anteriorly notched, pale yellow with ring of small dark brown/black spots. Oral tentacles digitiform.

Internal anatomy (Figs. 5a, 6a–f and 7a): Buccal mass (Fig. 5a) unpigmented. Buccal bulb similar in size to oral tube. Radular sac elongate and wedge shaped. Labial cuticle smooth. Radula composed of both smooth hamate and extremely elongate teeth (Fig. 6c). Radular formula 42 × 16.0.16 in the holotype NMP 041323, 34 × 15.0.15 in young juvenile CASIZ 204808, and 34 × 23.0.23 in older juvenile CASIZ 217210. In NMP 041323 inner three lateral teeth and two to three middle lateral teeth (Fig. 6d)

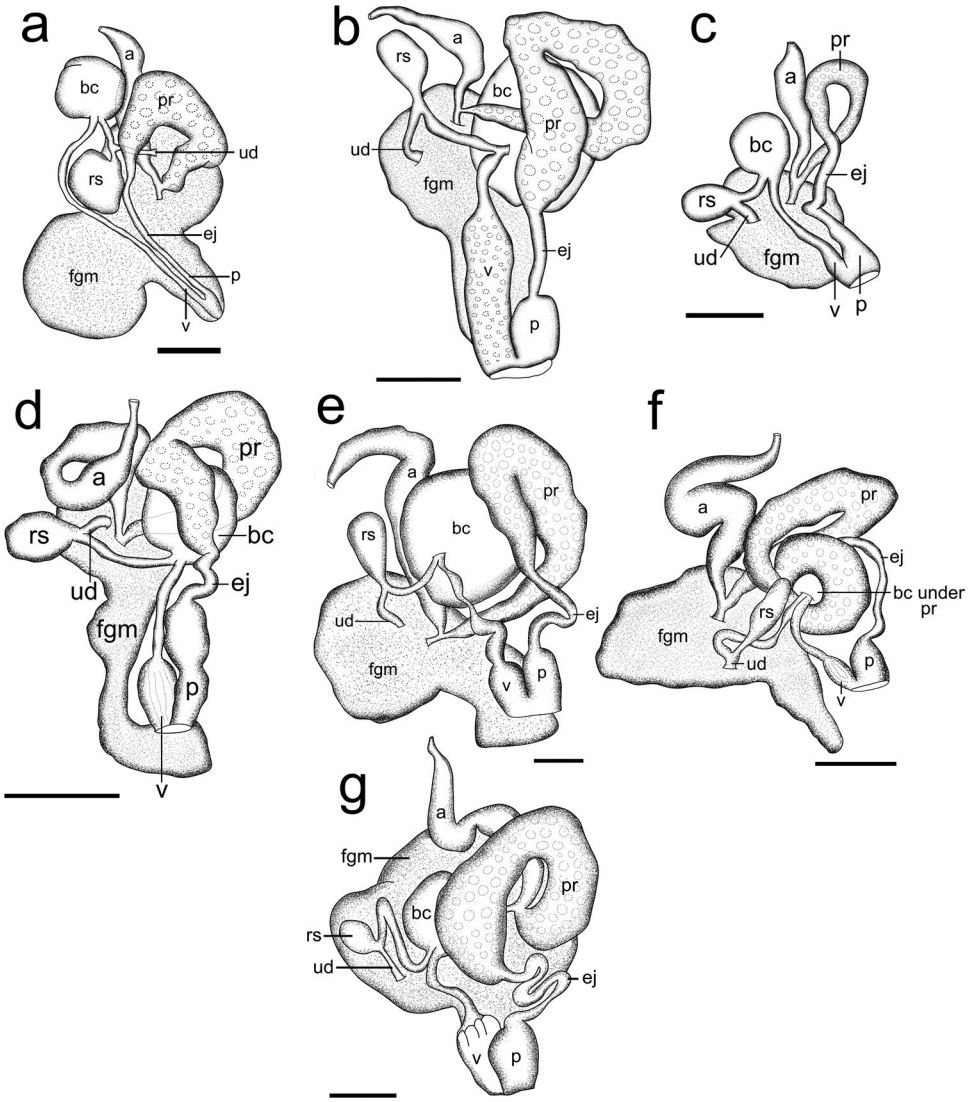

Fig. 7 Reproductive systems: **a** *Halgerda mango* sp. nov., holotype, NMP 041323, scale bar = 0.5 mm; **b** *Halgerda berberiani* sp. nov., holotype, UF 456643, scale bar = 1 mm; **c** *Halgerda biqiea* sp. nov., holotype, UF 455832, scale bar = 0.5 mm; **d** *Halgerda willeyi* Eliot, 1904, CASIZ 083676A, scale bar = 1 mm; **e** *Halgerda paulayi* sp. nov., holotype, CASIZ 192298, scale bar = 1 mm; **f** *Halgerda labyrinthus* sp. nov., paratype, CASIZ 160949, scale bar = 2 cm; **g** *Halgerda anosy* sp. nov., holotype, CASIZ 194054, scale bar = 0.5 mm. Abbreviations: a, ampulla; bc, bursa copulatrix; ej, ejaculatory duct; fgm, female gland mass; p, penis; pr, prostate; rs, receptaculum seminis; ud, uterine duct; v, vagina

hamate, broad based, slightly curved, with thick rounded cusps. Innermost tooth has approximately 12 greatly reduced denticles. Outer lateral teeth (Fig. 6e) thin, extremely elongate, with fine tips. Some outer teeth are broken and stacked together making counting difficult. Outermost tooth reduced version of outer laterals. Juvenile radulae vary from adults in outer lateral curvature (Fig. 6f) and inner lateral denticulation (Fig. 6a, b). Juvenile inner teeth denticulation includes 12–16 elongate denticles (first inner tooth), 3–6 elongate or semi-reduced denticles (second inner tooth), and sometimes one reduced denticle on third inner tooth.

Reproductive system (Fig. 7a): NMP 041323. Triaulic. Thin preampullary duct widens into thick ampulla, then narrows into postampullary duct which splits into vas deferens and short oviduct. Vas deferens rapidly expands into wide, looped granular prostate, then narrows into long, thin ejaculatory portion and connecting thin penis. Penis shares common genital atrium with similarly sized vagina. Narrow, elongate vagina continues into thin, elongate duct and proximally enters rounded bursa copulatrix. Thin, short duct connects bursa to slightly smaller, semi-rounded receptaculum seminis. Thin, elongate uterine duct also connects near receptaculum base and enters medium-sized, irregularly shaped female gland mass.

Geographical distribution: Known from the Philippines.

Ecology: Found on shallow reefs between 5 and 15 m and on coral rubble around 20 m.

Remarks: Our molecular phylogeny shows that *Halgerda mango* sp. nov. is sister to the similarly patterned species *H. dalanghita* and species delimitation analyses reveal that smaller specimens (previously cited as *Halgerda* sp. 3, Gosliner et al. 2018) are *H. mango* sp. nov. juveniles. All four species delimitation analyses support *H. mango* sp. nov. as a distinct species from *H. dalanghita* and reveal a minimum divergence of 8.3% in the COI gene and intraspecific variation ranged from 0.8 to 1.5%

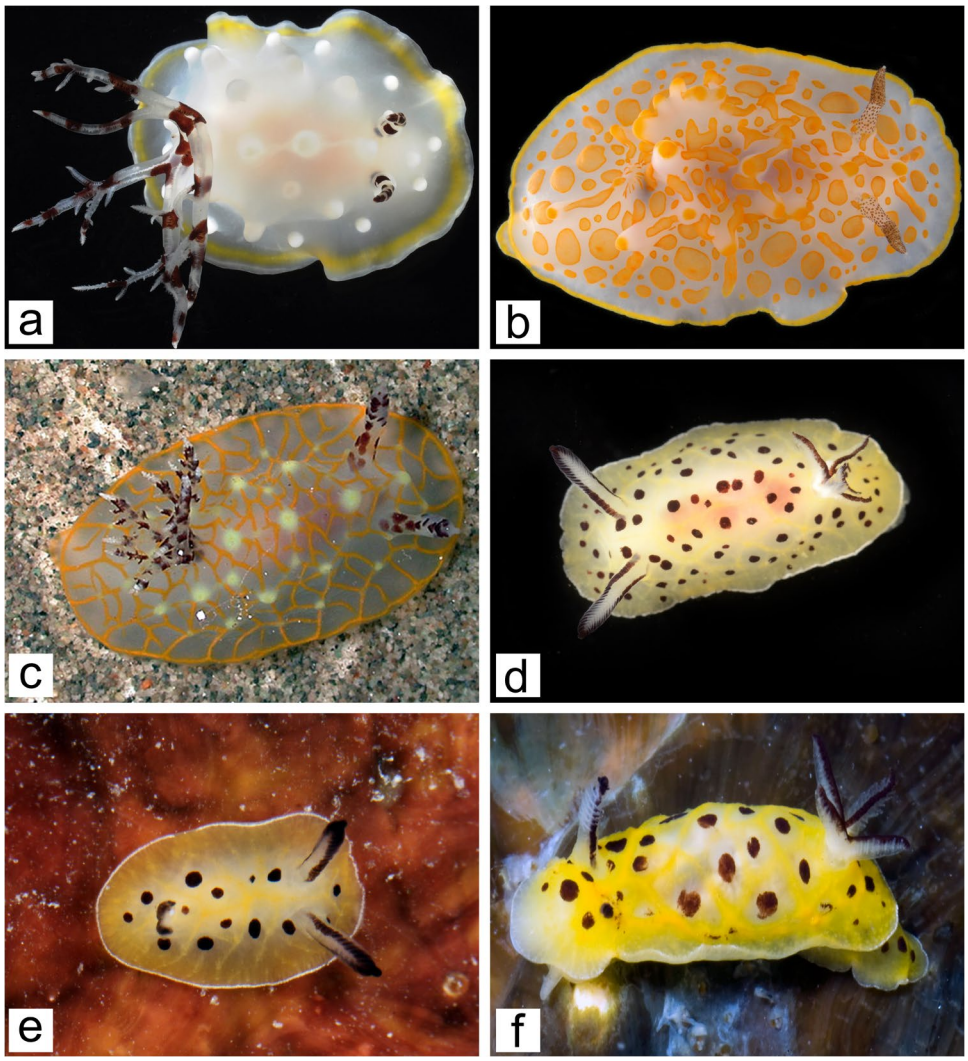

Fig. 8 Living specimens: **a** *Halgerda berberiani* sp. nov., holotype, UF 456643, Moorea, French Polynesia, photo by Richard Pyle; **b** *Halgerda aurantiomaculata* (Allan, 1932), UF 437371, Heron Island, Australia, photo by Florida Museum of Natural History; **c** *Halgerda terramtuentis* Bertsch & Johnson, 1982, CASIZ 171214, Maui, Hawaiian Islands, photo by Cory Pittman; **d**–**e** *Halgerda biqiea* sp. nov.; **d** holotype, UF 455832, Djibouti, photo by Gustav Paulay; **e** paratype, CASIZ 192299, Ablo Island, Saudi Arabia, photo by T.M. Gosliner; **f** *Halgerda brunneomaculata* Carlson & Hoff, 1993, UF 457854, Tahiti, French Polynesia, photo by Gustav Paulay

between the three *H. mango* sp. nov. specimens studied here. Morphologically, *H. mango* sp. nov. is similar to *H. dalanghita*, but both species exhibit noticeable differences in the external coloration of juvenile vs adult specimens. Therefore, morphological comparisons between adult *H. mango* sp. nov. and *H. dalanghita* and juvenile *H. mango* sp. nov. and *H. dalanghita* are made below.

Externally, adult *H. mango* sp. nov. have a uniform lemon-yellow coloration with minute, light brown flecking; pronounced ridging with elevated tips at the ridge junctions; six bipinnate (sometimes tripinnate) branchial leaves with a light brown dorsal stripe; and diffused brown subapical pigment along the rhinophores (Fig. 3f). In contrast, adult *H. dalanghita* are uniformly orange in coloration with white flecking across the mantle and less pronounced ridging which has minute brown flecking along the ridges and white spots at ridge junctions. The six branchial leaves are bipinnate with black/dark brown dorsal stripes and flecking along the rachises (Fahey and Gosliner 1999a, Fig. 4a; present study Fig. 3b, c). The rhinophores are similar to *H. mango* sp. nov.; however, the diffused pigment is darker and more prominent in *H. dalanghita*. Young juvenile *H. mango* sp. nov. are morphologically very similar to juvenile *H. dalanghita*, but there are external differences between the two species. In *H. mango* sp. nov., the numerous small to large spots are browner in coloration, and the dorsum ridging is less thick and more pronounced with elevated tips at the ridge junctions (Fig. 3d). In *H. dalanghita*, the spotting is darker and more black in coloration and the ridging thicker, more angled, and less pronounced with no elevated ridge junctions (Fig. 3a). Both species have bipinnate gills with dorsal stripes and rhinophores with dark pigment along the lamellae and splotches along the rhinophoral stalk, but in *H. mango* sp. nov., the dark pigment is noticeably lighter in color than that seen in *H. dalanghita*. The dorsum color in older juvenile *H. mango* sp. nov. is more yellow with the mantle spotting and rhinophore/gill pigment becoming lighter in color and more diffused (Fig. 3e).

Internally, both species have unpigmented buccal masses and similar patterns in the radular teeth including

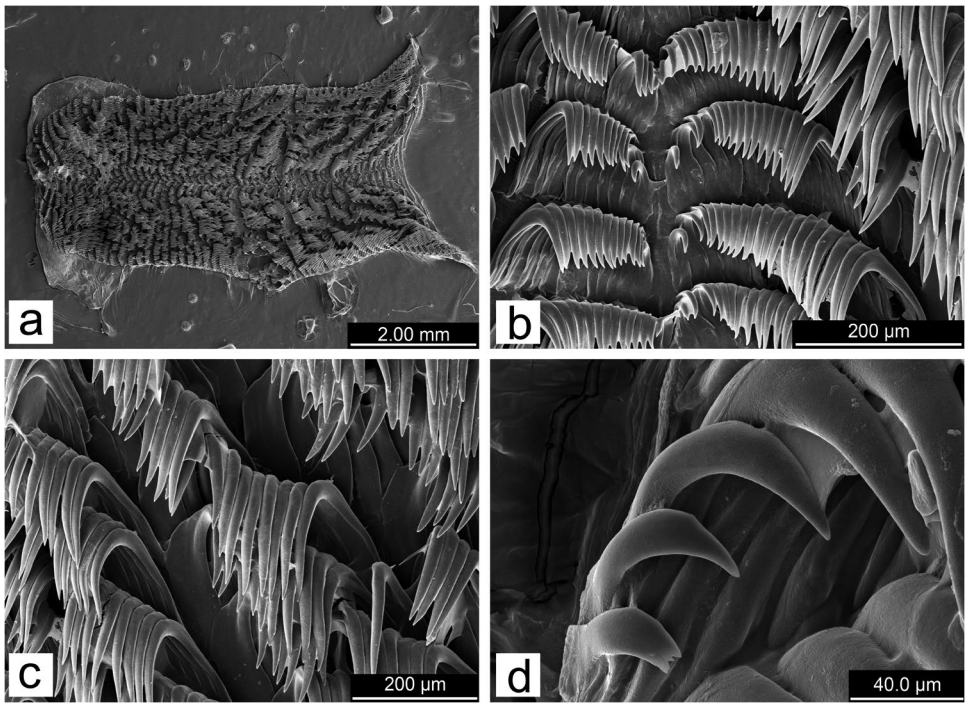

Fig. 9 *Halgerda berberiani* sp. nov., holotype, UF 456643, scanning electron micrographs of radula: **a** Entire radula; **b** inner lateral teeth; **c** mid-lateral teeth; **d** outer lateral teeth

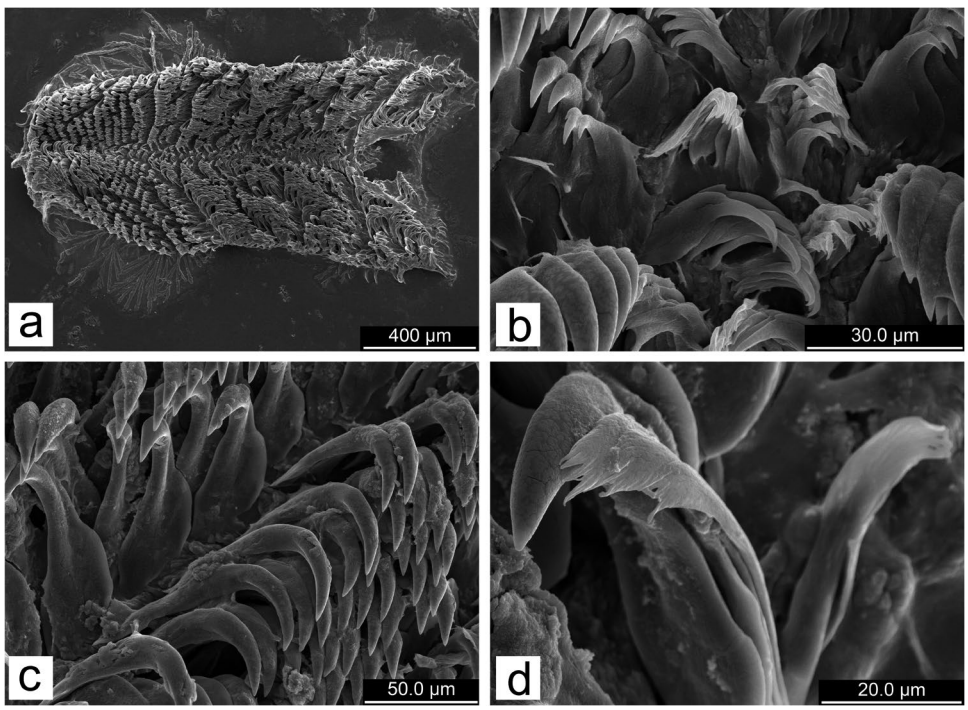

Fig. 10 *Halgerda biqiea* sp. nov., holotype, UF 455832, scanning electron micrographs of radula: **a** Entire radula; **b** inner lateral teeth; **c** mid-lateral teeth; **d** outer lateral teeth

denticulation in the inner laterals and thin, extremely elongate outer teeth with fine pointed tips. In adult *H. mango* sp. nov., there are fewer denticles (approximately 12) in the innermost tooth and a higher number of denticles (up to 16 and 6, respectively) in the first two inner teeth in *H. mango* sp. nov. juveniles. In contrast, there are more reduced denticles (approximately 14) present in the first lateral tooth of adult *H. dalanghita*, and the inner two lateral teeth of juvenile *H. dalanghita* have fewer denticles (12–13 and 3, respectively) along the first two inner teeth. The reproductive systems are also similar between the two species including a narrow, elongate vagina; narrow,

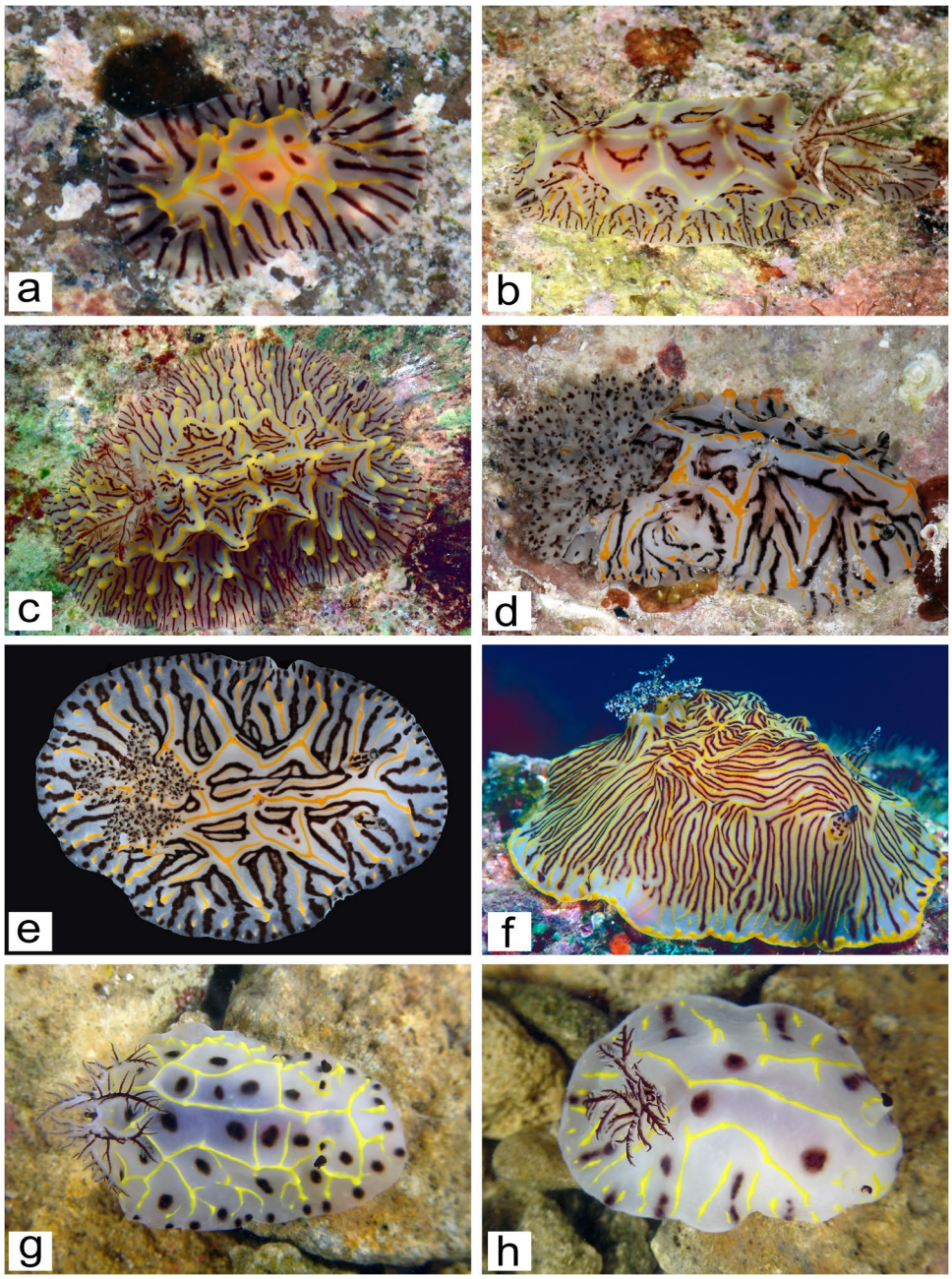

Fig. 11 Living specimens: **a–c** *Halgerda willeyi* Eliot, 1904; **a** CASIZ 201944, Maricaban Island, Philippines, photo by T.M. Gosliner; **b** CASIZ 204790, Verde Island, Philippines, photo by T.M. Gosliner; **c** CASIZ 083676A, Calumpan Peninsula, Philippines, photo T.M. Gosliner; **d–e** *Halgerda paulayi* sp. nov.; **d** holotype, CASIZ 192298, Ablo Island, Saudi Arabia, photo by T.M. Gosliner; **e** paratype, UF 476041, Jazirat Burcan, Saudi Arabia, photo by Gustav Paulay; **f** *Halgerda labyrinthus* sp. nov., holotype, CASIZ 070068, Okinawa, Japan, photo by R.F. Bolland; **g–h** *Halgerda anosy* sp. nov.; **g** holotype, CASIZ 194054, South Madagascar, photo by Marina Poddubetskaia; **h** CASIZ 194036, South Madagascar, photo by Marina Poddubetskaia

elongate penis and ejaculatory portion of the prostate; and thin elongate ducts between the vagina and the bursa copulatrix, the bursa and the receptaculum seminis, and an elongate uterine duct. Differences between the two species are minimal. The bursa copulatrix is twice the size of the receptaculum in *H. dalanghita*, and the preampullary duct abruptly expands into a thick ampulla, while in *H. mango* sp. nov., the bursa is only slightly larger than the receptaculum, and the preampullary duct gradually expands into a thick ampulla. The duct between the vagina and the bursa copulatrix is 1.5 × longer in *H. mango* sp. nov., and the ejaculatory portion of the prostate and the penis is an equal size to the vagina, rather than twice as thick as seen in *H. dalanghita*. Despite the similarities in adult and juvenile specimens of *H. mango* sp. nov. and *H. dalanghita*, there are external and some internal morphological differences and a strong genetic divergence between these two species.

Halgerda berberiani Donohoo & Gosliner sp. nov.
https://zoobank.org/E505E6C2-240E-43ED-94D4-C9EE04A4B517
(Fig. 5b, 7b, 8a and 9)

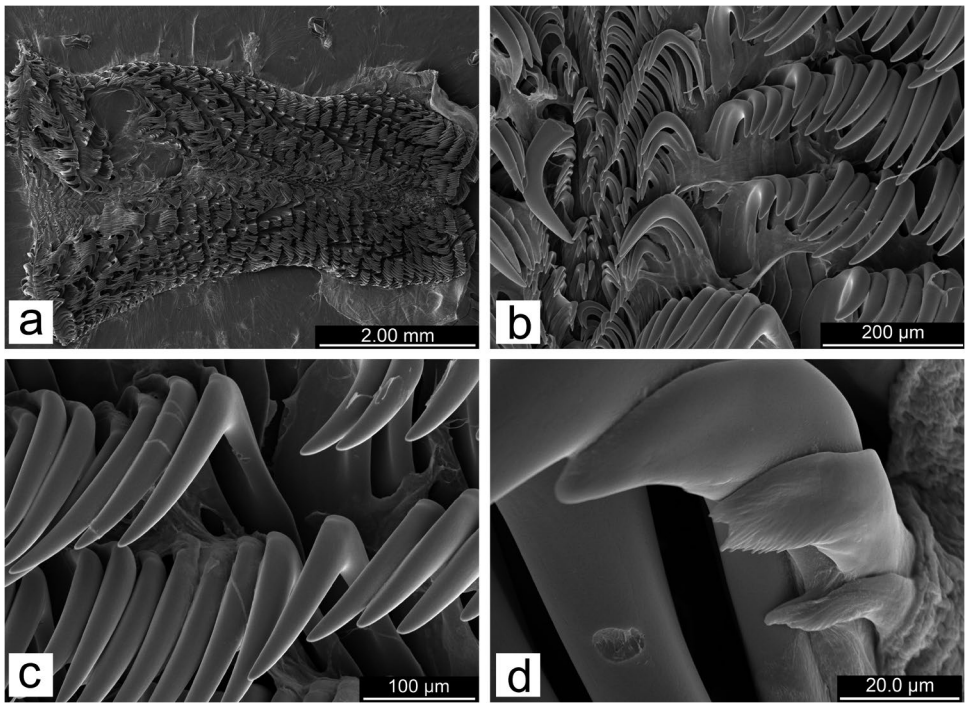

Fig. 12 *Halgerda willeyi* Eliot, 1904, CASIZ 083676A, scanning electron micrographs of radula: **a** Entire radula; **b** inner lateral teeth; **c** mid-lateral teeth; **d** outer lateral teeth

Halgerda sp. 1 Gosliner et al. (2015): 185, top right photograph. *Halgerda* sp. 5 Gosliner et al. (2018): 106, middle right photograph.

Material examined: Holotype: One specimen, UF 456643, dissected, 35 mm preserved, type locality: Moorea (17° 30′ 15.8″ S 149° 45′ 30.3″ W), Moorea Island, Society Islands, French Polynesia, 100 m depth, 04 February 2012, collected by John Earle, David Pence, Richard Pyle, and Rob Whitton. Paratype: One specimen, MNHN-IM-2000-27156, 34 mm preserved, locality: Tahiti (17° 46′ 52″ S 149° 24′ 4″ W), Tahiti Island, Society Islands, French Polynesia, 13 April 2013, collected by Alexander Fedosov.

Type locality: Moorea, Moorea Island, Society Islands, French Polynesia.

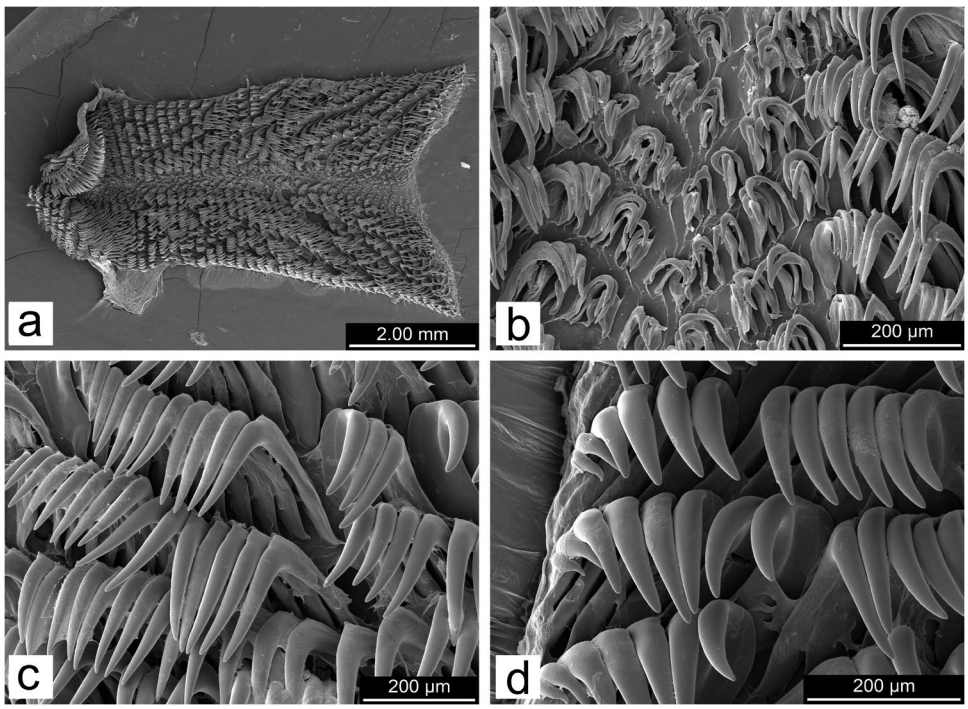

Fig. 13 *Halgerda paulayi* sp. nov., holotype, CASIZ 192298, scanning electron micrographs of radula: **a** Entire radula; **b** inner lateral teeth; **c** mid-lateral teeth; **d** outer lateral teeth

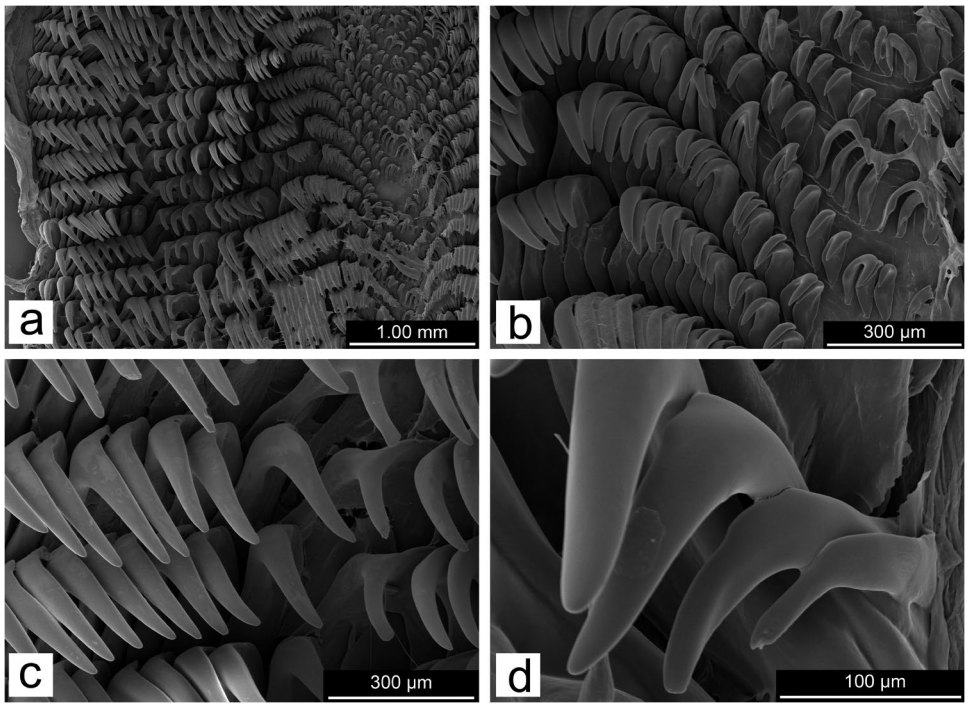

Fig. 14 *Halgerda labyrinthus* sp. nov., paratype, CASIZ 160949, scanning electron micrographs of radula: **a** Radula half row; **b** inner lateral teeth; **c** mid-lateral teeth; **d** outer lateral teeth

Etymology: This species is named in honor of Anthony Berberian who first photographed *Halgerda berberiani* in French Polynesia.

External morphology (Fig. 8a): Preserved animals 35 mm in length (Fig. 8a). Body oval, semi-rigid, and gelatinous. Living animal with dorsum color grayish white with large rounded opaque white tubercles. Viscera with yellow tint visible through mantle. Wide yellow submarginal mantle band offset from thin, semi-opaque white submarginal mantle band. Mantle underside grayish white. Gill surrounds elevated anus with four unipinnate branchial leaves. Gill branches translucent white with large reddish/dark brown semi-translucent spots. Opaque white glands visible in gill branches. Gill pocket smooth with similar dorsum coloration. Rhinophores tapered, perfoliate with similar

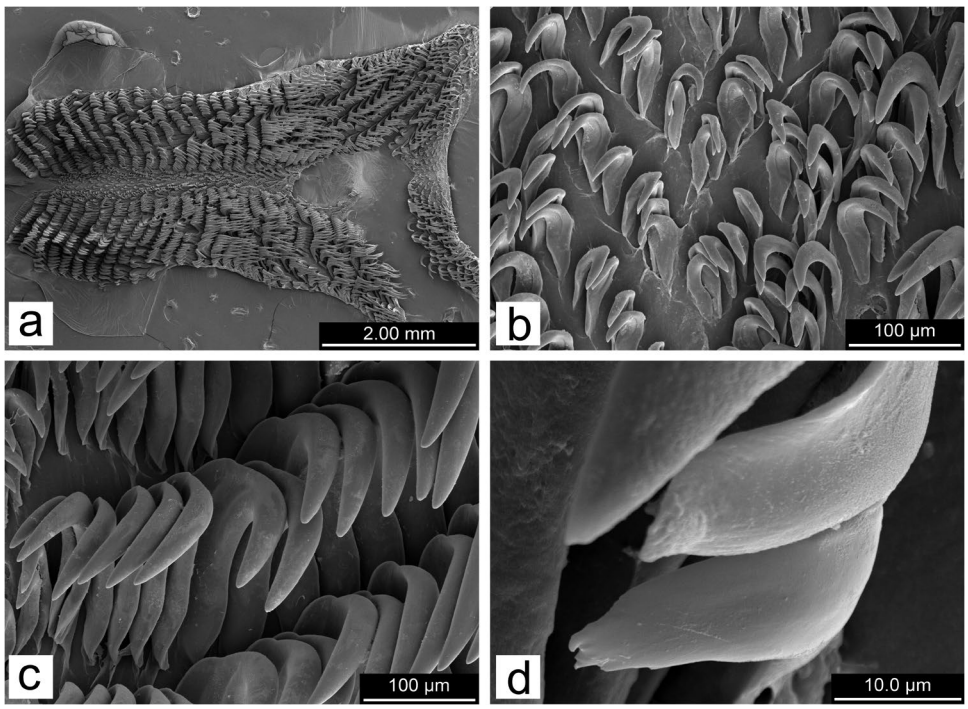

Fig. 15 *Halgerda anosy* sp. nov., paratype, CASIZ 194616B, scanning electron micrographs of radula: **a** Entire radula; **b** inner lateral teeth; **c** mid-lateral teeth; **d** outer lateral teeth

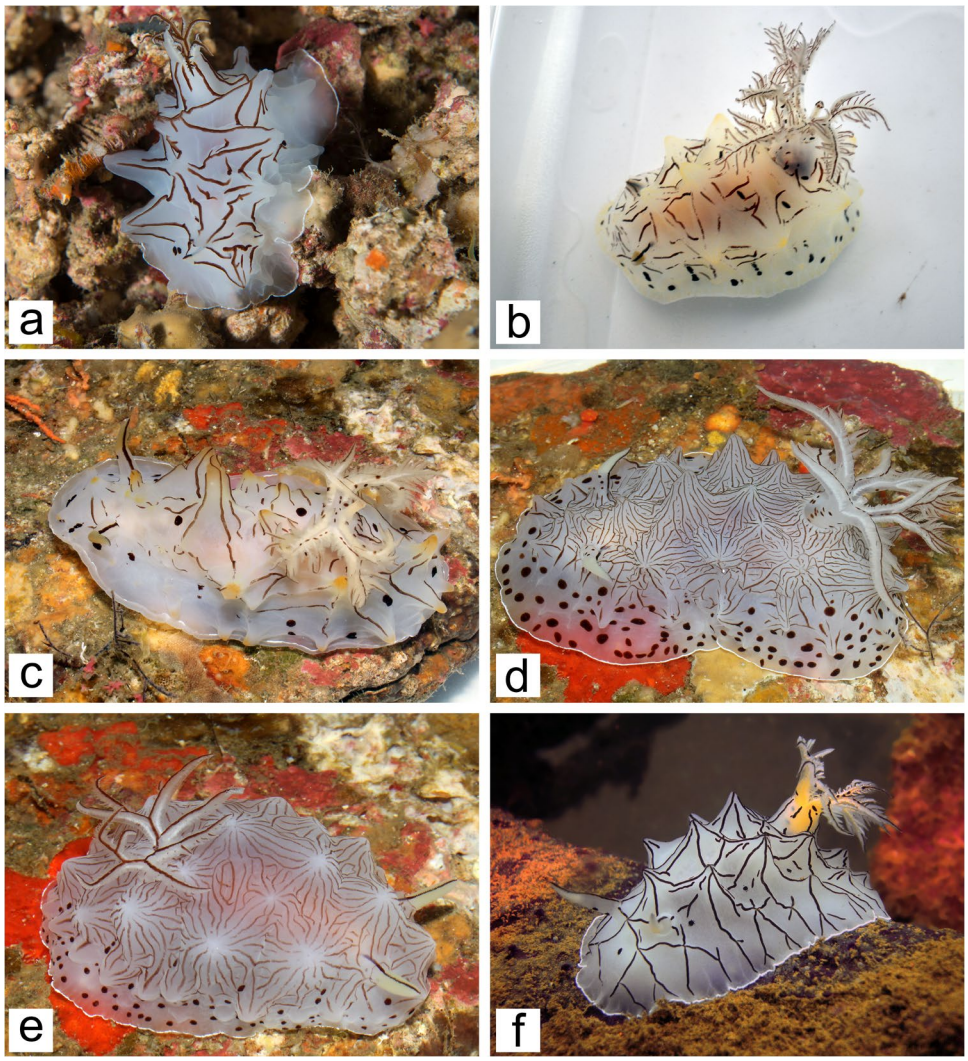

Fig. 16 Living specimens:. **a** *Halgerda mesophotica* sp. nov., holotype, NMP 041324, Balayan Bay, Philippines, photo by Terry Gosliner; **b** *Halgerda profunda* sp. nov., holotype, NMP 041325, Lubang Islands, Philippines, photo by Terry Gosliner; **c** *Halgerda takipsilim* sp. nov., holotype, NMP 041327, Verde Island, Philippines, photo by Terry Gosliner; **d**–**e** *Halgerda scripta* sp. nov.; **d** holotype, NMP 041326, Verde Island, Philippines, photo by Terry Gosliner; **e** paratype, CASIZ 204787, Verde Island, Philippines, photo by Terry Gosliner; **f** *Halgerda hervei* sp. nov., holotype, CASIZ 186494, New Caledonia Lagoon, New Caledonia, photo by Jean-François Hervé

gill coloration and 29 lamellae. Rhinophoral sheath and base similar to mantle coloration. Foot is broad, anteriorly notched, and grayish white. Oral tentacles digitiform and short.

Internal anatomy (Figs. 5b, 7b and 9a–d): Buccal mass (Fig. 5b) unpigmented; however, small light brown spots present around buccal opening. Oral tube elongated, narrowed anteriorly and approximately 1.5 × longer than buccal bulb. Radular sac elongate and folded over buccal bulb. Labial cuticle smooth. Radula composed of smooth hamate teeth (Fig. 9a). Radular formula 53 × 54.0.54 in the holotype UF 456643. First three inner lateral teeth small, broad based, with a slightly curved cusp. Inner lateral teeth (Fig. 9b) 4–15 gradually increase in size with a more elongate cusp and form a shallow V in the radula center. Middle lateral teeth (Fig. 9c) larger and more elongate than inner laterals. Outer lateral teeth (Fig. 9d) similar to middle laterals with shorter, rounded cusps. Outermost tooth paddle-shaped and semi-fimbriate with four small denticles.

Reproductive system (Fig. 7b): Triaulic. Thin, elongate preampullary duct widens into ampulla, then narrows into postampullary duct which splits into short, thin vas deferens and short, thin oviduct. Vas deferens thick, expands into wide, elongate, looped granular prostate, then quickly narrows into thin ejaculatory portion. Ejaculatory portion rapidly expands into short, wide penis which shares common genital atrium with vagina. Wide, elongate, nodular vagina narrows into thinner semi-elongate duct and proximally enters into large, rounded bursa copulatrix partially covered by granular prostate. Semi-elongate duct connects bursa to smaller, pyriform receptaculum seminis. Thin, elongate uterine duct also connects near receptaculum base and enters into medium-sized, pyriform-shaped female gland mass.

Geographical distribution: Known from Moorea and Tahiti, French Polynesia.

Ecology: Found on reef slopes at approximately 10–100 m.

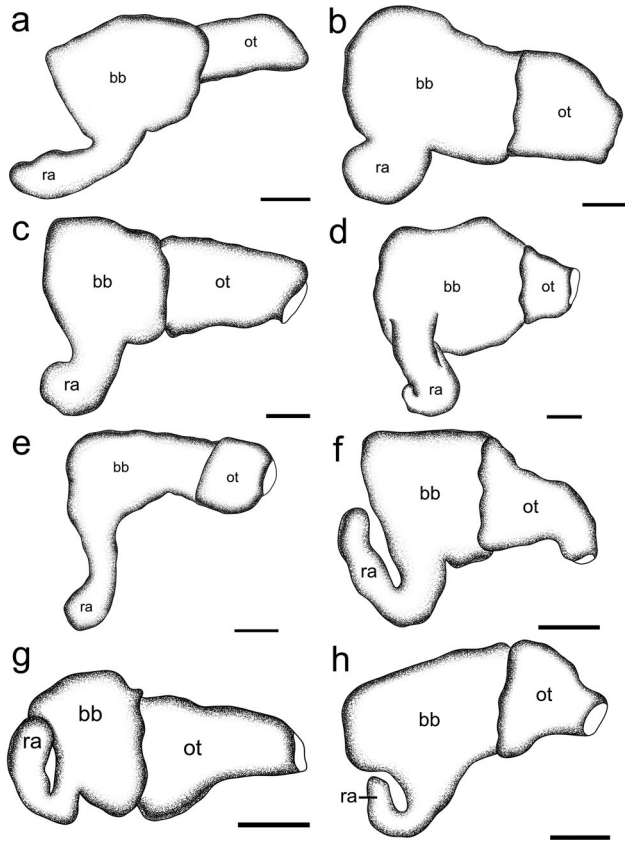

Fig. 17 Buccal masses: **a** *Halgerda mesophotica* sp. nov., holotype, NMP 041324, scale bar = 1 mm; **b** *Halgerda profunda* sp. nov., holotype, NMP 041325, scale bar = 1 mm; **c** *Halgerda takipsilim* sp. nov., holotype, NMP 041327, scale bar = 1 mm; **d** *Halgerda scripta* sp. nov., holotype, NMP 041326, scale bar = 1 mm; **e** *Halgerda hervei* sp. nov., holotype, CASIZ 186494, scale bar = 1 mm; **f** *Halgerda maaikeae* sp. nov., holotype, SAMC-A094639, scale bar = 1 mm; **g** *Halgerda pattiae* sp. nov., holotype, UF 422800, scale bar = 0.5 mm; **h** *Halgerda radamaensis* sp. nov., holotype, CASIZ 173456, scale bar = 0.5 mm. Abbreviations: bb, buccal bulb; ot, oral tube; ra, radular sac

Remarks: Molecular sequencing of the holotype of *Halgerda berberiani* sp. nov. (UF 456643) was unsuccessful for all genes studied; however, the morphological characteristics are distinct enough to distinguish *H. berberiani* sp. nov. as a new species within *Halgerda*. *Halgerda berberiani* sp. nov. is morphologically similar to *H. aurantiomaculata* (Fig. 8b) and *H. terramtuentis* (Fig. 8c), and morphological comparisons between the three are made below. Externally, the dorsum coloration of *H. berberiani* sp. nov. is a grayish white with large opaque white tubercles, an offset wide yellow mantle band, and a thin semi-opaque white mantle band, whereas *H. aurantiomaculata* is an opaque white color with numerous orange spots, and a single wide yellow mantle band (Willan and Brodie 1989, Figs. 1 and 2) and *H. terramtuentis* is translucent cream with white tipped tubercles, a network of orange lines, and an orange mantle band (Kay and Young 1969, Fig. 30; Bertsch and Johnson 1982, Fig. 15). The gill and rhinophore coloration vary slightly by species. In *H. berberiani* sp. nov., the gill and rhinophore spots are large with a reddish/dark brown coloration, while in *H. terramtuentis* the spots are smaller, more numerous, and black and in *H. aurantiomaculata* the brown/black spots are tiny and numerous.

The radular teeth in *H. berberiani* sp. nov. are similar to all *Halgerda*; however, the inner lateral teeth form a shallow V in the radula center, and the first three inner lateral teeth are small with a slightly curved cusp before increasing in size and developing more elongated cusps. The outermost tooth is also paddle-shaped and semi-fimbriate. Similarly, the first few inner lateral teeth in *H. aurantiomaculata* are smaller and less curved than the following inner teeth; however, the outermost tooth is reduced with an apical cleft (Willan and Brodie 1989, Figs. 25–32). In *H. terramtuentis* the radular teeth increase in length in the middle of each half-row, before decreasing to nearly "scythe-like" blades in the outermost teeth (Kay and Young 1969, as *H.* sp. cf. *graphica*, Fig. 28b; Bertsch and Johnson 1982, Fig. 16). The reproductive system also varies as *H. berberiani* sp. nov. has a large, rounded bursa copulatrix, a wide elongated nodular vagina, an elongated uterine duct, and a semi-elongated duct connecting the bursa copulatrix to the receptaculum seminis. In contrast, both *H. aurantiomaculata* and *H. terramtuentis* have a large, rounded bursa copulatrix ensheathed in the glandular portion of the prostate, a rounded glandular portion at the base of the duct connecting the vagina to the bursa copulatrix, a short uterine duct, and a much more elongated duct connecting the bursa copulatrix to the receptaculum seminis (Willan and Brodie 1989, Figs. 6, 7 and 8; Kay and Young 1969, Fig. 28a; respectively). Based on the unique internal and external characteristics including dorsum coloration and style of tubercles, *H. berberiani* sp. nov. is a distinct species within *Halgerda* despite the lack of molecular data for the species.

Halgerda biqiea Donohoo & Gosliner sp. nov.
https://zoobank.org/E2213338-54D8-4C78-B1E6-55983D95A9CC
(Fig. 5c, 7c, 8d, e and 10).

Halgerda brunneomaculata (misidentification) in: Gosliner et al. (2015): 185, bottom left photograph; Gosliner et al. (2018): 107, top left photograph.

Material examined: Holotype: One specimen, UF 455832, dissected and sequenced, 10 mm preserved, type locality: Gulf of Tadjoura (11° 33′ 44.2″ N 42° 41′ 51.3″ E), Djibouti, 15–20 m depth, 1 October 2012, collected by Gustav Paulay. Paratype: One specimen, CASIZ 192299, dissected and sequenced, 4 mm preserved, locality: Ablo Island Reef (18° 39′ 34.1″ N 40° 49′ 37.3″ E), Red Sea, Saudi Arabia, 05 March 2013, collected by Sancia E.T. van der Meij.

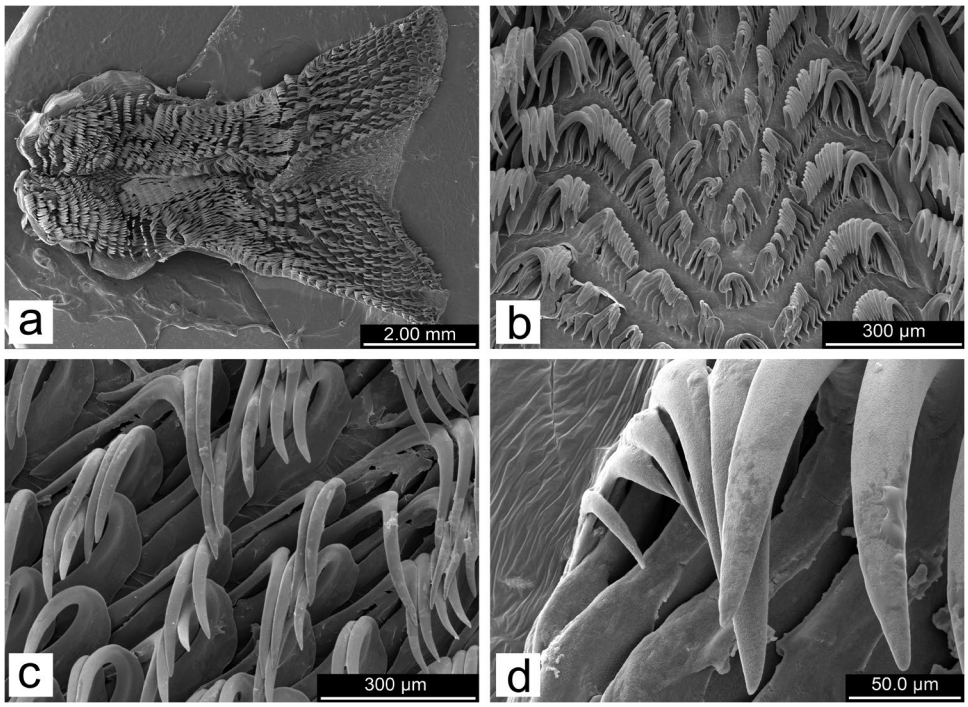

Fig. 18 *Halgerda mesophotica* sp. nov., holotype, NMP 041324, scanning electron micrographs of radula: **a** Entire radula; **b** inner lateral teeth; **c** mid-lateral teeth; **d** outer lateral teeth

Type locality: Gulf of Tadjoura, Djibouti

Etymology: This species is named "biqiea" after the Arabic word for spot and refers to the numerous small brown spots along the dorsal side of the mantle.

External morphology (Fig. 8d, e): Preserved animals 4–10 mm in length. Body elongate oval, rigid, and gelatinous. Dorsum color translucent pale yellow with numerous small to medium dark brown/black spots (Fig. 8d). Smaller specimens have fewer dark spots (Fig. 8e). Light yellow low ridging arranged in irregular pattern with slightly higher peaks and no tubercles. Viscera coloration visible through mantle in larger specimens. Thin, opaque white mantle band surrounds mantle edge. Mantle underside translucent pale yellow with ring of small to large dark brown/black spots. Gill surrounds elevated anus with four unipinnate branchial leaves. Gill coloration translucent white with dorsal dark brown stripe. Gill pocket smooth with similar dorsum coloration. Opaque white glands visible in gill branches. Rhinophores elongate, perfoliate, with similar dorsum coloration, dark brown /black lateral stripes, a rounded conical tip, and 10–12 lamellae. Rhinophoral sheath smooth with similar dorsum coloration. Foot broad, anteriorly notched, and pale yellow with numerous small to large dark brown/black spots. Oral tentacles digitiform.

Internal anatomy (Figs. 5c, 7c and 10a–d): Buccal mass (Fig. 5c) pigmented on oral tube with large single black spot and small dark brown/black spots present around buccal opening. Oral tube semi-elongate and approximately 1.5 × longer than buccal bulb. Radular sac short and unpigmented. Labial cuticle smooth. Radula composed of predominantly smooth hamate teeth (Fig. 10a). Radular formula 43 × 30.0.30 in the holotype UF 455832. Inner eight lateral teeth (Fig. 10b) small, broad based, with quickly tapered, slightly curved, cusp with single, large pectinate denticle along the outer edge and form a shallow V in the center. Middle lateral teeth (Fig. 10c) large, hamate with thicker, rounded cusps. Outer lateral teeth (Fig. 10d) similar to middle laterals with shorter, less curved cusps. Five outermost teeth reduced and fimbriate.

Reproductive system (Fig. 7c): Triaulic. Thin preampullary duct widens into thick ampulla, then narrows into elongate postampullary duct which splits into vas deferens and short oviduct. Vas deferens gradually thickens into elongate, looped granular prostate, which slightly narrows distally into thick, elongate ejaculatory portion. Ejaculatory portion expands into slightly wide penis which shares common genital atrium with smaller vagina. Semi-wide vagina gradually narrows proximally into thin, elongate duct and enters rounded bursa copulatrix. Short duct connects bursa to smaller, pyriform receptaculum seminis. Short uterine duct also connects near receptaculum base and enters small irregularly rounded female gland mass.

Geographical distribution: Known from the Gulf of Tadjoura, Djibouti and the Saudi Arabian Red Sea.

Ecology: Found on shallow patch reefs between 15 and 20 m.

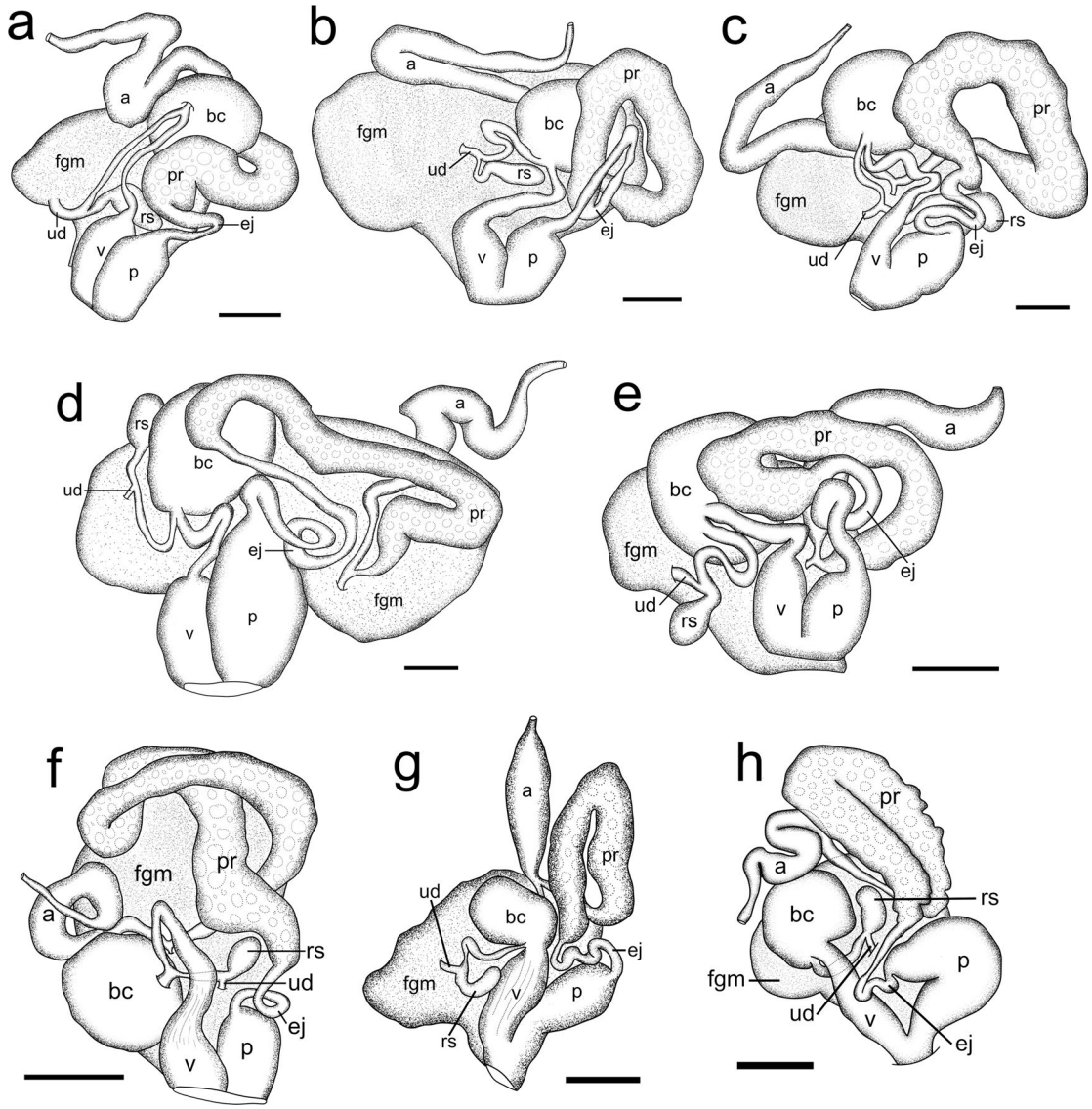

Fig. 19 Reproductive systems: **a** *Halgerda mesophotica* sp. nov., holotype, NMP 041324, scale bar = 0.5 mm; **b** *Halgerda profunda* sp. nov., holotype, NMP 041325, scale bar = 1 mm; **c** *Halgerda takipsilim* sp. nov., holotype, NMP 041327, scale bar = 1 mm; **d** *Halgerda scripta* sp. nov., holotype, NMP 041326, scale bar = 1 mm; **e** *Halgerda hervei* sp. nov., holotype, CASIZ 186494, scale bar = 1 mm; **f** *Halgerda maaikeae* sp. nov., holotype, SAMC-A094639, scale bar = 1 mm; **g** *Halgerda pattiae* sp. nov., holotype, UF 422800, scale bar = 0.5 mm; **h** *Halgerda radamaensis* sp. nov., holotype, CASIZ 173456, scale bar = 0.5 mm. Abbreviations: a, ampulla; bc, bursa copulatrix; ej, ejaculatory duct; fgm, female gland mass; p, penis; pr, prostate; rs, receptaculum seminis; ud, uterine duct; v, vagina

Remarks: Our molecular phylogeny shows that *Halgerda biqiea* sp. nov. from the Red Sea is sister to the similarly colored Indo-Pacific species *H. brunneomaculata* (Fig. 8f) and part of a well-supported clade that also includes *H. albocristata* and *H. toliara*. Both of the ABGD analyses and the COI ASAP, the bPTP and the GYMC analyses within the clade support *H. biqiea* sp. nov. as a distinct species. There is a minimum COI divergence of 7.1% between *H. biqiea* sp. nov. and *H. brunneomaculata*, as well as a minimum divergence of 11.8% between *H. biqiea* sp. nov. and *H. albocristata* and 11.6% between *H. biqiea* sp. nov. and *H. toliara*. There was no intraspecific variation within the COI gene in *H. biqiea* sp. nov. specimens collected in the Gulf of Tadjoura, Djibouti (UF 455832), and on Ablo Island Reef, Red Sea, Saudi Arabia (CASIZ 192299). Morphologically, *H. biqiea* sp. nov. is similar to *H. brunneomaculata*; however, there are some noticeable differences. Externally, the dorsum coloration of *H. biqiea* sp. nov. is translucent pale yellow with numerous small to medium dark brown/black spots, pale yellow ridging, a ring of dark brown/black spots on the mantle underside, and a foot with numerous dark brown/black spots. In contrast,

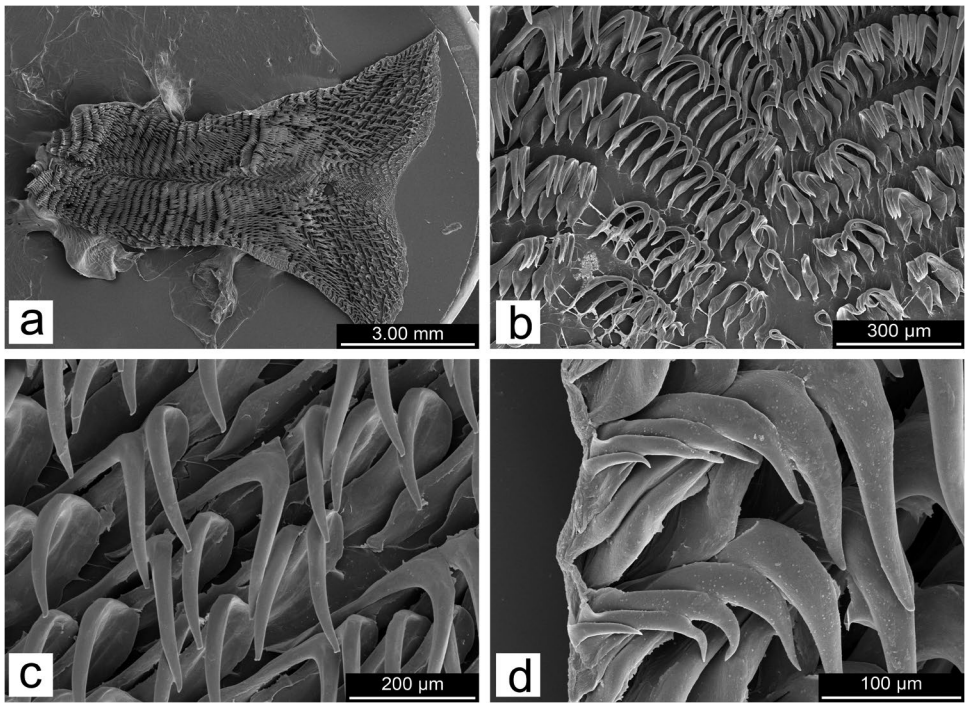

Fig. 20 *Halgerda profunda* sp. nov., holotype, NMP 041325, scanning electron micrographs of radula: **a** Entire radula; **b** inner lateral teeth; **c** mid-lateral teeth; **d** outer lateral teeth

H. brunneomaculata is translucent pale yellow with fewer large, brown spots, more vibrant yellow ridging, no spotting along the underside of the mantle, and only a handful of large brown spots on the foot which extends past the mantle (Carlson and Hoff 1993, Figs. 16, 17 and 18).

Internally, the radular teeth of *H. biqiea* sp. nov. are similar to *H. brunneomaculata* including the reduced, fimbriate five outermost teeth (Carlson and Hoff 1993, Fig. 20); however, the innermost eight teeth in *H. biqiea* sp. nov. are distinct. In *H. brunneomaculata* the innermost small tooth has a large, pectinate denticle along the inner edge (Carlson and Hoff 1993, Fig. 19), whereas in *H. biqiea* sp. nov., the innermost eight teeth each have a bulbous base with an abruptly tapered semi-curved cusp and a single, large pectinate denticle along the outer edge. Fahey and Gosliner (2000) noted that the buccal mass in *H. brunneomaculata*

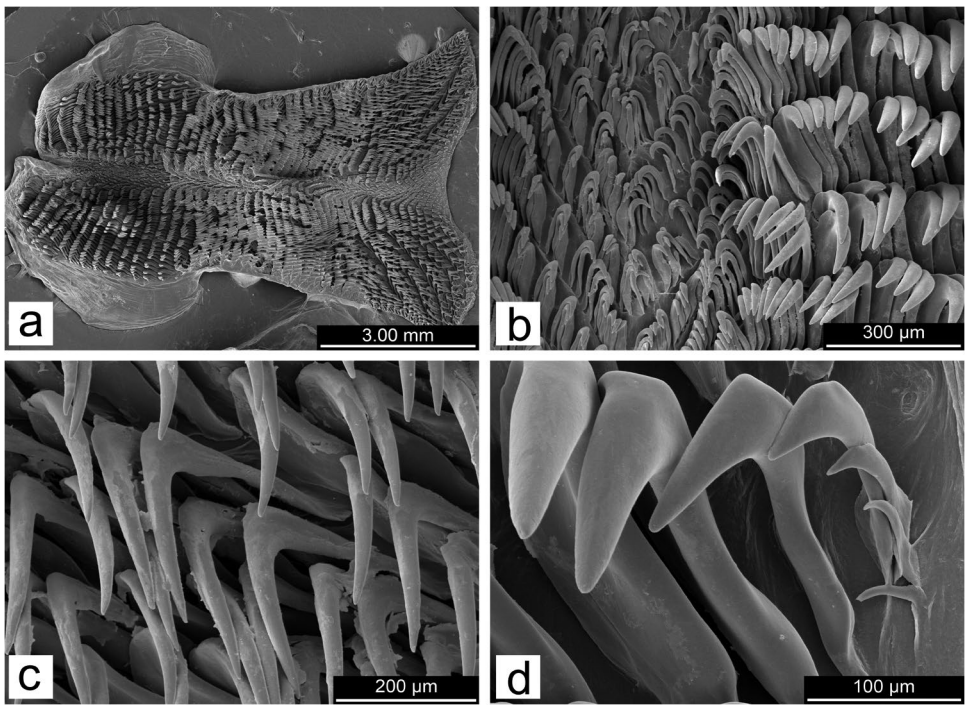

Fig. 21 *Halgerda takipsilim* sp. nov., holotype, NMP 041327, scanning electron micrographs of radula: **a** Entire radula; **b** inner lateral teeth; **c** mid-lateral teeth; **d** outer lateral teeth

lacked coloration but that there were small dark spots around the buccal opening. In *H. biqiea* sp. nov., the buccal mass has a single large black spot on the oral tube, as well as small dark brown/black spots around the buccal opening. The reproductive system also varies as *H. biqiea* sp. nov. has a small female gland mass; a short, wide penis with a thick elongated ejaculatory portion of the prostate; and an elongated duct connecting a large round bursa copulatrix to a semi-elongated vagina. In contrast, *H. brunneomaculata* has a much longer penis, an exceptionally thin elongated ejaculatory portion of the prostate, a nodular prostate much larger than the bursa copulatrix, and a similarly thin elongated duct connecting the vagina to the bursa copulatrix and the bursa copulatrix to the receptaculum seminis, as well as a thin elongated uterine duct (Carlson and Hoff 1993, Fig. 21).

Despite their many similarities, there are clear internal and external morphological differences and a strong genetic divergence that separate *H. biqiea* sp. nov. and *H. brunneomaculata*. Additionally, there is geographical separation between the two species. To date, *H. biqiea* sp. nov. is only found in the Saudi Arabian Red Sea and the nearby Gulf of Tadjoura, while *H. brunneomaculata* has been previously documented in the western Pacific including Guam; the Northern Mariana Islands; Fiji; Okinawa; New Caledonia; the Great Barrier Reef, Australia (Carlson and Hoff 1993; Debelius 1996; Ono 1999; Fahey and Gosliner 2000; Coleman 2001; Nakano 2004; Debelius and Kuiter 2007; Hervé 2010; Humann and DeLoach 2010); and French Polynesia (present study).

Halgerda willeyi Eliot, 1904
(Fig. 5d, 7d, 11a–c and 12)

Halgerda willeyi Eliot, (1904): 372–373, plate XXXII, Fig. 5; Eales (1938): 100–103, text-Figs. 17, 18, plate 1, Fig. 3; Gosliner et al. (1996): 160, second photograph from the bottom; Carlson and Hoff (2000): 161–162, Figs. 14, 18, 19 and 20; Coleman (2001): 58–59, bottom four photographs on 58, first photograph on 59; Yonow et al. (2002): 845–846, Figs. 7 and 11b; Nakano (2004): 130–131, bottom two photographs on 130, photographs labeled A–D, F on 131; Ono (2004): 142, bottom two photographs; Debelius and Kuiter (2007): 233, top four photographs; Gosliner et al. (2008): 179, top three photographs; Hervé (2010): 200–202; Humann and Deloach (2010): 316, bottom right photograph; Gosliner et al. (2015): 187, bottom two photographs; Gosliner et al. (2018): 109, top two photographs. *Halgerda elegans* Bergh (1905): 124–126; taf. II, Fig. 4a, taf. XV, Figs. 29–31; Johnson and Boucher (1983): 261–262, Fig. 4; Gosliner and Fahey (1998): 348–352, Figs. 1a, 2, 3, 4, 5 and 6; Ono (1999): 118–119, bottom photo on 118, small top left photo of juvenile on 119; Ono (2000): 118–119, bottom photo on 118, small top left photo of juvenile on 119; Ono (2004): 139, middle photograph; Debelius and Kuiter (2007): 229, top four photographs; Gosliner et al. (2008): 180, second photograph from the top; Humann and Deloach (2010): 316, middle right photograph; Gosliner et al. (2015): 186, top right photograph; Gosliner et al. (2018): 107, middle right photograph. *Halgerda* sp. 9 Debelius and Kuiter (2007): 233, middle four photographs. *Halgerda elegans* Bergh, 1905, syn. n.

Material examined: Two specimens, CASIZ 083676A, dissected, 35 mm preserved, locality: Twin Rocks, Calumpan Peninsula, Batangas Province, Luzon, Philippines, 15.8 m depth, 18 February 1992, collected by M. Miller. One specimen, CASIZ 177248, sequenced, 15 mm preserved, locality: Kirby's Rock (13° 41′ 28.0″ N 120° 50′ 29.0″ E), Caban Island, Maricaban Island, Batangas Province, Luzon, Philippines, 31.2 m depth, 16 March 2008, collected by T.M. Gosliner, Á. Valdés, M. Pola, L. Witzel, B. Moore, A. Alejandrino. One specimen, CASIZ 191259, sequenced, 6 mm preserved, locality: Rempi, Madang Province, Papua New Guinea, 16 November 2012, collected by Papua New Guinea Biodiversity Expedition 2012. One specimen, CASIZ 191495, sequenced, 13 mm preserved, locality: Madang, Papua New Guinea, 01 December 2012, collected by Pierre Laboute. One specimen, CASIZ 201944, sequenced, 8 mm preserved, locality: Sepok Wall (13° 45′ 34.3″ N 120° 55′ 34.1″ E), Maricaban Island, Batangas Province, Luzon, Philippines, 06 May 2014, collected by Alexis Principe. One specimen, CASIZ 204790, sequenced, 15 mm preserved, locality: Blackfish Corner (13° 34′ 31.7″ N 121° 02′ 30.3″ E), Verde Island, Luzon Island, Philippines, 80–94 m depth, 15 April 2015, collected by L. Rocha.

Type locality: Lifu (Lifou), Loyalty Islands, New Caledonia.

External morphology (Fig. 11a–c): Adult preserved animals 15–35 mm in length in specimens such as CASIZ 177248 and CASIZ 083676A (Fig. 11c) with similar adult description described for *H. willeyi* in Eliot (1904, plate XXXII, Fig. 5). Two additional external morphologies described here. Adult preserved specimens CASIZ 191495 and CASIZ 204790 (Fig. 11b) 13–15 mm in length. Dorsum color translucent white with low, irregular yellow and orange ridging and thick black/dark brown and orange lines within ridge valleys. Prominent yellow tubercles at ridge junctions. Central tubercles ringed with diffuse brown pigment. Small irregular spots and thin black/dark brown lines perpendicular to mantle edge. Thin, white mantle band along mantle edge. Mantle underside translucent white with short, thick black/dark brown lines perpendicular to mantle edge. Gill and rhinophores similar to Eliot (1904) description, i.e., two branchial plumes each split into three large mostly bipinnate branches. Gill coloration translucent white with dorsal and lateral brown stripes and white rachises. Opaque white glands visible in gill branches. Gill pocket smooth with similar dorsum coloration and perpendicular yellow-orange

ridges. Rhinophores tapered, perfoliate, translucent white with posterior black/dark brown stripe and shorter, similarly colored lateral stripes. Lamellae translucent white with lateral black/dark brown spots number 20–25. Rhinophoral sheath smooth with similar dorsum coloration and yellow ridges. Foot broad, anteriorly notched, and translucent white with numerous short black/dark brown perpendicular lines extends past mantle edge. Oral tentacles digitiform.

Juvenile preserved specimens CASIZ 191259 and CASIZ 201944 (Fig. 11a) 6–8 mm in length with similar description described for *H. elegans* in Bergh (1905, taf. II, Fig. 4a). Dorsum color translucent white with low, irregular yellow-orange ridging, large black spots between ridge valleys, and thick black lines alternating thinner, short black lines perpendicular to mantle edge. Prominent yellow tubercles at ridge junctions. Thin, white mantle band along mantle edge. Mantle underside translucent white with short, black lines and some small black spots perpendicular to mantle edge. Gill and rhinophores similar to Bergh (1905) description, i.e., two branchial plumes each split into three large mostly bipinnate branches. Gill coloration translucent white with prominent dorsal and lateral brown stripes and white rachises. Opaque white glands semi-visible in gill branches. Gill pocket smooth with similar dorsum coloration and perpendicular yellow-orange ridges. Rhinophores tapered, perfoliate, translucent white with posterior dark brown stripe and short similarly colored lateral stripes. Lamellae translucent white with large black blotches near the tips number 8–12. Rhinophoral sheath smooth with similar dorsum coloration and yellow-orange ridges. Foot broad, anteriorly notched, and translucent white with spaced apart short black perpendicular lines and small black spots extends past mantle edge. Oral tentacles digitiform.

Internal anatomy (Figs. 5d, 7d and 12a–d): Buccal mass (Fig. 5d) unpigmented. Oral tube semi-elongate and approximately 1.5×longer than buccal bulb. Radular sac slightly curved and unpigmented. Labial cuticle smooth. Radula composed of smooth hamate teeth (Fig. 12a). Radular formula 39×47.0.47 in CASIZ 083676A. Inner 25 lateral teeth (Fig. 12b) small, broad based, with elongated curved cusps form a steep V in radula center and gradually increase in size. Middle lateral teeth (Fig. 12c) larger and more elongate than inner laterals. Outer lateral teeth (Fig. 12d) similar to middle laterals with shorter cusps. Outermost two teeth are reduced and fimbriate.

Reproductive system (Fig. 7d): Triaulic. Thin preampullary duct widens into thick ampulla, then quickly narrows into postampullary duct which splits into short vas deferens and short oviduct. Vas deferens gradually thickens into wide, elongate, looped granular prostate, then abruptly narrows into thinner ejaculatory portion. Ejaculatory portion rapidly expands then contracts into the penis, which shares common genital atrium with vagina. Large, muscular vagina widens before proximally narrowing into thin, elongate duct and entering into large, rounded bursa copulatrix partially covered by granular prostate. Thin, elongate duct connects bursa to small oval-shaped receptaculum seminis. Uterine duct also connects near receptaculum base and enters medium-sized, pyriform-shaped female gland mass with elongated distal end.

Geographical distribution: Known from the Khuriya Muriya Islands (Eales 1938), the Ryukyu Islands, Japan (Gosliner and Fahey 1998; Ono 1999, 2000, 2004; Debelius and Kuiter 2007; Gosliner et al. 2008), the Philippines (Gosliner et al. 2008; present study), Indonesia (Gosliner and Fahey 1998), Papua New Guinea (Gosliner and Fahey 1998; Debelius and Kuiter 2007; Gosliner et al. 2008; present study), Australia (Gosliner et al. 2008), Vanuatu (Gosliner et al. 2008), the Loyalty Islands (Gosliner et al. 2008), and the Marshall Islands (Johnson and Boucher 1983; Gosliner et al. 2008).

Ecology: Found on living reefs crawling in the open or under rocks feeding on sponges.

Remarks: Our molecular phylogeny reveals that *Halgerda willeyi* is composed of three different morphologies: the original adult morphology as described in Eliot (1904) from Fiji; a new adult morphology described here; and a juvenile morphology formerly described as *Halgerda elegans* in Bergh (1905) from Indonesia. In our 16S ABGD, COI ASAP, bPTP, and GYMC analyses, the five specimens of *H. willeyi* are grouped together into one taxonomic unit, while our COI ABGD analysis over-partitions *H. willeyi* into four distinct taxonomic units and the 16S ASAP analysis groups *H. willeyi* with rest of the entire seventh clade. The COI maximum intraspecific variation between the five specimens studied here is only 1.8% (Supplementary Table S3), and the over-partitioning may be attributed to the low genetic diversity (2.9–4.8%) between *H. willeyi* and other members of the subclade: *H. gunnesi*, *H.* cf. *formosa*, *H. wasinensis*, *H.* aff. *wasinensis*, *H. anosy* sp. nov., and *H. dichromis* (Table 3).

All three color morphs share several external characteristics including: low, yellow-orange ridging with yellow tubercles at ridge junctions; perpendicular brown/black lines along the top and underside of the mantle edge; a thin white mantle band; a bipinnate gill composed of two branchial plumes each split into two or three large branches with dorsal and lateral brown stripes and white rachises; and translucent white rhinophores with a posterior dark brown stripe, similarly colored shorter lateral stripes, and dark colored spots or blotches along the lamellae. Variation within the three morphs is seen predominantly in the dorsum and tubercle patterning, as well as the stripes and spots along the gill and rhinophores. Similar to the original description of *H. willeyi* (Eliot 1904, plate XXXII, Fig. 5), adult specimens CASIZ 177248 and CASIZ 083676A (Fig. 11c) have more complex black and orange linework in the ridges and valleys than the other two morphologies. In the second adult color morph (Fig. 11b), seen in CASIZ 191495 and CASIZ 204790, the linework in the ridges and valleys is less complex, and the pigment more concentrated and the ridge

Table 3 Intra-specific range (bold) and minimum pairwise uncorrected *p*-distances (%) for COI between all *Halgerda* spp.

		1	2	3	4	5	6	7	8	9	10	11	12	13	14	15	16	17	18
1	*H. albocristata*	–																	
2	*H. anosy* sp. nov.	11.7	**0–0.6**																
3	*H. aurantiomaculata*	12.6	10.4	**0.3–0.5**															
4	*H. batangas*	13.1	10.2	3.6	**0–0.9**														
5	*H. biqiea* sp. nov.	11.8	11.5	12.9	13.1	–													
6	*H. brunneomaculata*	11.7	9.9	11.3	11.7	7.1	–												
7	*H. carlsoni*	12.9	11.3	3.6	2.2	13.7	12.6	**1.4–1.5**											
8	*H. dalanghita*	14	12.2	13.7	13.6	14	12.8	14.8	**0.5–1.7**										
9	*H. diaphana*	13.5	10.4	4.2	1.5	13.3	12.3	2.5	13.2	**0.2**									
10	*H. dichromis*	12.2	1.5	10.2	10.2	11.6	10.6	11.3	10.3	10.4	–								
11	*H.* cf. *formosa*	8.9	1.5	6.8	7.3	8.7	8	8	7.9	7.5	1.7	–							
12	*H. guahan*	10.6	7.5	9.8	10.9	10.6	10.8	11.3	11.9	11.1	7.5	6	**1.4**						
13	*H. gunnesi*	14.3	4.4	11.4	12.5	14.2	12.3	13.7	12.8	13	4.2	3.6	8.8	–					
14	*H. indotessellata*	12.8	11.5	11.5	11.9	12.5	11.1	13.3	13.9	12.8	11.8	8	10.6	12	**0.2–0.3**				
15	*H. jennyae*	8.7	7.1	7.5	8.5	8.2	8.7	8.7	9.2	8.3	7.1	6.1	0.5	7.8	8.7	–			
16	*H. labyrinthus* sp. nov.	13.1	10.9	4.1	0.8	13.1	11.7	2.8	13.4	2	10.9	7.7	11.1	12.3	12.1	8.7	–		
17	*H. leopardalis*	14	10.9	10.6	11.8	12.2	11	12.2	10.6	11.8	9.9	7.3	10.4	12	11.1	8.2	12.5	–	
18	*H. maaikeae* sp. nov.	12.2	11.6	11.1	12.3	13.1	11.8	13.8	13.9	13.1	11.8	9	9.1	12.3	5.8	7.8	12.7	12.4	–
19	*H. malesso*	13.1	10.9	3.4	1.1	13.5	11.9	2.2	13.9	0.6	10.6	7.5	11.4	13	12.8	8.5	1.7	11.8	13.2
20	*H. mango* sp. nov.	12.4	10.5	11.9	13.1	12.8	10.5	13.7	8.3	12.6	9.9	7	10.1	11.2	10.5	8.2	13.5	11.5	10.8
21	*H. meringuecitrea*	10.8	9.2	8.5	8.7	9.9	9.2	9.7	10.1	8.5	8.7	6.5	7.3	9.2	7.5	6.3	9.2	9.7	7.8
22	*H. mesophotica* sp. nov.	12.1	10.6	11	11.7	12	11.1	12.2	11.9	12.1	10.3	6.9	9.6	12.6	10.3	7.2	12.2	11.3	10.6
23	*H. mozambiquensis*	11.9	11.8	10.2	11.8	11.8	11.5	12.7	13.5	12.2	11.5	8.2	9.4	11.5	5.3	7.3	12.5	11.3	5.2
24	*H. nuarrensis*	12.9	11.1	3.1	2.6	12.8	11	2.3	12.8	2.5	11.1	7.8	10.9	11.8	11.9	8.5	3.3	11.4	12.3
25	*H. okinawa*	12.6	10.8	12	12.8	12.4	11.3	13.1	12.1	12.8	10.8	7.6	10.6	12.2	10.1	8.5	13.1	11.9	10.5
26	*H. pattiae* sp. nov.	11.4	10	8.7	9.9	10.2	9.9	10.4	10.4	9.9	10	7.3	9.5	10.9	9.2	7.8	10.4	9.7	8.5
27	*H. paulayi* sp. nov.	11.2	7.8	10.4	11.2	11	11.1	11.3	12.4	11.8	8.1	6	3.4	10	11.7	2.3	11.3	10.8	10.1
28	*H. profunda* sp. nov.	12.1	10.6	12	12.4	13	11.8	13.3	12.1	13.1	10.3	7.2	10.3	12.2	10.8	7.9	13.0	12.0	10.8
29	*H. scripta* sp. nov.	13.6	9.4	12	11.8	12	11.4	12.4	12.6	12.2	8.9	6.7	9.9	12.2	11.8	7.5	12	12	12.5
30	*H. takipsilim* sp. nov.	13	10.8	11.2	11.5	12.9	11.8	12.8	12.4	11.9	9.9	7.2	9.9	11.9	10.4	7.5	12.1	11.7	11.5
31	*H. terramtuentis*	13.7	11.1	3.7	1.5	14.2	11.9	2.5	14.1	2.2	10.6	7.2	11.8	12.8	12.9	8.7	2.2	12.0	13.6
32	*H. tessellata*	12.9	11.1	11.5	12.4	13.3	11.2	13.5	13.5	12.9	11.3	8.4	11.3	12.9	5.8	8.8	12.6	11.1	8.6
33	*H. theobroma*	12.7	10	7.8	8.2	10.8	9.9	8.2	12.8	8	10	6.4	9.5	10	10.1	7.7	8.7	11.1	10.9
34	*H. toliara*	0.8	11.7	13.1	13.3	11.6	11.1	13.5	13.7	14	11.9	8.9	9.8	12.7	12.4	8.9	14.1	13.7	11.3
35	*H.* aff. *wasinensis*	11.2	3.3	8.3	9.5	10.1	9.4	10.6	9.8	9.7	2.9	1.5	6.8	4.7	10.2	6	9.9	9.7	10.6
36	*H. wasinensis*	11	1.1	7.8	8.5	10.1	9.1	9.5	8.7	8.5	0.6	1.1	7	2.9	8.9	6.6	8.8	8	10
37	*H. willeyi*	12.9	3.6	11	11.4	12.5	10.4	12.7	11.9	12	4	3.4	8.3	3.6	11	7.6	11.4	10.7	11.1

Table 3 (continued)

		19	20	21	22	23	24	25	26	27	28	29	30	31	32	33	34	35	36	37
1	*H. albocristata*																			
2	*H. anosy* sp. nov.																			
3	*H. aurantiomaculata*																			
4	*H. batangas*																			
5	*H. biqiea* sp. nov.																			
6	*H. brunneomaculata*																			
7	*H. carlsoni*																			
8	*H. dalanghita*																			
9	*H. diaphana*																			
10	*H. dichromis*																			
11	*H.* cf. *formosa*																			
12	*H. guahan*																			
13	*H. gunnesi*																			
14	*H. indotessellata*																			
15	*H. jennyae*																			
16	*H. labyrinthus* sp. nov.																			
17	*H. leopardalis*																			
18	*H. maaikeae* sp. nov.																			
19	*H. malesso*	**0.5**																		
20	*H. mango* sp. nov.	12.9	**0.8–1.5**																	
21	*H. meringuecitrea*	9.2	9.2	**0–0.2**																
22	*H. mesophotica* sp. nov.	12.2	11.3	9	–															
23	*H. mozambiquensis*	12.2	10.1	7.8	9.6	–														
24	*H. nuarrensis*	2.5	12.7	8.8	10.8	11.6	–													
25	*H. okinawa*	12.6	10.7	9.1	5.5	9.8	11.5	–												
26	*H. pattiae* sp. nov.	10.6	9.1	6.0	9	9.2	9.7	10.4	–											
27	*H. paulayi* sp. nov.	11.3	10.8	9	11.3	9.9	11.4	11.5	10.6	**0.2–2.9**										
28	*H. profunda* sp. nov.	13.3	12	9.4	0.9	9.8	11.9	5.8	10.1	12	–									
29	*H. scripta* sp. nov.	12.2	11.2	8.4	7.3	9.9	11.6	6.7	11.1	9.7	7.3	**0–2.2**								
30	*H. takipsilim* sp. nov.	11.7	12.1	9.2	1.5	10.8	11.3	5.8	9.9	12	1.5	7.3	**0.2**							
31	*H. terramtuentis*	1.4	13.3	9.6	12.1	12.5	2.8	12.8	10.6	11.8	13.1	12.9	11.9	–						
32	*H. tessellata*	12.6	10.3	9.4	11.5	8	11.9	11.3	10.4	12	11.3	13	11.3	12.2	**0–0.6**					
33	*H. theobroma*	8.2	11.1	7.5	10.4	9.7	7.6	11.6	8.3	10.7	11.5	11.4	10.6	8.5	10.8	–				
34	*H. toliara*	13.6	13	10.8	11.9	12	13.8	12.8	11.3	10.5	11.9	13.3	12.8	13.9	12.6	12.7	**1.4**			
35	*H.* aff. *wasinensis*	9.7	8.7	7.3	8.6	9.4	10.2	9.4	8.9	6.8	8.9	8.2	8.7	9.4	10.9	8.8	10.8	–		
36	*H. wasinensis*	8.7	7.9	7.2	8.2	9.2	9	8.6	8.3	7.1	8.2	7.5	7.9	8.3	8.7	8	10.8	1.5	**0–1.7**	
37	*H. willeyi*	12.3	10.6	9.2	12.4	11.1	10.9	11.3	9.5	9.5	12.4	11.6	12.4	12.1	11.5	9.7	11.5	4.8	2.9	**0.3–1.8**

intersection tubercles are also ringed with a diffuse brown pigment not seen in the other two morphs. In juvenile specimens CASIZ 191259 and CASIZ 201944 (Fig. 11a), the dorsum and tubercle patterning are similar to that described for *H. elegans* in Bergh (1905, taf. II, Fig. 4a). Instead of complex linework in the ridges and valleys, there are large black spots and thicker perpendicular black lines along the mantle edge. The gill and rhinophores also have larger, more dark stripes and spots that are not quite as diffused as seen in older specimens.

Since Eliot (1904) did not provide a description of the radular teeth or the reproductive system in the original description of *H. willeyi*, we have dissected and described the internal anatomy of a specimen (CASIZ 083676A) that closely resembles Eliot's original external description. We disregarded the internal descriptions for *H. willeyi* found in Vayssière (1912) and Rudman (1978) as they are misidentifications of a new, similar species of *Halgerda* described and remarked upon in the *Halgerda paulayi* sp. nov. remarks section below. We are also unsure of which adult morph to which Eales (1938) refers, due to the lack of color from prior preservation and no external drawing; however, we are confident that Eales (1938) does refer to a true *H. willeyi* due to the presence of the numerous small inner radular teeth, the reduction in the shape of the outermost teeth, and the presence of a muscular vagina and large, spherical bursa copulatrix. The internal anatomy of the juvenile morphology previously described as *H. elegans* has a limited description in Bergh (1905). No details are given about the reproductive organs or their arrangement, but there is some description about the radular teeth (Bergh 1905, taf. XV, Figs. 29–31). Gosliner and Fahey (1998) further described the internal anatomy including the radula and reproductive system of *H. elegans* and was used for the internal comparisons of the three morphos. The external morphology of the *H. willeyi* dissected by Carlson and Hoff (2000) closely resembles the new adult morphology described here; however, it lacks details about the inner and middle lateral radular teeth. Carlson and Hoff (2000) did illustrate the outermost teeth and the reproductive system and was therefore used for some of the internal comparisons.

Internally, the buccal mass of all three morphologies lacks pigment and shares the predominantly smooth hamate teeth found in other species of *Halgerda*. In CASIZ 083676A, the numerous inner lateral teeth are small and broad-based with an elongated curved cusp, which is similar to the inner laterals described for *H. elegans* in Bergh (1905, taf. XV, Fig. 29) and the *H. elegans* specimen CASIZ 079348 in Gosliner and Fahey (1998, Fig. 2c–d). Gosliner and Fahey (1998) did find that *H. elegans* exhibits some variation in the radular teeth ranging from simple hamate to multifid middle laterals (Gosliner and Fahey 1998, Fig. 2, 3, 4 and 5). In all three morphs the outermost two to three teeth are reduced; however, the illustration of the outermost teeth in Carlson and Hoff (2000) lacks the fimbriate detail seen in the present study (Fig. 12d) and in Bergh's description of *H. elegans* (Bergh 1905, taf. XV, Fig. 31). In all three reproductive systems the large, spherical bursa copulatrix is partially covered by the granular portion of the prostate, the receptaculum seminis is oval-shaped and approximately half the size of the bursa, and the vagina is muscular and larger than the penis even in juvenile specimens previously considered as *H. elegans* (Gosliner and Fahey 1998, Fig. 6; Carlson and Hoff 2000, Figs. 18 and 19). Differences between the three reproductive systems are minimal but include the amount of the glandular prostate covering the bursa copulatrix in the second adult morph (Carlson and Hoff 2000, Figs. 18 and 19) and the penis expanding distally into an enlarged section of the ejaculatory portion of the prostate in CASIZ 083676A.

Since there are low genetic differences in the five specimens studied here, no geographical separation or morphological grouping, and numerous morphological similarities, we are confident that all three morphs represent a single species. Furthermore, there are no clear differences between *H. elegans* and *H. willeyi* other than slight variations in dorsum and tubercle patterning and as such *H. elegans* should be considered a junior synonym of *H. willeyi*.

Halgerda paulayi Donohoo & Gosliner sp. nov.
https://zoobank.org/D95DCF0F-EB8A-4831-93EA-5F1FE301666B
(Fig. 5e, 7e, 11d, e and 13)

Halgerda willeyi (misidentification) in: Vayssière (1912): 40–45, plate I, Fig. 7, plate VII, Figs. 98–104; Rudman (1978): 64–65, Figs. 4a and 5; Debelius (1998): 257, bottom two photographs; Yonow (2008): 163. *Halgerda* sp. 8 Debelius and Kuiter (2007): 232, middle two photographs. *Halgerda* sp. 1 Gosliner et al. (2008): 179, second photograph from the bottom. *Halgerda* sp. 2 Gosliner et al. (2015): 188, top two photographs. *Halgerda* sp. 7 Gosliner et al. (2018): 109, bottom two photographs.

Material examined: Holotype: One specimen, CASIZ 192298, dissected and sequenced, 45 mm preserved/alive, type locality: Ablo Island Reef (18° 39′ 34.1″ N 40° 49′ 37.3″ E), Red Sea, Saudi Arabia, 05 March 2013, collected by Patrick L. Norby. Paratypes: One specimen, UF 476040, dissected and sequenced, 35 mm preserved, locality: Jazirat Burcan (27° 54′ 35.6″ N 35° 03′ 55.5″ E), Red Sea, Saudi Arabia, 17–18 m depth, 28 September 2013, collected by Gustav Paulay, Seabird McKeon, Daisuke Uyeno, Jenna Moore, and Casey Zakroff. One specimen, UF 476041, dissected and sequenced, 50 mm preserved, locality: Jazirat Burcan (27° 54′ 35.6″ N 35° 03′ 55.5″ E), Red Sea, Saudi Arabia, 28 September 2013, collected by Gustav Paulay, Seabird McKeon, Daisuke Uyeno, Jenna Moore, and Casey Zakroff.

Type locality: Ablo Island Reef, Red Sea, Saudi Arabia

Etymology: This species is named in honor of Dr. Gustav Paulay, for his numerous contributions to molluscan research and his extensive collection of nudibranch sea slugs and other invertebrate taxa, which has greatly increased our understanding of marine biodiversity.

External morphology (Fig. 11d, e): Preserved animals 35–50 mm in length. Body oval, rigid, and gelatinous. Dorsum color bluish white with thick, black connected lines. Pronounced ridging in irregular pattern with yellow/orange coloration. Prominent yellow/orange tubercles at ridge intersections. Small yellow/orange tubercles, minute white tubercles, perpendicular black lines, and black spots along mantle edge. Mantle marginal band absent. Mantle underside bluish white with numerous short perpendicular black lines, medium black splotches, and small black spots along mantle edge. Large gill surrounds anus with four tripinnate branchial leaves split into two posterior and two anterior gill branches. Posterior gill branches further split into two large branches. Gill branches and rachises translucent white with blue tint and numerous small randomly dispersed black spots. Opaque white glands visible in gill branches. Gill pocket smooth with similar dorsum coloration and yellow-orange ridges. Rhinophores tapered, perfoliate, and translucent white with blue tint, a posterior black stripe, and small to medium black splotches along stalk and lamellae. Lamellae number 20–30. Rhinophoral sheath color bluish white with yellow-orange ridges. Foot broad, anteriorly notched, and white with small black spots interspersed with short perpendicular black lines. Oral tentacles digitiform.

Internal anatomy (Figs. 5e, 7e and 13a–d): Buccal opening and buccal mass (Fig. 5e) pigmented on oral tube with small random black spots. Oral tube similar in size to buccal bulb. Radular sac curved and unpigmented. Labial cuticle smooth. Radula composed of smooth hamate teeth (Fig. 13a). Radular formula 43 × 40.0.40 in the holotype CASIZ 192298 and 37 × 30.0.30 in the paratype UF 476,040. In CASIZ 192298 inner eight to ten lateral teeth (Fig. 13b) small, broad based, with narrow, sharply curved cusps form a V in the center. Middle lateral teeth (Fig. 13c) larger than inner laterals with larger, less curved, slightly flared, rounded cusps. Outer lateral teeth (Fig. 13d) similar to middle laterals with shorter, unflared cusps. Outermost two to three teeth reduced, straighter than other lateral teeth with occasional single denticle.

Reproductive system (Fig. 7e): Triaulic. Thin preampullary duct gradually thickens into ampulla, then quickly narrows into postampullary duct which splits into thin, short vas deferens and thin, short oviduct. Vas deferens gradually thickens into wide, looped granular prostate, then narrows into thin, elongate ejaculatory portion. Ejaculatory portion rapidly expands into large penis, which shares common genital atrium with similarly sized vagina. Vagina abruptly narrows and gradually thins into elongate duct before entering large, rounded bursa copulatrix partially covered by granular prostate. Thin, elongate duct connects bursa to smaller, pyriform receptaculum seminis. Thin, elongate uterine duct also connects near receptaculum base and enters small, pyriform-shaped female gland mass with elongated distal end.

Geographical distribution: Known from the Red Sea, including Saudi Arabia (Rudman 1978; Gosliner et al. 2008, present study), the Gulf of Aqaba (Debelius 1998), Yemen (Debelius and Kuiter 2007), and the Gulf of Tadjoura, Djibouti (Vayssière 1912).

Ecology: Found on shallow reefs and on steep slopes of fringing reef faces between 10 and 25 m.

Remarks: Our molecular phylogeny and all four species delimitation analyses reveal that *Halgerda paulayi* sp. nov. from the Red Sea is a distinct species within *Halgerda* and is separated from the similarly patterned *H. willeyi* by a minimum divergence of 9.5% in the COI gene. In our COI ABGD, COI ASAP, and bPTP analyses, the paratype UF 476040 collected from Jazirat Burcan, Saudi Arabia, is over-partitioned from the paratype UF 476041 also collected from Jazirat Burcan and the holotype CASIZ 192298 collected from Ablo Island, Saudi Arabia, due to a high intraspecific genetic divergence of 2.9%. Morphologically (Supplementary Figure S5), this paratype specimen is smaller than the other two specimens and has less pronounced ridging, thicker perpendicular black lines along the mantle edge, and finely tripinnate branches as a result. Internally, there are fewer inner lateral teeth and fewer rows; however, there are no discernable differences between the paratype and holotype reproductive systems. The over-partitioning may also be attributed to the low genetic diversity between *H. paulayi* sp. nov. and the other two members of this clade: *H. jennyae* and *H. guahan*. Within the COI gene, *H. paulayi* sp. nov. and *H. jennyae* are separated by a low genetic divergence of 2.3–2.9%, while *H. paulayi* sp. nov. and *H. guahan* are separated by a slightly higher genetic divergence of 3.4–4.2%.

Morphologically, these three species are very distinct. For example, *H. guahan* has low orange ridging along the dorsum with no additional dorsum coloration (Carlson and Hoff 1993, Fig. 3a), whereas *H. jennyae* has more pronounced ridging with high tubercles and a complex pattern of thin brown lines along the irregular ridges and valleys (Tibiriçá et al. 2018, Figs. 11d, e). In contrast, *H. paulayi* sp. nov. has pronounced yellow/orange ridging with thick black lines along the dorsum, ridge valleys, and mantle edge (Fig. 11d, e). These three species form a clade within the seventh subclade and share a similar spotting pattern on the rhinophores and gills that varies between stripes and solid coloration within rest of the subclade.

This species is also compared here to *Halgerda johnsonorum* Carlson & Hoff, 2000, described from the Marshall Islands and documented from New Caledonia (Gosliner et al. 2008). This species has low orange ridges that have low

acutely pointed apices at the junction of ridges in contrast to steeper, more rounded ridge junctions found in *H. paulayi* sp. nov. In *H. johnsonorum*, the body is more translucent, and there are several fine black radiating lines between the ridges whereas the body of *H. paulayi* sp. nov. is opaque bluish white, and there is a single thicker line between the mantle ridges. The base of the rhinophore has numerous black spots in *H. johnsonorum* versus only 1–3 spots on the rhinophore base of *H. paulayi* sp. nov., and *H. paulayi* sp. nov. has a much more prominent black line on the entire posterior face of the rhinophore base. Internally, there are differences, as well. In *H. paulayi* sp. nov., the hamate outer lateral tooth has only a single denticle (Fig. 13d), whereas in *H. johnsonorum* the outer tooth is narrow with a bifid apex (Carlson and Hoff 2000, Fig. 15). Most significantly, the reproductive system of *H. paulayi* sp. nov. has large bulbous bases to both the vagina and penial sac (Fig. 7e), whereas these structures are both narrow and not significantly enlarged in *H. johnsonorum* (Carlson and Hoff 2000, Fig. 17). *Halgerda johnsonorum* as described from the Marshall Islands has some significant external differences to specimens recorded from New Caledonia as *H. johnsonorum* (Gosliner et al. 2018; 110, upper right photo). In the New Caledonia specimens, the gill is much less divided and has black lines rather than pots on the branches and the narrow, more elongate rhinophores lack spotting and have only a prominent thin black line on their posterior face. A more detailed examination of New Caledonia specimens is necessary, but these differences suggest that they may represent a distinct, undescribed species.

Further morphological comparisons are made below between *H. paulayi* sp. nov. and the similarly patterned *H. willeyi*. Externally, the dorsum coloration of *H. paulayi* sp. nov. is bluish white with thick, black connected lines; pronounced irregularly patterned yellow/orange ridging and tubercles; and perpendicular thick black and orange lines along the mantle edge. In contrast, the dorsum coloration of *H. willeyi* is translucent white with low, irregular yellow and orange ridging, prominent lemon-yellow tubercles, and numerous thin perpendicular black lines along the mantle edge. The mantle underside and foot are similarly patterned between the two species with black perpendicular lines; however, in *H. paulayi* sp. nov., the mantle underside perpendicular lines are shorter than in *H. willeyi* and there are also small to medium black spots and blotches along both the mantle underside and the foot. The gill plumes are also uniquely distinct as *H. paulayi* sp. nov. has four tripinnate branchial leaves that further divide into six large branches which are colored translucent white with a blue tint and numerous randomly dispersedly small black spots. In *H. willeyi* there are two mostly bipinnate branchial leaves further divided into six large branches which are also translucent white but have dorsal brown stripes, diffused lateral brown stripes, and white rachises. The rhinophores are similar between the two species; however, *H. paulayi* sp. nov. has a higher number of small and large black spots along the stalk and lamellae, while *H. willeyi* has fewer spots along the stalk and lamellae which are browner in color. Additionally, adult specimens of *H. paulayi* sp. nov. studied here are generally larger in size (35–50 mm in length) than those of *H. willeyi* (13–35 mm in length). These two species are also geographically separated with *H. johnsonorum* being restricted to the western and central Pacific, possibly being endemic to the Marshall Islands whereas *H. paulayi* sp. nov. is restricted to the Red Sea and the Gulf of Aden. No specimens resembling either of these species have been found in any localities situated between the Red Sea and the Central Pacific.

Internally, the buccal opening and the oral tube of the buccal mass in *H. paulayi* sp. nov. are pigmented with small random black spots, whereas in *H. willeyi* neither are pigmented. The radular teeth in *H. paulayi* sp. nov. are similar to all *Halgerda*; however, there are only eight to ten small inner lateral teeth which have a more elongate stem and a sharply curved cusp and the outermost two to three teeth are reduced and straighter than the other lateral teeth. In contrast, there are 25 inner lateral teeth with a thicker elongated cusp in *H. willeyi* and the outermost two teeth are reduced and fimbriate. The reproductive system also varies as *H. paulayi* sp. nov. has a large, rounded bursa copulatrix partially covered by the granular prostate, a smaller pyriform receptaculum seminis, and a similarly sized large penis and vagina. In *H. willeyi* the rounded bursa copulatrix is much smaller and predominantly covered by the slightly smaller granular prostate, the receptaculum seminis is half the size of the bursa and oval-shaped, and the penis is smaller than the vagina, but tapers distally but tapers distally before expanding into the ejaculatory portion (present study, Fig. 7d).

Due to the morphological similarities between these two species, specimens of *H. paulayi* sp. nov. from the Red Sea have been previously misidentified as *H. willeyi*. Vayssière (1912) extensively described specimens from the Gulf of Tadjoura, Djibouti, but questions whether they are a variation of *H. willeyi* or a new species of *Halgerda* entirely. We are confident that these specimens are in fact *H. paulayi* sp. nov. based on the thick, connected black lines in coordination with the yellow/orange ridging across the mantle, the whitish tripinnate gill with numerous small black spots (Vayssière 1912, plate I, Fig. 7), the elongated stems in the first few inner radular teeth (Vayssière 1912, plate VII, Fig. 100), and the reduced, straighter outermost teeth (Vayssière 1912, plate VII, Fig. 101). Rudman (1978) described the anatomy of a specimen from Jeddah, Saudi Arabia, Red Sea; however, upon closer review this specimen is also *H. paulayi* sp. nov. due to the thick black, connected lines along the irregularly patterned ridging, the thick black perpendicular lines along the mantle edge, and the large, white-colored gill with

numerous small black spots (Rudman 1978, Fig. 4a). Rudman also mentioned that the oral tube of the buccal mass is pigmented with spots, that there are seven small inner lateral teeth (Rudman 1978, Fig. 5a) and that the outermost two to three teeth are "simple flattened plates" or more accurately described as reduced and straight when compared with other lateral teeth (Rudman 1978, Fig. 5b), which also correlates with the morphology of *H. paulayi* sp. nov. described in the present study. In 1988, Frances Velkovrh collected a specimen of *H. paulayi* sp. nov. off the island of Cres near Baldarin Bay, Croatia in the northern Adriatic Sea. This specimen, previously identified as *H. willeyi*, was introduced into the Mediterranean via migration from the Red Sea through the Suez Canal or potentially through ballast water in traveling ships (Turk 2001; Rudman 2001). No further specimens have been recorded from the Mediterranean since 1988.

There are clear internal and external morphological differences, a strong genetic divergence, and even some geographical separation between *H. paulayi* sp. nov. *H. johnsonorum,* and *H. willeyi*. To date, *H. paulayi* sp. nov. is found in the Red Sea and the nearby Gulf of Tadjoura, Djibouti, while a specimen of *H. willeyi* has been previously documented off the coast of Oman in the Khuriya Muriya Islands, Arabian Sea it has been extensively documented throughout the western Pacific (See *H. willeyi* geographical distribution).

Halgerda labyrinthus Donohoo & Gosliner **sp. nov.**
https://zoobank.org/5706F284-DA7C-42ED-8472-90E6B3703C3E
(Fig. 5f, 7f, 11f and 14)

Halgerda willeyi (misidentification) in: Ono (1999): 119, top right photograph; Ono (2000): 119, top right photograph; Keiu (2000): 103, top two photographs; Nakano (2004): 131, photograph labeled E; Ono (2004): 142, large middle photograph. *Halgerda* sp. 11 Debelius and Kuiter (2007): 234, top four photographs.

Material examined: Holotype: One specimen, CASIZ 070174, 95 mm alive, type locality: Horseshoe Cliffs (26° 30′ 00.0″ N 127° 50′ 09.0″ E), Onna Village, Okinawa, Ryukyu Islands, Japan, 51.8 m depth, 14 March 1987, collected by R.F. Bolland. Paratypes: One specimen, CASIZ 070068, 84 mm alive, locality: Maeda Point (26° 26′ 50.0″ N 127° 46′ 09.0″ E), Maeda Sake, Okinawa, Ryukyu Islands, Japan, 27.4 m depth, 04 June 1989, collected by R.F. Bolland. One specimen, CASIZ 160949, dissected and sequenced, 95 mm preserved, locality: Seragaki (26° 30′ 40.0″ N 127° 53′ 00.0″ E), Okinawa, Ryukyu Islands, Japan, 41.2 m depth, 05 October 2001, collected by R.F. Bolland.

Type locality: Horseshoe Cliffs, Onna Village, Okinawa, Ryukyu Islands, Japan.

Etymology: The name *labyrinthus* refers to the maze-like pattern of the numerous fine lines decorating the dorsum of this species.

External morphology (Fig. 11f): Preserved and living animals 84–95 mm in length. Body oval, semi-rigid, and gelatinous. Dorsum color white with numerous thin, black connected lines interspersed with yellow connected lines. Semi-pronounced ridging in irregular pattern with yellow coloration. Yellow mantle marginal band with continuing perpendicular black and yellow lines, raised yellow spots and occasional black spots near mantle edge. Mantle underside white with perpendicular lines of small black spots. Large gill surrounds anus with four tripinnate branchial leaves split into two posterior and two anterior gill branches. Posterior gill branches further split into two large branches. Gill branches translucent yellow with translucent white rachises and numerous small randomly dispersed black spots. Gill pocket smooth with white coloration and radiating yellow lines. Rhinophores tapered, perfoliate with thick stalks. White lamellae number 25–35 with small black spots. Rhinophore stalks white with small black spots and lateral black stripes. White rhinophoral sheath smooth with yellow ridges. Foot broad, anteriorly notched, and white with random small black spots and perpendicular lines with spots along foot edge. Oral tentacles digitiform.

Internal anatomy (Fig. 5f, 7f and 14a–d): Buccal mass (Fig. 5f) unpigmented. Buccal bulb approximately 1.5 × longer than oral tube. Radular sac semi-elongate, club shaped, and unpigmented. Labial cuticle smooth. Radula composed of smooth hamate teeth (Fig. 14a). Radular formula 65 × 48.0.48 in the paratype CASIZ 160949. Inner 16 lateral teeth (Fig. 14b) small, broad based, with slightly curved cusps form a shallow V shape. Middle lateral teeth (Fig. 14c) larger than inner laterals with more curved, elongate, rounded cusps. Outer lateral teeth (Fig. 14d) larger than middle laterals and slightly less curved. Outermost two teeth reduced with irregular tips.

Reproductive system (Fig. 7f): Triaulic. Thin preampullary duct gradually widens into ampulla, then narrows into postampullary duct which splits into short vas deferens and short oviduct. Vas deferens gradually thickens into looped, granular prostate wrapped around bursa copulatrix, before narrowing into thin, elongate ejaculatory portion. Ejaculatory portion abruptly expands into penis, which shares common genital atrium with smaller vagina. Muscular vagina abruptly narrows proximally into thin, elongate duct and enters into large, rounded bursa copulatrix hidden under glandular prostate portion. Thin, elongate duct connects bursa to smaller, irregular-shaped receptaculum seminis. Short uterine duct also connects near receptaculum base and enters small, irregularly oval-shaped female gland mass with elongated distal end.

Geographical distribution: Known from the Ryukyu Islands, Japan (present study), Kerama Islands (Ono 1999, 2000), the Izu Peninsula, Japan (Keiu 2000; Debelius and Kuiter 2007), and Taiwan (Debelius and Kuiter 2007).

Ecology: Found on steep reef faces and coral rubble between 20–55 m.

Remarks: In our molecular phylogeny *Halgerda labyrinthus* sp. nov. is a distinct species in a large clade composed of *H. theobroma*, *H. batangas*, *H. terramtuentis*, *H. malesso*, *H. diaphana*, *H. carlsoni*, *H. nuarrensis*, and *H. aurantiomaculata*. The bPTP analysis successfully separates *H. labyrinthus* sp. nov. from the *H. batangas* polytomy; however, the COI ABGD, COI ASAP, and GMYC analyses fails to make this distinction and groups *H. labyrinthus* sp. nov. with *H. batangas*. The 16S ABGD and 16S ASAP analyses also groups *H. labyrinthus* sp. nov. with *H. paulayi* sp. nov. and *H. guahan*, as well as *H. willeyi*, respectively. This may be attributed to the low interspecific variation between some of the species within this clade (Table 2). For instance, the distance between *H. labyrinthus* sp. nov. and *H. batangas* is only 0.8–1.4% in the COI gene; while the greatest distance is 4.5% between *H. labyrinthus* sp. nov. and *H. aurantiomaculata*. Morphologically, *H. labyrinthus* sp. nov. is similar to *H. willeyi* and *H. paulayi* sp. nov. and further morphological comparisons are made below. There is a strong minimum divergence of 11.4% in the COI gene between *H. labyrinthus* sp. nov. and the similarly patterned *H. willeyi* and a similar divergence of 11.3% between *H. labyrinthus* sp. nov. and *H. paulayi* sp. nov. from the Red Sea.

Externally, *H. labyrinthus* sp. nov. varies from the previous comparison between *H. willeyi* and *H. paulayi* sp. nov. (see *H. paulayi* sp. nov. 'remarks' section above) due to the white dorsum coloration with numerous thin, black connected lines interspersed with thin, yellow lines; semi-pronounced yellow ridging; and a yellow mantle marginal band with raised yellow and black spots and perpendicular black and yellow lines along the mantle edge. The mantle underside and foot are similarly patterned to *H. willeyi* and *H. paulayi* sp. nov. with black perpendicular lines; however, in *H. labyrinthus* sp. nov., there are fewer lines with each line composed of sequential small black spots. There are also random small black spots interspersing the short lines along the foot. The gill plume is similar to *H. paulayi* sp. nov. with four tripinnate branchial leaves furthered divided into six large branches patterned with numerous small black spots; however, the branchial leaves are translucent yellow rather than white and the rachises are white rather than translucent white with a blue tint. The rhinophores are also similar to *H. paulayi* sp. nov. with a posterior black stripe, lateral black stripes, and small black spots; however, in *H. labyrinthus* sp. nov., there are more lateral stripes and small black spots as well as thicker rhinophoral stalks. Additionally, adult specimens of *H. labyrinthus* sp. nov. are two to three times larger (> 80 mm in length) than specimens of *H. paulayi* sp. nov. (35–50 mm in length) *and H. willeyi* (13–35 mm in length) studied here, are generally less rigid when preserved, and found at depths greater than 25 m.

Internally, the buccal opening and buccal mass of *H. labyrinthus* sp. nov. are similar to *H. willeyi* (i.e., unpigmented) and the radular teeth are similar to all *Halgerda*; however, there are 16 small inner lateral teeth which form a shallower V in the center of the radula. The middle and outer laterals are thicker and less elongated in the cusp and the two outermost teeth are reduced with curved cusps and irregular tips rather than reduced and straight (*H. paulayi* sp. nov.) or reduced and fimbriate (*H. willeyi*). The reproductive system in *H. labyrinthus* sp. nov. is similar to both *H. willeyi* and *H. paulayi* sp. nov., however, the bursa copulatrix is completely covered by the granular portion of the prostate; the receptaculum is small, more elongate, and irregularly shaped; and the uterine duct is much shorter than either found in *H. willeyi* or *H. paulayi* sp. nov. The penis and vagina are both smaller in *H. labyrinthus* sp. nov., but the vagina is similarly muscular to the one found in *H. paulayi* sp. nov. (present study, Fig. 7e).

Previously, specimens of *H. labyrinthus* sp. nov. have been either mis-identified as *H. willeyi* or suggested as a variation of *H. willeyi* due to the similarities in dorsum coloration and patterning. This may be attributed to a lack of geographical separation between the two species, since both are found in Okinawa, Japan. There is, however, geographical separation between *H. labyrinthus* sp. nov. and the similarly patterned *H. paulayi* sp. nov. as the former is found only in Japan and Taiwan and the latter is found only in the Saudi Arabian Red Sea. Despite the similarities between these three species, there are strong morphological characteristics and a large genetic distance that separate them, making each a distinct species within *Halgerda*.

Given the small genetic difference between *H. labyrinthus* sp. nov. and *H. batangas*, we also compare these species to each other. *Halgerda labyrinthus* sp. nov. is a large species ranging from 84–95 mm, whereas *H. batangas* reaches a maximum length of 40 mm. Additionally, *H. batangas* lacks any black lines on the notum that dominate the body color of *H. labyrinthus* sp. nov., while *H. labyrinthus* sp. nov. lacks bright orange tubercles and fine orange lines found in *H. batangas*. Internally, the radula of *H. labyrinthus* sp. nov. has only the outermost tooth with a bifid apex, whereas in *H. batangas* the outermost tooth is strap-shaped and the adjacent two teeth are bifid (Carlson and Hoff 2000, Fig. 9). The configuration of the reproductive system also differs in the two species. In *H. labyrinthus* sp. nov., the vagina is narrow and muscular but lacks a ring of glandular structures immediately proximal to its opening. In *H. batangas*, the muscular vagina is as wide as the penis and has a ring of glandular structures immediately proximal to the vagina (Carlson and Hoff 2000, Fig. 11). Furthermore, *H. labyrinthus* sp. nov. is found in deep water from 27–51 m depth, whereas *H. batangas* has been found from 2–20 m depth. García-Méndez et al. (2022) has shown that despite low genetic divergence (0.18%

in COI gene) in species of *Dondice*, it was acceptable to separate similar but distinct species on the basis of consistent morphological and ecological differences. We contend that the evidence clearly supports a similar separation of *H. labyrinthus* sp. nov. and *H. batangas*.

Halgerda anosy Donohoo & Gosliner sp. nov.
https://zoobank.org/5A554E81-6B77-4250-9AE3-96E1FFCAB1B3
(Fig. 5g, 7g, 11g–h and 15)

Material examined: Holotype: One specimen, CASIZ 194054, dissected and sequenced, 45 mm preserved/alive, type locality: South Madagascar (24° 57′ 00.0″ S 47° 06′ 30.0″ E), Madagascar, 10 m depth, 12 May 2010, collected by the South Madagascar Expedition. Paratypes: Three specimens, CASIZ 194616A (50 mm preserved) sequenced, CASIZ 194616B (35 mm preserved) dissected, type locality: South Madagascar (24° 57′ 00.0″ S 47° 06′ 24.0″ E), Madagascar, 5–6 m depth, 06 May 2010, collected by the South Madagascar Expedition. Other material examined: One specimen, CASIZ 194036, sequenced, 55 mm preserved/alive, type locality: South Madagascar (25° 13′ 30.0″ S 47° 13′ 48.0″ E), Madagascar, 88 m depth, 08 May 2010, collected by the South Madagascar Expedition. One specimen, CASIZ 194045, sequenced, 35 mm preserved, type locality: South Madagascar (25° 00′ 12.0″ S 47° 06′ 12.0″ E), Madagascar, 22–28 m depth, 30 April 2010, collected by the South Madagascar Expedition. One specimen, CASIZ 194046, sequenced, 20 mm preserved, type locality: South Madagascar (25° 00′ 12.0″ S 47° 06′ 12.0″ E), Madagascar, 22–28 m depth, 30 April 2010, collected by the South Madagascar Expedition.

Type locality: South Madagascar, Madagascar.

Etymology: This species is named "anosy" after the Malagasy word for island or land of the islands and refers to the type locality of the island of Madagascar.

External anatomy: Preserved animals 20–55 mm in length (Figs. 11g–h). Body oval, rigid, and gelatinous. Dorsum color bluish white with many medium dark brown/black spots along mantle edge. Low yellow ridging in irregular pattern with semi-projected yellow tubercles at ridge intersections. A single large dark brown/black spot or two conjoined small dark brown/black spots present within ridge depressions. Viscera with dark blue/purple coloration semi-visible through mantle. Smaller specimens (Fig. 11h) have less pronounced ridging with fewer, lighter colored spots and barely visible viscera. Thin white line present along mantle edge. Mantle underside bluish white with anterior mantle edge small dark brown/black spots clearly visible through mantle and larger dark brown/black spots only semi-visible through mantle. Gill surrounds elevated anus with four highly bipinnate branchial leaves split into two posterior and two anterior gill branches. Posterior gill branches further split into two large branches. Gill coloration bluish white with central anterior dark brown/black stripe and bluish white rachises. Gill pocket smooth with similar dorsum coloration. Opaque white glands present within branchial leaves. Rhinophores tapered, perfoliate, with 5–6 white lamellae, then 18–22 dark brown/black lamellae, and a white apical tip. Rhinophore stalks bluish white with small posterior dark brown/black spot. Rhinophoral sheath smooth with yellow coloration. Foot is broad, anteriorly notched, bluish white with small to medium dark brown/black spots. Oral tentacles digitiform.

Internal anatomy (Fig. 5g, 7g and 15a–d): Buccal mass (Fig. 5g) unpigmented; however, small dark spots present around buccal opening. Buccal bulb approximately 1.5 × larger than oral tube. Radular sac short, rounded, and unpigmented. Labial cuticle smooth. Radula composed of smooth hamate teeth (Fig. 15a). Radular formula 48 × 44.0.44 in the paratype CASIZ 194616B. Inner 15 lateral teeth (Fig. 15b) small, broad based, with curved, elongate, rounded cusps forming a slightly spaced V shape. Some of the first three inner teeth are bifurcated. Middle lateral teeth (Fig. 15c) are larger, thicker, and slightly more elongated than inner laterals. Outer lateral teeth (Fig. 15d) are slightly larger than middle laterals and less curved. Outermost two teeth reduced and semi-fimbriate.

Reproductive system (Fig. 7g): Triaulic. Thin preampullary duct widens into thick ampulla, then gradually narrows into postampullary duct which splits into short vas deferens and short oviduct. Vas deferens quickly expands into wide, elongate, looped granular prostate which abruptly narrows into thin, elongate, convoluted ejaculatory portion. Ejaculatory portion quickly expands into large penis, which shares a common genital atrium with a similarly size vagina. Vagina contains finger-like projections before proximally narrowing into thin, elongate duct and entering into rounded bursa copulatrix partially covered by granular prostate. Elongate duct connects bursa to smaller, semi-rounded receptaculum seminis. Thin, elongate uterine duct also connects near receptaculum base and enters large, semi-rounded female gland mass.

Geographical distribution: Known from South Madagascar.

Ecology: Found on patch reefs and fringing reefs between 5–50 m.

Remarks: *Halgerda anosy* sp. nov. is part of a large, unresolved, subclade including *H. dichromis*, *H.* aff. *wasinensis*, *H. wasinensis*, and *H.* cf. *formosa*. The COI ABGD analysis successfully separates out *H. anosy* sp. nov. from the previously mentioned species; however, 16S ABGD, the COI and 16S ASAP, the GMYC, and the bPTP analysis fail to recover *H. anosy* sp. nov. and the previously mentioned species as distinct species and instead groups them together in various large taxonomic units. This over and under grouping

Table 4 Morphological comparisons of mesophotic and deep-sea *Halgerda* spp.

	H. abyssicola	*H. azteca*	*H. fibra*	*H. orstomi*	*H. mesophotica* sp. nov	*H. okinawa*	*H. profunda* sp. nov.	*H. scripta* sp. nov.	*H. takipsilim* sp. nov.
Dorsum	Reticulated ridging, with dark ridge outlines, pronounced pale tubercles	Reticulated ridging, pronounced tubercles, random dark spots	Irregular ridging, pronounced tubercles, radiating thin dark lines	Low reticulated ridging, pronounced tubercles with dark apex, dark spots or lines	Sporadic black spots, extremely large, conical tubercles, radiating brown lines	Large conical yellow tubercles, black ridges, black spots	Irregular dark black ridging large, conical light-yellow tubercles	Large conical tubercles, radiating thin black lines	Large random black spots, irregular brown ridging, prominent conical yellow tubercles
Mantle margin	Perpendicular dark lines and dark spots	Perpendicular dark lines and spots	Small dark spots or lines	Perpendicular dark lines	Thin, white band	Yellow band, sporadic black spots	Thin, white band, small black spots	Thin, white band, numerous black spots	Thin, white band
Gill plume	Four sparsely pinnate branches, large secondary leaves, ventral dark stripe	Two sparsely pinnate branches, four leaves, dorsal dark stripe	Two sparsely pinnate branches, six leaves, dorsal brown stripe, ventral dark spots	Four pinnate branches, three secondary leaves, ventral brown stripe, dorsal dark spots	Four highly bipinnate branches, large secondary leaves, dorsal brown stipe	Four yellow branches, large secondary leaves, black dorsal spots	Four highly bipinnate branches, large secondary leaves, thin black stripes, small black spots	Four branches, large secondary leaves, dorsal black stripe, small black spots	Two bipinnate branches, four leaves, semi-translucent white
Radula formula	35 × 57.0.57	27 × 43.0.43	51 × 65.0.65	43 × 47.0.47	41 × 74.0.74	45 × 49.0.49	48 × 57.0.57	50 × 70.0.70	48 × 52.0.52
No. of smaller inner teeth	10	7–8	8	20	31		15	27	17
Outermost teeth	Three reduced with denticles	Four reduced and curved	Three reduced versions of outer laterals	Three to four reduced with fine denticles	Three reduced versions of outer laterals	Three reduced versions of outer laterals	Three reduced, thinner, and straighter	Three to five reduced, slightly curved	Three reduced, thinner, slightly curved
Vagina	Large, bulbous	Large, bulbous, with sphincter	Large, bulbous	Large, bulbous, with sphincter	Large, wide	Thin, elongate	Large, wide	Large, wide	Slightly wide, elongate
Type locality	Vanuatu	New Caledonia	Philippines	Vanuatu	Philippines	Okinawa	Philippines	Philippines	Philippines
Depth	207–420 m	230–367 m	90–400 + m	92–251 m	60 m	53–76 m	90 m	65–80 m	80–90 m

may be attributed to the low interspecific variation between some of the species within this clade (Table 2). There is a minimum divergence of 3.3%, 1.5%, 2.9%, and 1.1% in the COI gene between *H. anosy* sp. nov. and *H.* cf. *formosa*, *H. dichromis*, *H.* aff *wasinensis*, and the *H. wasinensis* complex, respectfully. There is also minimal intraspecific variation (0.0–0.6%) between the five specimens studied here from South Madagascar.

Morphologically, *H. anosy* sp. nov. is most similar with a specimen of *H.* cf. *formosa* (MHN-YT1682) from Mozambique and *H. wasinensis*. Externally, the dorsum coloration of *H. anosy* sp. nov. is bluish white with many dark brown to black spots along the mantle edge, low yellow ridging with semi-projected yellow tubercles at ridge junctions, and either a single large or two conjoined small dark brown to black spots present within ridge depressions. In contrast, the dorsum coloration of *H.* cf. *formosa* is whitish with a gray tinge and a handful of large dark brown to black spots along the mantle edge and occasionally present in some of the low, angled, yellow ridge depressions (Tibiriçá et al. 2018, Fig. 3a). There are no tubercles at the ridge junctions; however, there are numerous minute white tubercles along the mantle edge. Both species have a thin white mantle band along the mantle edge, semi-visibility of the dark brown to black spots through the mantle underside, and several smaller dark brown to black spots along the foot. The gill plumes are distinct as *H. anosy* sp. nov. has four large bluish white bipinnate gill branches, each with a central anterior dark brown to black stripe and bluish white rachises, while in *H.* cf. *formosa* the gill plume is whiter with four large tripinnate branchial leaves each with black-lined branches and black branch tips. The rhinophores are similar between the two species with dark brown to black lamellae and a white apical tip; however, in *H. anosy* sp. nov., the posterior dark brown to black spots along the rhinophoral stalk are much smaller than the posterior, longitudinal band seen in *H.* cf. *formosa*. *Halgereda wasinensis* is highly variable in the amount of black pigment present (Tibiriçá et al. 2018) but always has at least some irregular dark blotches rather than the regular spots that form circles or ovals in *H. anosy* sp. nov. The ridge network lines of *H. anosy* sp. nov. are more distinctly yellow in contrast to orange lines of *H. wasinensis*. The base of the gill branches in *H. wasinensis* is thick with a much more extensive area of opaque white than in *H. anosy* sp. nov. In *H. wasinensis* the posterior base of the rhinophores has an extensive black line that extends the entire length of the rhinophore stalk in contrast to an isolated black spot at the base of the rhinophore stalk in *H. anosy* sp. nov.

Internally, both *H. anosy* sp. nov. and *H.* cf. *formosa* have unpigmented buccal masses in contrast to that described for *H. wasinensis* (Rudman 1978; Tibiriçá et al. 2018), however, in *H. anosy* sp. nov., there are small dark spots around the buccal opening and the radular sac is short and rounded, whereas in *H.* cf. *formosa*, there is no mention of the presence or absence of pigment around the buccal opening and the radular sac is more elongate. In *H. anosy* sp. nov. and *H. wasinensis* (Rudman 1978; Tibiriçá et al. 2018), the inner lateral teeth are small with curved, elongate, rounded cusps which form a spaced-out V shape in the center of the radula, while in *H.* cf. *formosa* the inner lateral teeth are less elongate and much more tightly packed to form a steep V shape in the radula center (Tibiriçá et al. 2018, Fig. 4b). The middle teeth are larger and less elongate in *H. anosy* sp. nov. with more rounded tips than in *H.* cf. *formosa* or *H. wasinensis*, and the outermost two teeth are reduced and semi-fimbriate. In *H.* cf. *formosa* the middle teeth are also larger, but more elongate than those in *H. anosy* sp. nov. and the tips are more pointed (Tibiriçá et al. 2018, Fig. 4c). The three outermost teeth in *H.* cf. *formosa* are also reduced, but much more fimbriate (Tibiriçá et al. 2018, Fig. 4d) than are those of *H. anosy* or *H. wasinensis*. All three species reproductive systems share some similarities including a small receptaculum seminis, an elongate ejaculatory portion, a large penis, and deep finger-like projections in the proximal portion of the vagina. Notable differences from *H.* cf. *formosa* include a much larger female gland mass in *H. anosy* sp. nov. and *H. wasinensis* and the bursa copulatrix is only partially covered by the granular portion of the prostate. The differences in the size of the female gland mass could be easily due to different levels of maturity in the specimens examined. More significantly, in *H.* cf. *formosa and H. wasinensis,* there is a muscular sphincter at the entry to the vagina which is absent in *H. anosy* sp. nov. (Tibiriçá et al. 2018, Fig. 5a, b). The pronounced internal and external differences between *H. anosy* sp. nov., *H. wasinensis*, and *H.* cf. *formosa* (MHN-YT1682) supports *H. anosy* sp. nov. as new species within *Halgerda*.

Halgerda mesophotica Donohoo & Gosliner sp. nov.
https://zoobank.org/E20B641A-6EFF-40F4-A69C-C491BFD21A46
(Fig. 16a, 17a, 18 and 19a)

Halgerda sp. 4 Gosliner et al. (2015): 190, top right photograph. *Halgerda* sp. 11 Gosliner et al. (2018): 112, top right photograph. *Halgerda* sp. Stiefel (2011).

Type material: Holotype, One specimen, NMP 041324, formerly CASIZ 193832, dissected and sequenced, 55 mm preserved, type locality: Mapating, Tingloy, Balayan Bay, Luzon Island, Philippines, 61 m depth, 11 December 2013, collected by E. Jessup.

Type locality: Mapating, Tingloy, Balayan Bay, Luzon Island, Philippines.

Etymology: The name *mesophotica* refers to the depth (i.e. the middle mesophotic zone) in which this species is found.

External morphology: Preserved animal 55 mm in length (Fig. 16a, Supplementary Figure S6a). Body oval, semi-rigid,

and gelatinous. Dorsum color translucent white with sporadic small dark brown/black spots and extremely large, conical tubercles. Central tubercles with series of radiating thick brown lines. Outer tubercles shorter with no coloration. Thin, white mantle band along mantle edge. Mantle underside translucent white with random small to medium brown and dark brown spots near foot. Elevated gill surrounds anus with four pinnate/bipinnate branchial leaves split into two posterior and two anterior gill branches. Each posterior branch splits into two–three large secondary branches. Gill branches long, thin with few very short pinnae extending from each branch. Leaves and rachis translucent white with thick brown dorsal stripe. White glands visible in gill branches. Gill sheath smooth with similar dorsum coloration and radiating series of brown lines. Rhinophores long, tapered, and perfoliate with 34 cream-colored lamellae. Rhinophoral stalk and lamellae translucent white with posterior dark brown stripe. Rhinophoral sheath smooth with similar dorsum coloration and brown lines. Foot is broad, anteriorly notched, and translucent white. Oral tentacles digitiform.

Internal anatomy (Fig. 17a, 18a–d and 19a): Buccal mass (Fig. 17a) unpigmented. Buccal bulb 1.5 × longer than elongate oral tube. Radular sac elongate, irregular shaped, and unpigmented. Labial cuticle smooth. Radula composed of smooth hamate teeth with no denticles (Fig. 18a). Radular formula 41 × 74.0.74 in the holotype NMP 041324. Inner 31 lateral teeth (Fig. 18b) small, broad-based with elongated stems, sharply curved elongated cusps form a V in the center. Middle lateral teeth (Fig. 18c) larger than inner laterals with more curved, elongated, rounded cusps. Outer lateral teeth (Fig. 18d) larger and thicker than middle laterals. Outermost three teeth reduced versions of the outer laterals with more pointed tips.

Reproductive system (Fig. 19a): Triaulic. Thin preampullary duct quickly widens into thick ampulla, then narrows into postampullary duct which splits into the vas deferens and oviduct. Vas deferens rapidly expands into wide, elongate, and curved granular prostate which abruptly narrows gradually into thin, elongate, curved ejaculatory portion. Ejaculatory portion rapidly expands into large, wide penis and shares common genital atrium with similarly sized vagina. Large, wide vagina abruptly narrows proximally into very thin, elongate duct and enters large, rounded bursa copulatrix partially covered by granular prostate. Very thin, elongate duct connects bursa to smaller, tapered receptaculum seminis. Thin, semi-elongate uterine duct connects near receptaculum base and enters medium-sized, irregularly pyriform-shaped female gland mass.

Geographical distribution: Known from the Philippines.

Ecology: Found on deep reefs in the mesophotic zone at approximately 60–70 m (Steifel 2011).

Remarks: In our molecular phylogeny, *Halgerda mesophotica* sp. nov. is part of a well-supported mesophotic clade including *H. scripta* sp. nov., *H. okinawa*, *H. profunda* sp. nov., and *H. takipsilim* sp. nov. The COI and 16S ABGD, the COI ASAP, the GYMC, and bPTP analyses successfully separates *H. mesophotica* sp. nov. from *H. okinawa* and *H. scripta* sp. nov.; however, the 16S ASAP analysis does group *H. mesophotica* sp. nov. with one specimen of *H. scripta* sp. nov. and the rest of the mesophotic clades. There are genetic differences greater than 5.5% in the COI gene; however, all four delimitation analyses group *H. mesophotica* sp. nov. with *H. profunda* sp. nov. and *H. takipsilim* sp. nov. This may be attributed to the low genetic divergences (0.9–1.5%) in the COI gene between the three species; however, there are strong morphological differences in each species (summarized in Table 4). Therefore, *H. mesophotica* sp. nov. is morphologically compared with *H. profunda* sp. nov. and *H. takipsilim* sp. nov. in the *H. takipsilim* sp. nov. remarks section below.

Halgerda profunda Donohoo & Gosliner sp. nov.
https://zoobank.org/2FC8EF5F-4198-4DDC-9F70-D0E3671CF95D
(Fig. 16b, 17b, 19b and 20)

Halgerda sp. 5 Gosliner et al. (2015): 190, middle left photograph. *Halgerda* sp. 12 Gosliner et al. (2018): 112, middle left photograph.

Type material: Holotype, One specimen, NMP 041325, formerly CASIZ 201240, dissected and sequenced, 60 mm preserved, type locality: Lubang (13° 45′ 41.6″ N 120° 07′ 47.2″ E), Lubang Island, Occidental Mindoro, Philippines, 91.45 m depth, 15 May 2014, collected by the VIP Team.

Type locality: Lubang, Lubang Island, Occidental Mindoro, Philippines.

Etymology: This species is named "profunda" after the Latin word for deep and refers to the deep depths of the lower mesophotic zone in which this species is found.

External morphology: Preserved animal 60 mm in length (Fig. 16b). Body oval, rigid, and gelatinous. Dorsum color translucent white with small black spots along mantle edge. Irregular dark black ridging with large, conical light yellow-tipped tubercles. Thin, white mantle band along mantle edge. Mantle underside translucent white with small dark brown/black spots near mantle edge. Elevated gill surrounds anus with four highly bipinnate branchial leaves split into two posterior and two anterior gill branches. Each posterior branch splits into two–three large secondary branches each bearing an elongate lateral pinnae. Leaves and rachis translucent white with dorsal thin black stripes and small black spots. Thin area of white glands visible in gill branches. Anal papilla with black pigment at apex. Gill sheath smooth with similar dorsum coloration and small black spots. Rhinophores tapered, and perfoliate with 24 cream-colored lamellae. Rhinophoral stalk and lamellae translucent white with posterior black stripe. Rhinophoral sheath smooth with similar dorsum coloration and radiating black lines. Foot is

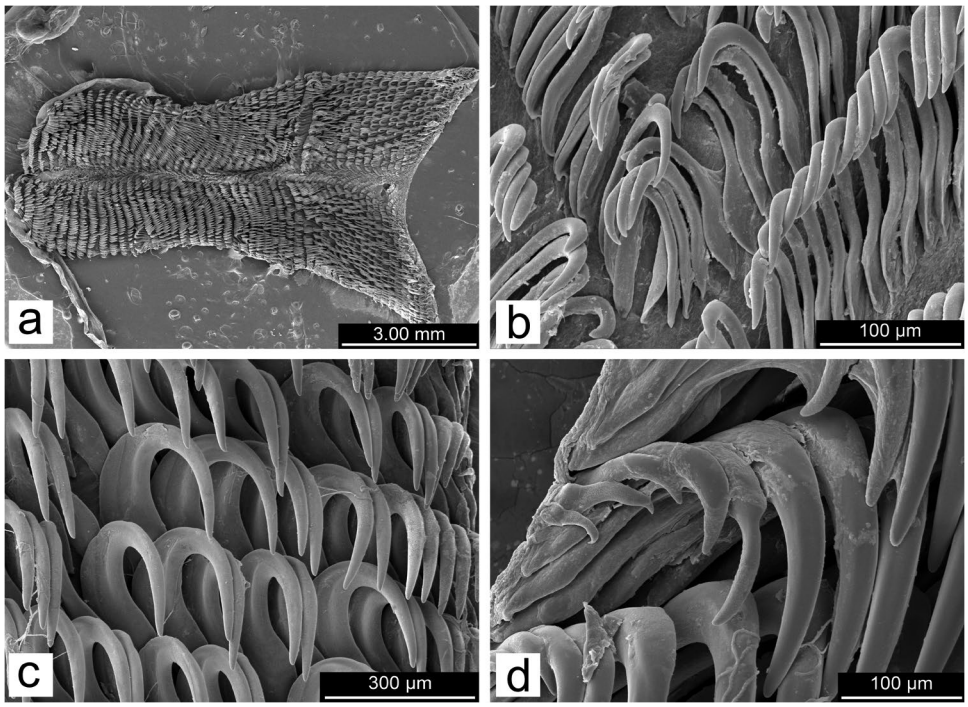

Fig. 22 *Halgerda scripta* sp. nov., holotype, NMP 041326, scanning electron micrographs of radula: **a** Entire radula; **b** inner lateral teeth; **c** mid-lateral teeth; **d** outer lateral teeth

broad, anteriorly notched, translucent white with small dark brown/black spots and medium dark brown/black blotches. Oral tentacles digitiform.

Internal anatomy (Fig. 17b, 19b and 20a–d): Buccal mass (Fig. 17b) unpigmented; however, dark brown/black blotches present around buccal opening. Buccal bulb 2 × longer than oral tube. Radular sac short, rounded, and unpigmented. Labial cuticle smooth. Radula composed of smooth hamate teeth with no denticles (Fig. 20a). Radular formula 48 × 57.0.57 in the holotype NMP 041325. Inner 15 lateral teeth (Fig. 20b) small, broad-based with thin elongated stems and thin elongated cusps form a V in the center. Middle lateral teeth (Fig. 20c) larger and thicker than inner laterals with more sharply curved cusps and rounded tips. Outer lateral teeth (Fig. 20d) larger and thicker than middle laterals with shorter curved cusps. Outermost three teeth reduced, thinner, and straighter than other teeth with slightly curved tips.

Reproductive system (Fig. 19b): Triaulic. Thin, elongate preampullary duct gradually widens into semi-thick ampulla, then quickly narrows into postampullary duct which splits into vas deferens and oviduct. Vas deferens quickly expands into wide, elongate, and looped granular prostate which abruptly narrows into thin, very elongate, and looped ejaculatory portion. Ejaculatory portion rapidly expands into large, wide penis which shares common genital atrium with slightly thinner, similarly sized vagina. Large, wide vagina quickly narrows proximally into gradually thinning duct and enters large, rounded bursa copulatrix partially covered by granular prostate. Thin, elongate duct connects bursa to small, thin oblong receptaculum seminis. Short, thin uterine duct connects near receptaculum base and enters large, semi-pyriform shaped female gland mass.

Geographical distribution: Known from the Philippines (Gosliner et al. 2015, 2018; present study).

Ecology: Found on deep reefs in the mesophotic zone at approximately 90 m.

Remarks: In the mesophotic clade, *Halgerda profunda* sp. nov. is sister to *H. takipsilim* sp. nov. and is successfully separated from *H. okinawa* and *H. scripta* sp. nov. during all but the 16S ASAP analyses. The COI ABGD revealed genetic differences greater than 5.8% in the COI gene between *H. profunda* sp. nov. and the previously mentioned species. Since there are low genetic differences between *H. profunda* sp. nov., *H. mesophotica* sp. nov., and *H. takipsilim* sp. nov. all three species are morphologically compared below in the remarks section following *H. takipsilim* sp. nov and summarized in Table 4.

Halgerda takipsilim Donohoo and Gosliner sp. nov.
https://zoobank.org/8D18AF28-4A4A-4882-AB6C-F3FBB34EBAC2
(Fig. 16c, 17c, 19c and 21)

Halgerda sp. 6 Gosliner et al. (2015): 190, middle right photograph. *Halgerda* sp. 13 Gosliner et al. (2018): 112, middle right photograph.

Type material: Holotype, One specimen, NMP 041327, formerly CASIZ 204791, dissected and sequenced, 45 mm preserved, type locality: South Pinnacle (13° 31′ 59.5″ N 121° 06′ 11.8″ E), Verde Island, Luzon Island, Philippines, 80 m depth, 13 April 2015, collected by E. Jessup. Paratype: One specimen, CASIZ 201241, sequenced, 30 mm

preserved, type locality: Lubang (13° 45′ 41.6″ N 120° 07′ 47.2″ E), Lubang Island, Occidental Mindoro, Philippines, 91.45 m depth, 15 May 2014, collected by the VIP Team.

Type locality: South Pinnacle, Verde Island, Luzon Island, Philippines.

Etymology: This species is named "takipsilim" after the Filipino word for twilight and refers to the great depths (i.e., the lower mesophotic zone) in which this species is found.

External morphology: Preserved animal 30–45 mm in length (Fig. 16c). Body oval, semi-rigid, and gelatinous. Dorsum color semi-translucent white with randomly distributed large black spots. Irregular brown ridging with large, conical bright yellow-tipped, rounded tubercles. Thin, white mantle band along mantle edge. Mantle underside semi-translucent white with sporadic small brown spots. Elevated gill surrounds anus with four highly bipinnate, branchial leaves split into two posterior and two split anterior gill branches. Each posterior branch splits into two–three large secondary branches. Leaves and rachis semi-translucent white with small brown dotted dorsal lines and numerous small single brown spots. White glands visible in gill branches. Anal papilla without dark pigment. Gill sheath smooth with similar dorsum coloration. Rhinophores elongated, tapered, and perfoliate with 37–40 light yellow lamellae. Rhinophoral stalk semi-translucent white with posterior dark brown stripe and small black spot. Rhinophoral sheath smooth with similar dorsum coloration. Foot is broad, anteriorly notched, and semi-translucent white. Ring of small dark brown/black spots near foot bottom. Ring of large brown blotches near top of foot connecting to mantle. Oral tentacles digitiform.

Internal anatomy (Figs. 17c, 19 and 21a–d): Buccal mass (Fig. 17c) unpigmented; however, small brown flecks/spots present around buccal opening. Oral tube 1.5 × longer than buccal bulb. Radular sac semi-elongate, irregularly rounded, and unpigmented. Labial cuticle smooth. Radula composed of smooth hamate teeth with no denticles (Fig. 21a). Radular formula 48 × 52.0.52 in the holotype NMP 041327. Inner 17 lateral teeth (Fig. 21b) small, broad-based with short, highly curled cusps form a V in the center. Middle lateral teeth (Fig. 21c) larger and thicker than inner laterals with more elongated, sharply curved cusps. Outer lateral teeth (Fig. 21d) larger and thicker than middle laterals with shorter, rounded cusps. Outermost three teeth reduced, thinner, and slightly more curved than other lateral teeth.

Reproductive system (Fig. 19c): Triaulic. Thin, elongate preampullary duct gradually widens into slightly wide ampulla, then gradually narrows into postampullary duct which splits into short oviduct and short vas deferens. Vas deferens gradually expands into wide, elongate, looped granular prostate and then abruptly narrows into thin, elongated, and curved ejaculatory portion. Ejaculatory portion rapidly expands into large, wide penis which shares common genital atrium much smaller and thinner vagina. Slightly wide, elongate vagina narrows proximally into thinner, elongated duct and enters large, rounded bursa copulatrix partially covered by granular prostate. Very thin, elongate duct connects bursa to thin, elongate, oblong-shaped receptaculum seminis. Short, thin uterine duct connects near receptaculum base and enters small-medium sized irregularly rounded female gland mass.

Geographical distribution: Known only from the Philippines.

Ecology: Found on deep reefs in the mesophotic zone between 80–90 m.

Remarks: In all of our delimitation analyses, *H. mesophotica* sp. nov., *H. profunda* sp. nov., and *H. takipsilim* sp. nov. are grouped together as a single taxonomic unit due to low genetic differences. All three species were found originally in the Philippines; however, *H. mesophotica* sp. nov. was found in Balayan Bay at a slightly shallower depth (60 m), *H. profunda* sp. nov. was found at Lubang Island at 90 m in depth, and *H. takipsilim* sp. nov. was found at Verde Island at 80 m depth and at Lubang Island at 90 m in depth. Externally, all three species have a semi-translucent/translucent white dorsum with sporadic small black spots; large, rounded to conical tubercles; spots along the mantle underside and foot; and a thin white mantle band; however, there are distinct patterns in the ridging and tubercles. In *H. profunda* sp. nov., the irregular ridging is dark black in color with large, yellow-tipped conical tubercles, whereas in *H. takipsilim* sp. nov., the irregular ridging is brown, and the bright yellow-tipped tubercles have a broader base and a quickly elongating, more rounded tip. In *H. mesophotica* sp. nov., there is no ridging, and each tubercle has a series of brown lines radiating from the tip. The rhinophores and gills also vary between the three species. All three have the dark posterior stripe along the rhinophoral stalk, but it varies in color. In *H. mesophotica* sp. nov. and *H. takipsilim* sp. nov., the stripe is dark brown, while in *H. profunda* sp. nov., the stripe is black. Additionally, the lamellae in *H. takipsilim* sp. nov. are light-yellow in color, rather than cream as seen in *H. mesophotica* sp. nov. and *H. profunda* sp. nov. All three species have a gill composed of four bipinnate leaves with two anterior branches and two posterior branches with two to three large secondary branches; however, the branching of the gill, coloration, and patterning vary. In *H. mesophotica* sp. nov., the gill branches are thin and elongate with very short pinnae as is found in *H. scripta* sp. nov. In *H. profunda* sp. nov., the gill branches are elongate and wide with elongate lamellae, whereas in *H. takipsilim* sp. nov., the gill branches are short with fewer pinnae that have very faint dark pigment. In *H. mesophotica* sp. nov., the leaves and rachises are translucent white with a thick brown dorsal stripe and radiating brown lines along the gill sheath, while in *H. profunda* sp. nov., the leaves and rachises are

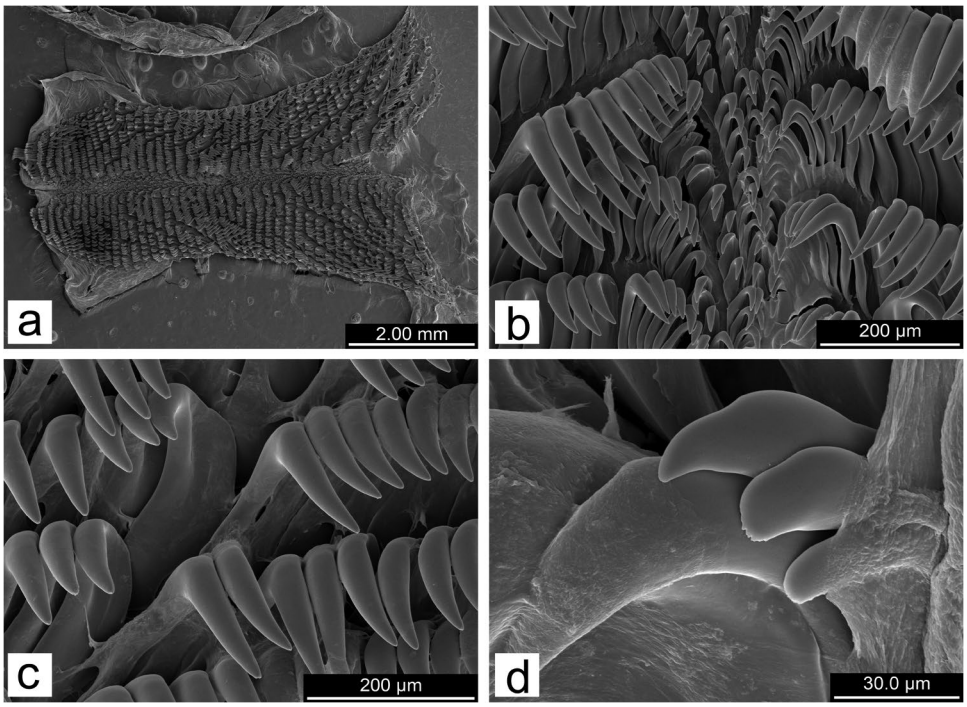

Fig. 23 *Halgerda hervei* sp. nov., holotype, CASIZ 186494, scanning electron micrographs of radula.: **a** Entire radula;, **b** inner lateral teeth;, **c** mid-lateral teeth;, and **d** outer lateral teeth

translucent white, and the dorsal stripes are thin and black with extra small black spots. In *H. takipsilim* sp. nov., the leaves and rachises are semi-translucent cream with small brown dotted lines and numerous single brown spots along the dorsal side.

Internally, the buccal mass, radular teeth and the reproductive systems are similar, but there are noticeable differences. The buccal mass of *H. mesophotica* sp. nov. and *H. profunda* sp. nov. is larger than the oral tube and the radular sac is elongate in *H. mesophotica* sp. nov. but short in *H. profunda* sp. nov. In contrast, *H. takipsilim* sp. nov., the buccal mass is much shorter than the oral tube and the radular sac is moderately elongate. In *H. mesophotica* sp. nov., there are no markings around the buccal opening, while there are dark brown/black blotches around the buccal opening in *H. profunda* sp. nov. and small brown flecks/spots in *H. takipsilim* sp. nov. The radular teeth in *H. mesophotica* sp. nov. include 31 small inner lateral teeth with elongated stems and sharpy curved cusps, while in *H. profunda* sp. nov., there are only 15 small inner lateral teeth with thin elongated stems and thin elongated cusps, and in *H. takipsilim* sp. nov., there are only 17 small inner lateral teeth with elongated stems and short, highly curved cusps. All three species have similar middle and outer lateral teeth (i.e., larger and more elongated); however, in *H. mesophotica* sp. nov., the three outermost teeth are reduced versions of the outer laterals with more pointed tips. In contrast, the three outermost teeth in *H. profunda* sp. nov. are reduced, thinner, straighter, and only slightly curved at the tips. The outermost three teeth in *H. takipsilim* sp. nov. are also reduced and thinner but more curved than in *H. profunda* sp. nov. and less elongated than those in *H. mesophotica* sp. nov.

In all three species the reproductive system is composed of a large, spherical bursa copulatrix partially covered by the granular portion of the prostate; a large penis approximately half the width of the bursa; and a much smaller receptaculum seminis. In *H. mesophotica* sp. nov. and *H. profunda* sp. nov., the vagina is a similar size to the penis, but in *H. takipsilim* sp. nov., the vagina is much smaller and more elongated. The ejaculatory portion of the prostate is elongated in all three species, but in *H. mesophotica* sp. nov. and *H. takipsilim* sp. nov. it only curves once or twice and in *H. profunda* sp. nov. it is looped and twice as long. The size and length of the ducts connecting the proximal end of the vagina to the bursa copulatrix and the bursa to the split into the receptaculum seminis/uterine duct also varies between species. In *H. mesophotica* sp. nov., both ducts are thin, elongated and a similar length, whereas in *H. profunda* sp. nov., the vagina to bursa duct is initially wide and then gradually narrows and the bursa to receptaculum duct is consistently thin. In *H. takipsilim* sp. nov. both ducts are a similar length; however, the vagina to bursa duct is twice as thick as the bursa to receptaculum duct. The female gland mass is a similar size in *H. mesophotica* sp. nov. and *H. takipsilim* sp. nov., but twice as large in *H. profunda* sp. nov.

Despite the similarities between *H. mesophotica* sp. nov., *H. profunda* sp. nov., and *H. takipsilim* sp. nov., there are consistent, unique internal and external characteristics

(Table 4) that separate these three species from one another and support their distinctness as species within *Halgerda*. Examination of five specimens *H. scripta* sp. nov. below demonstrates the consistency of color pattern in species of this clade and further supports the distinctness of the other members of this clade, based on features of their color pattern.

Halgerda scripta Donohoo & Gosliner sp. nov.
https://zoobank.org/54C1BFC7-21E9-447E-8B74-3FDA94C7D574
(Fig. 16d–e, 17d, 19d and 22)

Halgerda sp. 7 Gosliner et al. (2015): 190, bottom left photograph. *Halgerda* sp. 14 Gosliner et al. (2018): 112, bottom left photograph.

Type material: Holotype, One specimen, NMP 041326, formerly CASIZ 204,788, dissected and sequenced, 50 mm preserved, type locality: South Pinnacle (13° 31′ 59.5″ N 121° 06′ 11.8″ E), Verde Island, Luzon Island, Philippines, 80 m depth, 13 April 2015, collected by E. Jessup and L. Rocha. Paratypes: One specimen, CASIZ 193823, dissected and sequenced, 35 mm preserved, type locality: Kirby's Rock (13° 41′ 40.6″ N 120° 50′ 32.5″ E), Maricaban Island, Batangas Province, Luzon, Philippines, 70 m depth, 12 December 2013, collected by L. Rocha. One specimen, CASIZ 201239, sequenced, 45 mm preserved, type locality: Lubang (13° 45′ 41.6″ N 120° 07′ 47.2″ E), Lubang Island, Occidental Mindoro Province, Philippines, 91.5 m depth, 15 May 2014, collected by the VIP Team. Other material examined: One specimen, CASIZ 204787, sequenced, 35 mm preserved, type locality: South Pinnacle (13° 31′ 59.5″ N 121° 06′ 11.8″ E), Verde Island, Luzon Island, Philippines, 80 m depth, 13 April 2015, collected by L. Rocha. One specimen, CASIZ 204789, sequenced, 45 mm preserved, locality: Blackfish Corner (13° 34′ 31.7″ N 121° 02′ 30.0″ E), Verde Island, Luzon Island, Philippines, 66–80 m depth, 16 April 2015, collected by B. Shepherd.

Type locality: South Pinnacle, Verde Island, Luzon Island, Philippines.

Etymology: The name *scripta* refers to the fine, script like linework ornamenting the dorsum of this species.

External morphology: Preserved animals 35–50 mm in length (Fig. 16d, e). Body oval, rigid, and gelatinous. Dorsum color bluish white with numerous medium black spots along mantle margin. Large conical tubercles with radiating thin black lines. Thin, white mantle band along mantle edge. Mantle underside bluish white with random small to medium brown/dark brown spots. Elevated gill surrounds anus with four bipinnate branchial leaves split into two posterior and two anterior gill branches. Each posterior branch splits into two–three large secondary branches. Leaves and rachis semi-translucent white with dorsal black stripe and random small black spots. White glands visible in gill branches. Anal papilla unpigmented or with black pigment at apex. Gill sheath smooth with similar dorsum coloration and radiating series of thin black lines. Rhinophores long, tapered, and perfoliate with 32–35 cream-colored lamellae. Rhinophoral stalk semi-translucent white with posterior black stripe and small lateral black spots. Rhinophoral sheath smooth with similar dorsum coloration and radiating thin black lines. Foot is broad, anteriorly notched, and bluish white with small random dark brown/black spots. Oral tentacles digitiform.

Internal anatomy (Figs. 17d, 19d and 22a–d): Buccal mass (Fig. 17d) unpigmented; however, small dark brown/black spots present around buccal opening. Buccal bulb approximately 2.5 × larger than oral tube. Radular sac elongate, semi-folded over, and unpigmented. Labial cuticle smooth. Radula composed of smooth hamate teeth with no denticles (Fig. 22a). Radular formula 50 × 70.0.70 in the holotype NMP 041326 and 45 × 50.0.50 in the paratype CASIZ 193823. In NMP 041326 inner 27 lateral teeth (Fig. 22b) small, broad-based with elongated sharply curved cusps form a steep V in the center. Middle lateral teeth (Fig. 22c) are larger, thicker than inner laterals with longer curved cusps and rounded tips. Outer lateral teeth (Fig. 22d) are larger, thicker, and less curved than middle laterals. Outermost three to five teeth gradually reduced with slightly curved tips.

Reproductive system (Fig. 19d): Triaulic. Thin preampullary duct gradually widens into thick ampulla, then gradually narrows into postampullary duct which splits into short vas deferens and short oviduct. Vas deferens rapidly expands into wide, extremely elongate, fairly straight granular prostate which abruptly narrows into thin, elongate, and looped ejaculatory portion. Ejaculatory portion quickly expands into very large, wide penis, which shares common genital atrium with slightly smaller vagina. Wide vagina, half-length of penis, abruptly narrows proximally into thin elongate duct and enters into large, rounded bursa copulatrix partially covered by granular prostate. Very thin, elongate duct connects bursa to small, oval-shaped receptaculum seminis. Short, very thin uterine duct connects near receptaculum base and enters large female gland mass.

Geographical distribution: Known from the Verde Island Passage, Philippines.

Ecology: Found on deep reefs in the mesophotic zone between 65–80 m.

Remarks: Our molecular phylogeny places *Halgerda scripta* sp. nov. at the base of a mesophotic clade including *H. okinawa*, *H. mesophotica* sp. nov., *H. profunda* sp. nov., and *H. takipsilim* sp. nov. The species delimitation analyses clearly indicate that *H. scripta* sp. nov. is a distinct species within the mesophotic clade with a genetic divergence of 6.7–8.2% in the COI gene. However, our 16S ABGD and ASAP analyses grouped one specimen of *H. scripta* sp. nov.

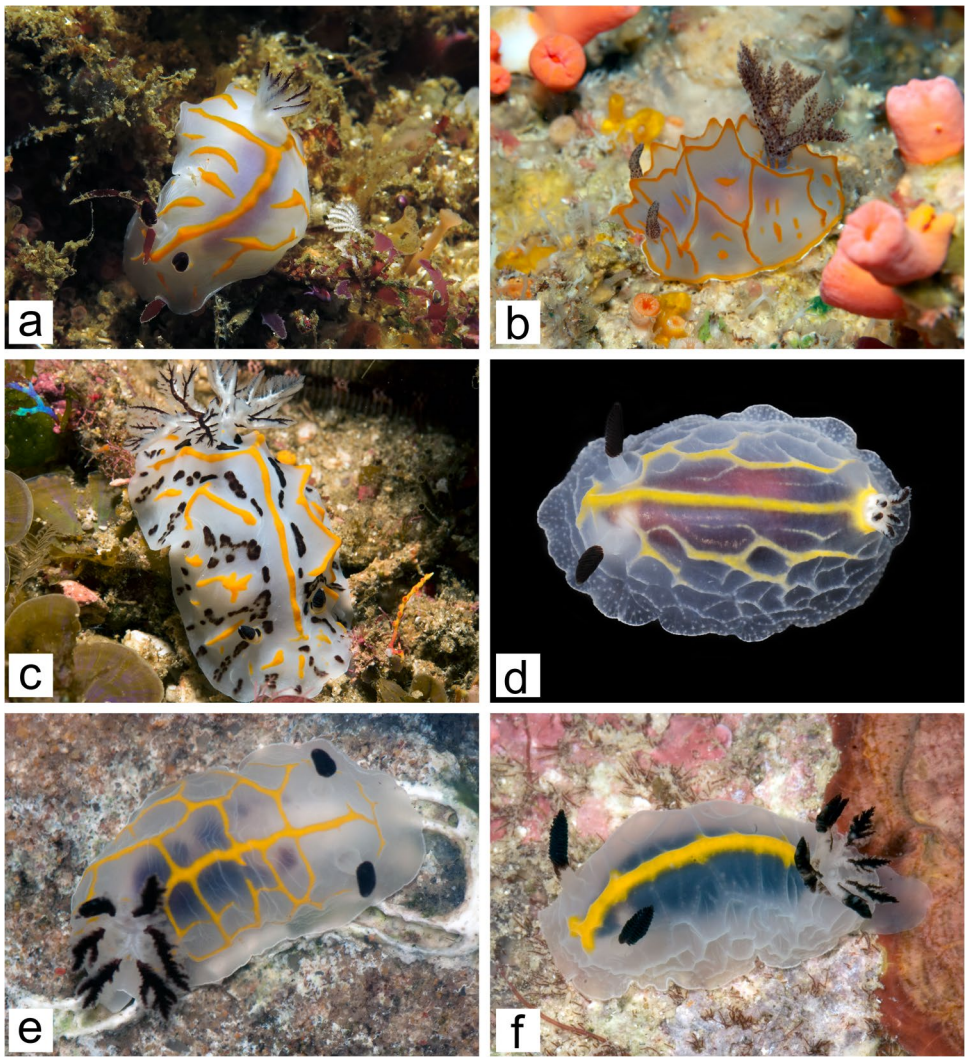

Fig. 24 Living specimens: **a** *Halgerda maaikeae* sp. nov., holotype, SAMC-A094639, Aliwal Shoal, South Africa, photo by Brian Sellick; **b** *Halgerda diaphana* Fahey & Gosliner, 1999b, UF 351996, Okinawa, Japan, photo by Gustav Paulay; **c** *Halgerda dichromis* Fahey & Gosliner, 1999a, CASIZ 231104, KwaZulu-Natal, South Africa, photo by Brian Sellick; **d** *Halgerda pattiae* sp. nov., holotype, UF 422800, Mayotte Island, France, photo by Arthur Anker and François Michonneau; **e** *Halgerda meringuecitrea* Tibiriçá et al., 2018, MB28-004527, Zavora, Mozambique, photo by Yara Tibiriçá; **f** *Halgerda radamaensis* sp. nov., holotype, CASIZ 173456, Iles Radama, Madagascar, photo by T.M. Gosliner

with *H. mesophotica* sp. nov., *H. profunda* sp. nov., and *H. takipsilim* sp. nov. and our COI ABGD and bPTP analyses over-partitioned the same specimen of *H. scripta* sp. nov. collected on Maricaban Island (CASIZ 193823) from the other four specimens including the holotype NMP 041326 collected on Verde Island. Externally, this paratype specimen is smaller than either the holotype or the other paratypes. Internally, there are fewer inner lateral teeth and fewer rows; however, there are no discernable differences between the paratype and holotype reproductive systems (Supplementary Figure S7). Ong et al. (2017) suggested that there may be genetic isolation within the Verde Island Passage (VIP) after they found an intraspecific genetic divergence of 1.7% in the COI gene between two Gastropteridae specimens collected 22 km apart on the north and south sides of the VIP. This may explain the high maximum intraspecific genetic divergence of 2.2% between the *H. scripta* sp. nov. specimen CASIZ 193823 and the holotype NMP 041326 since there is a 21 km separation between Maricaban Island and the Verde Island.

Halgerda scripta sp. nov. shares some morphological similarities with other members of the mesophotic clade (Table 4); however, it most similar with *H. jennyae* in its color pattern. Externally, the dorsum coloration of *H. scripta* sp. nov. is bluish white with prominent conical tubercles and radiating thin black lines, numerous medium black spots along the mantle margin with a thin white mantle band, small random dark brown/black spots along the foot, and small to medium brown/dark brown spots along the underside of the mantle. In contrast, *H. jennyae* has a translucent white dorsum with high tubercles, a complex pattern of thin brown lines along the irregular ridges and valleys, a thin white mantle band, and the foot and mantle underside have numerous small to medium brown spots (Tibiriçá et al. 2018, Figs. 11d, e). There are also differences in the coloration of the rhinophores and gills. In *H. scripta* sp. nov., the rhinophores are semi-translucent white with cream lamellae and a posterior black stripe and small lateral black spots, whereas in *H. jennyae* the rhinophore stalks are translucent with yellowish lamellae and brown lines on the dorsal and

lateral sides. The gill in *H. jennyae* is translucent white the numerous brown spots, while in *H. scripta* sp. nov., the gill is semi-translucent white with a dorsal black stripe and random small black spots.

Internally, the buccal mass of *H. scripta* sp. nov. is unpigmented and the radular teeth are similar to other *Halgerda*; however, there are 27 small inner teeth which from a sharp V in the center of the radula. Additionally, the middle and outer lateral teeth have long curved cusps with rounded tips and the outermost three to five teeth gradually reduce in size and curvature. In *H. jennyae* the buccal mass is pigmented and the radular teeth are pigmented in yellow or gold. The inner 16–18 lateral teeth are similar to *H. scripta* sp. nov.; however, the middle and outer lateral teeth are much thicker the entire length of the curved cusp (Tibiriçá et al. 2018, Fig. 15a–c). The outermost three to five teeth are also slightly more curved than those in *H. scripta* sp. nov. (Tibiriçá et al. 2018, Fig. 15d). The reproductive system varies as *H. scripta* sp. nov. has a small receptaculum seminis; a large penis connected to an extremely elongate and looped ejaculatory portion; a slightly shorter, vagina; and a large, rounded bursa copulatrix which is only slightly covered by a portion of the elongated granular prostate. In contrast, the receptaculum seminis in *H. jennyae* is slightly larger though similarly shaped to *H. scripta* sp. nov.; the penis and vagina are small, similarly sized and the ejaculatory portion is much shorter; and the granular prostate completely covers the slightly smaller bursa copulatrix (Tibiriçá et al. 2018, Fig. 14b).

There are some morphological similarities between *H. scripta* sp. nov. and *H. jennyae*; however, our molecular analyses clearly indicate that these are two distinct species as they are found in completely different clades and separated by a minimum divergence of 7.5% in the COI gene.

Halgerda hervei Donohoo & Gosliner sp. nov.
https://zoobank.org/C5A09FCC-573C-4FB8-AF4C-3D3C0560B71F
(Fig. 16f, 17e, 19e and 23)

Halgerda sp. 1 Hervé (2010): 197–198. *Halgerda* sp. 8 Gosliner et al. (2015): 191, top left photograph. *Halgerda* sp. 3 Gosliner et al. (2008): 183, first photograph. *Halgerda* sp. 5 Debelius and Kuiter (2007): 229, bottom two photographs. *Halgerda* sp. 15 Gosliner et al. (2018): 113, top left photograph. *Halgerda* sp. Bas (2022).

Type material: Holotype, One specimen, CASIZ 186494, dissected, 40 mm alive, type locality: La Joliette (21° 36′ 49.4″ S 166° 14′ 54.7″ E), Thio, New Caledonia Lagoon, New Caledonia, 15 m depth, 27 May 2006, collected by Jean-François Hervé.

Type locality: La Joliette, Thio, New Caledonia Lagoon, New Caledonia.

Etymology: This species is named in honor of Jean-François Hervé, who collected and photographed the type specimen from New Caledonia.

External morphology: Preserved animal 40 mm in length (Fig. 16f, Supplementary Figures S6b–d). Body oval, semi-rigid, and gelatinous. Dorsum color semi-translucent white with sporadic small black spots. Irregular dark brown/black ridging with large, pronounced tubercles at junctions. tubercles semi-translucent white with series of connected radiating dark brown/black lines. Thin, white mantle band and perpendicular dark brown/black lines along mantle edge. Mantle underside semi-translucent white with occasional small to medium light brown spots. Elevated gill surrounds unpigmented anus with two bipinnate, branchial leaves split into two posterior and two anterior gill branches. Upper one-third of leaves and rachis translucent white with thin dark brown/black dorsal stripes. Lower two-thirds of leaves translucent yellow with ventral dark brown/black spots. White glands visible in gill branches. Gill sheath smooth with similar dorsum coloration and radiating series of black lines. Rhinophores long, tapered, and perfoliate with 26 lamellae. Rhinophoral stalk and lamellae translucent white with posterior dark brown/black stripe. Small black spots present near stalk base. Rhinophoral sheath smooth with similar dorsum coloration, small black spots, and radiating black lines. Foot is broad, anteriorly notched, and semi-translucent white with sporadic small to medium light brown spot. Oral tentacles digitiform.

Internal anatomy (Figs. 17e, 19e and 23a–d): Buccal mass (Fig. 17e) unpigmented; however, small light brown spots present around buccal opening. Buccal bulb 2.5 × longer than short, rounded oral tube. Radular sac elongated, rounded, and unpigmented. Labial cuticle smooth. Radula composed of smooth hamate teeth with no denticles (Fig. 23a). Radular formula 45 × 47.0.47 in the holotype CASIZ 186494. Inner 19 lateral teeth (Fig. 23b) small, thick with sharply curved cusps form a steep almost vertical V in the center. Middle lateral teeth (Fig. 23c) larger and thicker than inner laterals with a more elongated, curved cusp with rounded tips. Outermost lateral teeth (Fig. 23d) are slightly larger and thicker than middle laterals with shorter curved cusps. Outermost two teeth are small, paddle-shaped, and semi-fimbriate.

Reproductive system (Fig. 19e): Triaulic. Preampullary duct quickly widens into thick ampulla, then quickly narrows into postampullary duct which splits into short vas deferens and short oviduct. Vas deferens rapidly expands into wide, elongate, and curved granular prostate which abruptly narrows into thinner, elongate, and looped ejaculatory portion. Ejaculatory portion rapidly expands into large, wide penis which shares common genital atrium with slightly smaller, slightly longer, vagina. Large, wide vagina abruptly narrows proximally into thinner semi-elongate duct and enters large,

rounded bursa copulatrix partially covered by granular prostate. Thin, short duct connects bursa to smaller, rounded receptaculum seminis. Short, thin uterine duct connects near receptaculum base and enters medium-sized, irregularly oval-shaped female gland mass.

Geographical distribution: Known from New Caledonia.

Ecology: Found on shallow to moderately deep reefs rich in sediments between 15–40 m (Hervé 2010; Bas 2022).

Remarks: Molecular sequencing of the holotype of *Halgerda hervei* sp. nov. (CASIZ 186494) was unsuccessful for all genes studied; however, the morphological characteristics are distinct enough to distinguish *H. hervei* sp. nov. from the similarly patterned *H. jennyae* and *H. mesophotica* sp. nov. Morphological comparisons of *H. hervei* sp. nov. to *H. jennyae and H. mesophotica* sp. nov. are made below. Externally, *H. hervei* sp. nov. is semi-translucent white with small black dots, an irregularly dark brown/black ridging with large, pronounced tubercles; and radiating dark brown/lines from the tips of the tubercles and similarly colored lines perpendicular to the edge of the mantle. *Halgerda jennyae* is also translucent white with high tubercles; however, there is a complex pattern of thin brown lines along the ridges and valleys of the irregular ridging and numerous small to medium brown spots along the foot and dorsum (Tibiriçá et al. 2018, Figs. 11d, e). *Halgerda mesophotica* sp. nov. is also translucent white with sporadic black dots, but the extremely large and conical tubercles have a series of radiating thick brown lines and there is no linework along the edge of the mantle. The rhinophores are similar between *H. hervei* sp. nov. and *H. mesophotica* sp. nov. due to the translucent white coloration, cream-colored lamellae, and posterior dark stripe along the rhinophoral stalk; however, there are also small black spots and radiating black lines along the rhinophoral sheath in *H. hervei* sp. nov. that are absent in *H. mesophotica* sp. nov. In contrast, the rhinophores in *H. jennyae* are translucent with yellow lamellae and brown lines along the dorsal and lateral sides. The bipinnate branchial plume in *H. hervei* sp. nov. is two-toned with the upper one-third of leaves and rachises translucent white with a thin dark dorsal stripe, while the lower-two thirds are translucent yellow with ventral dark spots. The gill plume in *H. mesophotica* sp. nov. is similar; however, there are fewer large secondary branches, and the leaves and rachises are translucent white with a thick brown dorsal stripe and no spots. In *H. jennyae* the gill is also semi-translucent white with a dorsal black stripe, but there are also numerous small random black spots along the rachises and leaves.

Internally, the radula of *H. hervei* sp. nov. is more similar to *H. jennyae*, while the reproductive system is more similar to H. *mesophotica* sp. nov. In *H. hervei* sp. nov., there are small light brown spots around the buccal opening and no pigment on the buccal mass, while in *H. jennyae* the buccal mass is pigmented. In contrast, there is no pigmentation on the buccal mass or around the buccal opening in *H. mesophotica* sp. nov. In *H. hervei* sp. nov., the oral tube is much smaller than the buccal bulb while in *H. mesophotica* sp. nov., they are much more similar in size with the buccal bulb being 1.5 × the length of the oral tube. The radular teeth in *H. hervei* sp. nov. include 19 small inner lateral teeth with thick, sharply curved cusps; while in *H. mesophotica* sp. nov., there are 31 small inner lateral teeth with elongated stems and sharply curved cusps. In *H. jennyae* there are 16–18 small inner lateral teeth with thick cusps, that are shorter than those in *H. hervei* sp. nov. (Tibiriçá et al. 2018, Fig. 15a). The outermost radular teeth are different in all three species. In *H. hervei* sp. nov., the outermost three teeth are reduced with the outermost two teeth small, paddle-shaped, and semi-fimbriate. In *H. mesophotica* sp. nov., the three outermost teeth are reduced versions of the other outer laterals with more pointed tips and in *H. jennyae* the three to five outermost teeth are also reduced and similar to the other outer teeth, but less elongated and pointed than those in *H. mesophotica* sp. nov. (Tibiriçá et al. 2018, Fig. 15d). The reproductive systems of *H. hervei* sp. nov. and *H. mesophotica* sp. nov. share a large spherical bursa copulatrix partially covered by the granular portion of the prostate, a large vagina and penis, and a much smaller semi-rounded receptaculum seminis. However, in *H. hervei* sp. nov., the ejaculatory portion of the vas deferens is longer than in *H. mesophotica* sp. nov. with a distinct loop. The vagina of *H. hervei* sp. nov. gradually narrow and has a narrow distal portion that enters the bursa copulatrix, whereas in *H. mesophotica* sp. nov., the bulbous vagina abruptly narrows and is uniformly narrow to its junction with the bursa. Additionally, the duct connecting the vagina to the bursa and the bursa to the receptaculum/uterine duct split is much shorter and thicker in *H. hervei* sp. nov. In contrast, the smaller bursa is completely covered by the granular prostate in *H. jennyae*, the penis and vagina smaller, the ejaculatory portion shorter, and the receptaculum is also slightly larger (Tibiriçá et al. 2018, Fig. 14b). Based on the unique internal and external characteristics including dorsum and tubercle patterning, the translucent yellow gill, a short oral tube, athe paddle-shaped semi-fimbriate outer radular teeth, *H. hervei* sp. nov. is a distinct species with *Halgerda* despite the lack of molecular data for the species. Ecologically, *H. hervei* sp. nov. and *H. jennyae* are found in moderately shallow water 10–40 m and 20 m, respectively, whereas *H. mesophotica* sp. nov. is found at mesophotic depths from 61–70 m.

Halgerda maaikeae Donohoo & Gosliner sp. nov.
https://zoobank.org/5DF422FE-F830-46F0-B1F0-8BEA39CD5AC0
(Fig. 17f, 19f, 24a and 25)

Halgerda sp. 2 Sellick et al. (2020): 14, bottom right photograph.

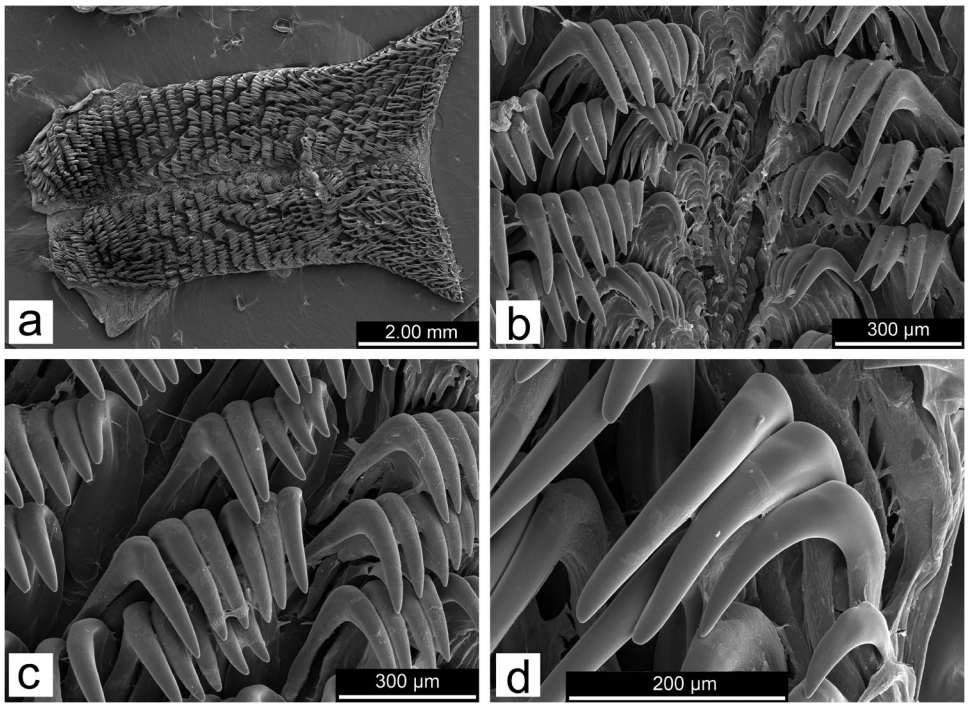

Fig. 25 *Halgerda maaikeae* sp. nov., holotype, SAMC-A094639, scanning electron micrographs of radula: **a** entire radula; **b** inner lateral teeth; **c** mid-lateral teeth; and **d** outer lateral teeth

Material examined: Holotype: One specimen, SAMC-A094639, formerly CASIZ 231106, dissected and sequenced, 41 mm alive, type locality: Aliwal Shoal (30° 20′ 00.6″ S 30° 47′ 37.8″ E), KwaZulu-Natal Province, South Africa, 27.5 m depth, 02 September 2019, collected by Brian Sellick. Paratype: One specimen, CASIZ 231070, dissected and sequenced, 29 mm alive, type locality: Aliwal Shoal (30° 19′ 57.0″ S 30° 47′ 31.8″ E), KwaZulu-Natal Province, South Africa, 28 m depth, 17 July 2019, collected by Brian Sellick.

Type locality: Aliwal Shoal, KwaZulu-Natal Province, South Africa

Etymology: This species is named in honor of Maaike, the owner of the dive center that helps facilitate specimen collections with Brian Sellick in South Africa.

External morphology: Living animals 29–41 mm length (Fig. 24a). Body oval, semi-rigid, and gelatinous. Dorsum color semi-translucent white with low unconnected irregularly patterned orange ridging. Reddish purple viscera semi-visible through mantle. Thin white marginal band along mantle edge. Mantle underside semi-translucent white. Gill surround slightly elevated anus with seven bipinnate branchial leaves. Gill coloration semi-translucent white with dorsal dark brown/black stripe. Gill pocket smooth with similar dorsum coloration. Opaque white glands present in gill branches. Rhinophores tapered, perfoliate with semi-translucent white stalks and 14–16 dark brown/black lamellae. Rhinophoral sheath smooth with similar dorsum coloration. Foot is broad, anteriorly notched, semi-translucent white, and extends slightly beyond mantle. Oral tentacles digitiform.

Internal anatomy (Figs. 17f, 19f and 25a–d): Buccal mass (Fig. 17f) unpigmented. Oral tube slightly longer than buccal bulb and narrowed anteriorly. Radular sac very elongate, rounded tip, and unpigmented. Labial cuticle smooth. Radula composed of smooth hamate teeth without denticles (Fig. 25a). Radular formula 35 × 35.0.35 in the holotype SAMC-A094639. Inner 14 lateral teeth (Fig. 25b) small, broad-based with short, thick, highly curved cusps form a steep V in the radula center. Middle lateral teeth (Fig. 25c) larger and thicker than middle laterals with more elongated cusps and rounded tips. Outer lateral teeth (Fig. 25d) larger and more elongate than middle laterals. Outermost two teeth greatly reduced versions of other outer laterals.

Reproductive system (Fig. 19f): Triaulic. Thin preampullary duct continues into thin ampulla which quickly expands, loops, and then gradually narrows into postampullary duct which splits into short vas deferens and short, thin oviduct. Vas deferens gradually expands into similarly wide, elongate granular prostate which widens, loops, and then abruptly narrows into thin, elongate, looped ejaculatory portion. Ejaculatory portion quickly expands into large, wide penis which shares common genital atrium with slightly smaller muscular vagina. Large, wide vagina gradually narrows proximally into thinner elongate duct which enters large, bursa copulatrix slightly covered by vagina. Thin, semi-elongate duct connects bursa to small oval-shaped receptaculum seminis. Short, thin uterine duct connects near receptaculum base and enters large, oblong-shaped female gland mass.

Geographical distribution: Known from South Africa.

Table 5 Morphological comparisons of previously described and newly described *Halgerda* species with white/translucent white mantles and yellow/orange ridging

	Halgerda diaphana	*Halgerda dichromis*	*Halgerda meringuecitrea*	*Halgerda toliara*	*Halgerda maaikeae* sp. nov.	*Halgerda pattiae* sp. nov.	*Halgerda radamaensis* sp. nov.
Dorsum	Moderate orange ridging with secondary lines, low tubercles	Moderate unconnected orange ridging with secondary black spots, no tubercles	Low yellow-orange ridging, no tubercles	Low orange ridging with no tubercles	Low unconnected orange ridging, no tubercles	Wide yellow longitudinal line, low yellow ridging, small yellow and white tubercles	Wide yellow longitudinal line, moderate ridging with no color, small semi-white/white tubercles
Mantle margin	Thick orange band and then thin white band	Thin, semi-opaque white band	Thin, white band	Thin, white band and small yellow tubercles	Thin, white band	Thin, white band and small semi-opaque white tubercles	Thin, white band and small semi-white/white tubercles
Gill plume	Four pinnate, sometimes bipinnate leaves, with black speckles	Two tripinnate branches, with dorsal black stripe	Five to six unipinnate, sometimes bipinnate leaves, with rachis and top two-thirds dark brown	Four pinnate leaves with one-half to one-third black	Seven bipinnate leaves with dorsal dark brown/black stripe	Five unipinnate leaves with dorsal dark brown stripe	Six unipinnate leaves with rachis and top two-thirds black
Radula formula	53×43.0.43	48×41.0.41	41×25–30.0.25–30	43×30.0.30	35×35.0.35	38×35.0.35	32×29.0.29
No. of smaller inner teeth	10	20	13–14	4	14	16	15
Outermost teeth	Three reduced, blunt, and denticulate	Three reduced and fimbriate/pointed	Two to three reduced with pointed hook	Three reduced and fimbriate	Two reduced	Two to three reduced and fimbriate	Four reduced with outer three fimbriate
Vagina	Large, wide, glandular	Short, narrow with wide muscular and glandular portions	Large, wide, and muscular	Narrow and elongate	Large, wide, and muscular	Large, wide, and muscular	Narrow and elongate
Type locality	Okinawa	South Africa	Mozambique	Madagascar	South Africa	Mayotte Island	Madagascar

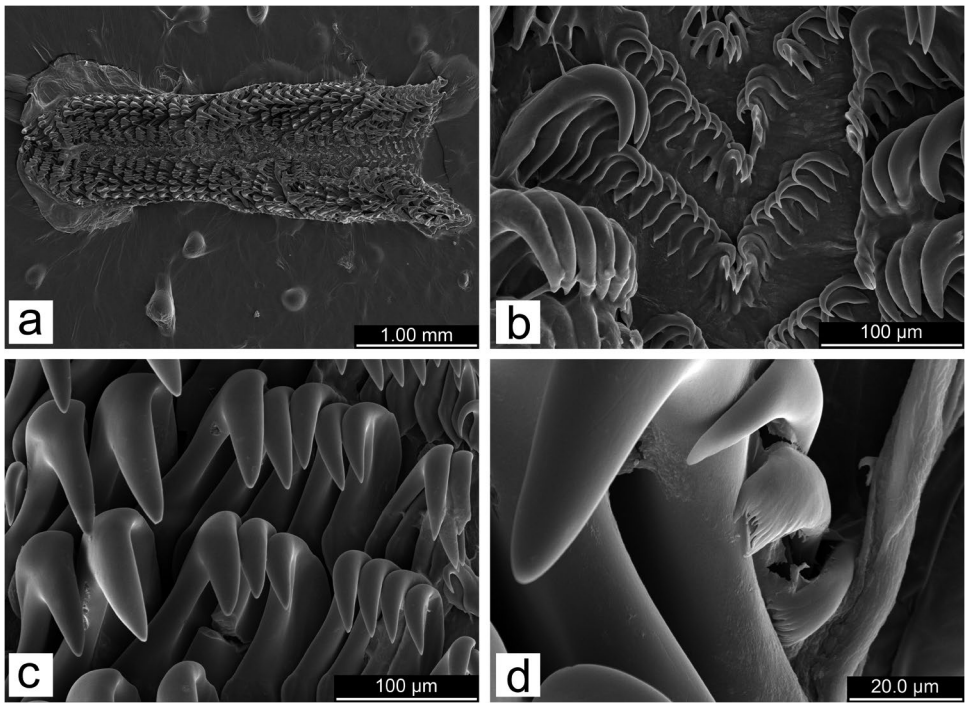

Fig. 26 *Halgerda pattiae* sp. nov., holotype, UF 422800, scanning electron micrographs of radula: **a** Entire radula; **b** inner lateral teeth; **c** mid-lateral teeth; **d** outer lateral teeth

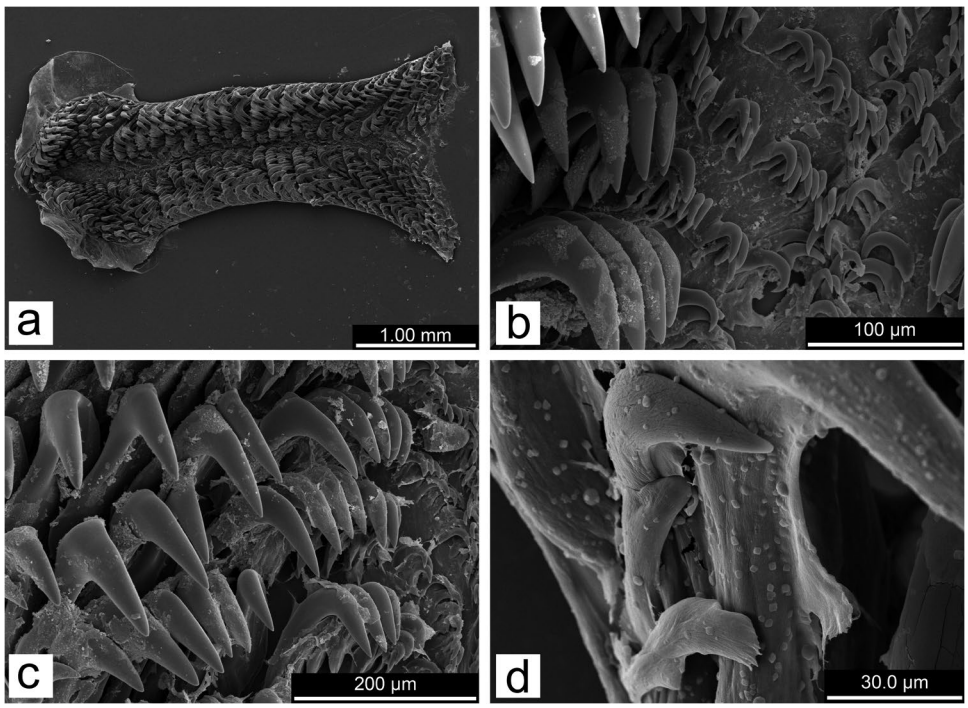

Fig. 27 *Halgerda radamaensis* sp. nov., holotype, CASIZ 173456, scanning electron micrographs of radula: **a** Entire radula; **b** inner lateral teeth; **c** mid-lateral teeth; **d** outer lateral teeth

Ecology: Found on deeper reef faces below 25 m (Sellick et al. 2020).

Remarks: In our molecular phylogeny *Halgerda maaikeae* sp. nov. from South Africa is part of an unresolved clade including *H. mozambiquensis*, *H. indotessellata*, and *H. tessellata*. Within this clade, *H. maaikeae* sp. nov. is separated from *H. mozambiquensis* genetically by a minimum divergence of 5.2% in the COI gene and morphologically by the lack of large, dark brown spots found between the orange ridging seen in *H. mozambiquensis* (Tibiriçá et al. 2018, Fig. 11b). In comparison to *H. indotessellata* and *H. tessellata* there is a minimum COI genetic divergence of 5.8% and 8.6%, respectively. Externally, *H. maaikeae* sp. nov. also lacks the brown pigmentation with white spots between the pronounced

ridging seen in both species and the rhinophores are a solid black *in H. maaikeae* sp. nov. rather than spotted as seen in *H. indotessellata* and *H. tessellata* (Tibiriçá et al. 2018, Fig. 11a; Bergh 1880b, Tafel F, Figs. 22 and 23; respectively).

Morphologically, *H. maaikeae* sp. nov. is most similar to *H. diaphana* (Fig. 24b) from Okinawa and *H. dichromis* (Fig. 24c) from South Africa, so further morphological comparisons are made below and summarized in Table 5. The four species delimitation analyses support *H. maaikeae* sp. nov. as a distinct species and there is a strong minimum COI divergence of 13.1% between *H. maaikeae* sp. nov. and *H. diaphana* and 11.8% between *H. maaikeae* sp. nov. and *H. dichromis*. Externally, *H. maaikeae* sp. nov. is semi-translucent white with low, unconnected orange ridging, no tubercles, and a thin white marginal band near the mantle edge. The rhinophores and seven bipinnate branchial leaves are also semi-translucent white with black lamellae and a dark brown/black dorsal stripe, respectively. The dorsal color of *H. diaphana* is more translucent white with moderately pronounced and connected orange ridging, secondary orange lines, low tubercles, and a thick orange marginal band offset from a thinner, white marginal band near the mantle edge. The rhinophores and four pinnate (sometimes bipinnate) branchial leaves are translucent white with numerous black speckles (Fahey and Gosliner 1999b, Fig. 1c). *Halgerda dichromis* is more grayish white in coloration with moderately pronounced, unconnected orange and black ridging, secondary black spots, no tubercles, and a thin white marginal band (Fahey and Gosliner 1999a, Fig. 4b). The rhinophores and branchial leaves are similarly patterned to *H. maaikeae* sp. nov., but the rhinophores also have a white apical tip and there are fewer, more highly pinnate branchial leaves.

Internally, the radular teeth and reproductive systems vary noticeably between the three species. In *H. maaikeae* sp. nov., there are 14 small inner lateral teeth with short, thick, highly curved cusps that form a steep V shape in the middle of the radula. In *H. diaphana* there are only 10 small inner lateral teeth with very short and pointed cusps (Fahey and Gosliner 1999b, Fig. 5b) and in *H. dichromis* there are 20 small inner lateral teeth with less curved and more pointed cusps (Fahey and Gosliner 1999a, Fig. 7b). The middle and outer teeth are larger with more elongate cusps in all three species, but the outermost teeth vary drastically. In *H. maaikeae* sp. nov., the two outermost teeth are greatly reduced versions of the other outer laterals, while in *H. diaphana* the three outermost teeth are similarly reduced with blunt tips and denticulation (Fahey and Gosliner 1999b, Fig. 5a), and in *H. dichromis* the three outermost teeth are either fimbriate or pointed depending on the row (Fahey and Gosliner 1999a, Fig. 7a). The reproductive system of *H. maaikeae* sp. nov. includes a small receptaculum seminis; a large, spherical bursa copulatrix uncovered by the prostate; a large, wide penis connecting to an elongate, looped ejaculatory portion of the prostate; a wide, looped, elongated granular portion of the prostate; and a large, wide, muscular vagina (slightly smaller than the penis) that narrows proximally. In contrast, *H. diaphana* has a large, spherical bursa copulatrix covered by the granular portion of the prostate and the ejaculatory portion of the prostate is much shorter and connects into a wide, elongated penis that is slightly smaller than the large and glandular vagina (Fahey and Gosliner 1999b, Fig. 2c). In *H. dichromis*, the large and spherical bursa copulatrix is also covered by the granular portion of the prostate and connects to a thin, elongated ejaculatory portion of the prostate, which expands into a large, wide penis (Fahey and Gosliner 1999a, Fig. 3c). The vagina is smaller and composed of a large, glandular portion that narrows into a short, muscular portion, before narrowing and connecting to the bursa. Despite the morphological similarities, there are clear internal and external differences and strong genetic divergences between *H. maaikeae* sp. nov., *H. diaphana*, and *H. dichromis*, which supports each of them as distinct species within *Halgerda*.

Halgerda pattiae Donohoo & Gosliner sp. nov.
https://zoobank.org/E4F5CACA-4254-452F-ACA3-B3BFDBEDA649
(Fig. 17g, 19g, 24d and 26)

Halgerda toliara Poddubetskaia (2003). *Halgerda* cf. *toliara* Poddubetskaia (2004).

Material examined: Holotype: One specimen, UF 422800, dissected and sequenced, 10 mm preserved, type locality: Mayotte Island (12° 51′ 18.5″ S 45° 16′ 06.8″ E), Comoros Archipelago, 15–17 m depth, 02 June 2008, collected by Arthur Anker and François Michonneau.

Type locality: Mayotte Island, Comoros Archipelago.

Etymology: This species is named in honor of Patti Ann Kerscher, the first author's very supportive and beloved mother.

External morphology: Preserved animals 10 mm in length (Fig. 24d, Supplementary Figure S6e). Body oval, semi-rigid, and gelatinous. Dorsum color translucent white with low irregular ridging formed by series of low conical tubercles Anteriorly forked wide yellow longitudinal line along central ridge begins before rhinophores and rings the gill pocket. Central lateral ridges maybe also be light yellow or translucent white with translucent white or vibrant yellow small tubercles which gradually lose color towards mantle edge. (Supplementary Figure S6f). Numerous small semi-opaque white conical tubercles present along lateral ridges and mantle edge. Thin white marginal band along mantle edge. Viscera with reddish purple coloration visible through mantle. Mantle underside translucent white. Gill surrounds slightly elevated anus with five unipinnate branchial leaves. Gill coloration white with translucent white rachis and dorsal dark brown stripe. Gill pocket smooth. Opaque white glands semi-visible within branchial leaves. Rhinophores tapered,

perfoliate with translucent white stalks and 15 dark brown lamellae forming the rhinophoral club. Rhinophoral sheath smooth with similar dorsum coloration. Foot is broad, anteriorly notched, and translucent white. Oral tentacles digitiform.

Internal anatomy (Figs. 17g, 19g and 26a–d): Buccal mass (Fig. 17g) unpigmented. Oral tube 1.5 × longer than buccal bulb. Radular sac elongate, curved, slightly expanded at tip, and unpigmented. Labial cuticle smooth. Radula composed of smooth hamate teeth with no denticles (Fig. 26a). Radular formula 38 × 35.0.35 in the holotype UF 422800. Inner 16 lateral teeth (Fig. 26b) small, broad-based with slightly elongated, gently curved, thin cusps and pointed tips form a V in the center. Middle lateral teeth (Fig. 26c) larger and thicker than inner laterals with more elongated cusps and rounded tips. Outer lateral teeth (Fig. 26d) slightly larger than middle laterals with more elongated tips. Outermost two–three teeth greatly reduced and fimbriate.

Reproductive system (Fig. 19g): Triaulic. Thin preampullary duct rapidly expands into thick ampulla, then gradually narrows into postampullary duct which splits into short vas deferens and short oviduct. Vas deferens gradually expands into similarly wide, elongate granular prostate which widens, loops, and then abruptly narrows into thin, elongate, curved ejaculatory portion. Ejaculatory portion quickly expands into large, wide, elongate penis which shares common genital atrium with similarly sized muscular vagina. Large, wide muscular vagina abruptly narrows proximally and enters medium-sized, irregularly rounded bursa copulatrix. Very thin, elongate duct connects bursa to small, oblong receptaculum seminis. Short, slightly thin uterine duct connects near receptaculum base and enters medium sized irregularly rounded female gland mass.

Geographical distribution: Known from Mayotte Island in the Comoros Archipelago.

Ecology: Found on exposed coral and rocks between 15–17 m.

Remarks: Our molecular phylogeny shows that *Halgerda pattiae* sp. nov. from Mayotte Island in the Comoros Archipelago is sister to the similarly colored *H. meringuecitrea* (Fig. 24e) from Mozambique. All four species delimitation analyses support *H. pattiae* sp. nov. as a distinct species from *H. meringuecitrea* and reveal a minimum divergence of 6.0% in the COI gene. *Halgerda pattiae* sp. nov. is also similarly colored to *H. toliara* from Madagascar; however, there is a stronger genetic divergence of 11.3% between these two species. Furthermore, these two species are found within separate well-supported clades in our molecular phylogeny. Due to their morphological similarities, further comparisons between *H. pattiae* sp. nov., *H. meringuecitrea*, and *H. toliara* are made below and summarized in Table 5.

Externally, *H. pattiae* sp. nov. is translucent white with low yellow ridging that gradually loses color; a wide, forked, yellow longitudinal line along the central ridge; and numerous small yellow and white tubercles along the ridge edges and offset from the thin, white mantle band along the mantle margin. The rhinophores are translucent white with dark brown lamellae and there are five, unipinnate white branchial leaves with translucent white rachis and a dorsal dark brown stripe. The dorsum of *H. meringuecitrea* is also translucent white; however, the low yellow-orange ridging is less pronounced and more uniform in color and there are no tubercles present along the ridging or offset from the thin, white mantle band along the mantle margin (Tibiriçá et al. 2018, Fig. 11g). Also, the central yellow line of *H. pattiae* sp. nov. extends around the gill pocket, whereas it terminates anteriorly of the gill pocket in *H. meringuecitrea*. The rhinophores of *H. meringuecitrea* are similar in coloration to *H. pattiae* sp. nov. There are five to six unipinnate (occasionally bipinnate) translucent white branchial leaves with dark brown coloration along the top two-thirds of the rachis. In *H. toliara*, the dorsum is whiter in coloration with more extensive low orange ridging (Fahey and Gosliner 1999a, Fig. 4c). There are no tubercles present along the ridging; however, there are small yellow/orange tubercles offset from the thin, white mantle band along the mantle margin. The rhinophores are similar to both *H. pattiae* sp. nov. and *H. meringuecitrea*; however, the lamellae are darker and blacker in coloration. The gill is composed of only four pinnate leaves which are translucent white with approximately one-half to one-third black in coloration.

Internally, the radular teeth and reproductive systems also noticeably vary between these species. In *H. pattiae* sp. nov., there are 16 small inner lateral teeth with slightly elongated, gently curved, thin cusps, while in *H. meringuecitrea*, there are 13–14 small inner lateral teeth with shorter, thicker, more abruptly curved cusps (Tibiriçá et al. 2018, Fig. 16b), and in *H. toliara*, there are only four small inner lateral teeth which are more similar in size and shape to *H. pattiae* sp. nov. (Fahey and Gosliner 1999a, Fig. 8a). The middle and outer teeth are all larger and more elongate in each species, but the outermost teeth vary slightly. In *H. pattiae* sp. nov. and *H. toliara*, the outermost two to three lateral teeth are reduced and fimbriate (Fahey and Gosliner 1999a, Fig. 8b), while in *H. meringuecitrea*, the two to three outermost teeth are also reduced with a slightly pointed hook (Tibiriçá et al. 2018, Fig. 16c, d). The reproductive system of *H. pattiae* sp. nov. is composed of a thick ampulla; a large, wide, elongate penis and a similarly sized muscular vagina; a medium-sized irregularly rounded bursa copulatrix; and a small, oblong receptaculum seminis. In contrast, *H. meringuecitrea* has a narrower ampulla and elongated penis; a much smaller bursa copulatrix and a minute, rounded receptaculum seminis. The vagina is similarly muscular to the one found in *H. pattiae* sp. nov.; however, it gradually narrows in the proximal portion and is overall smaller in size and width (Tibiriçá et al. 2018, Fig. 14c). In *H. toliara*, the penis is short and bulbous and the vagina is narrow and extremely elongated, while

the rounded bursa copulatrix is very large and the rounded receptaculum seminis is approximately one-sixth the size of the bursa (Fahey and Gosliner 1999a, Fig. 3d).

The slight variation in external morphology, particularly the extent of the dorsal yellow pigment, and the noticeable differences in the radula and reproductive systems of *H. pattiae* sp. nov., *H. meringuecitrea*, and *H. toliara* are supported by strong genetic divergences, which help distinguish these three distinct, but similar species within *Halgerda*. The presence of ridges formed by lines of small tubercles, the presence of yellow pigment encircling the gill and the details of the reproductive system noted above clearly differentiate *H. pattiae* sp. nov. from other described species of *Halgerda*.

Halgerda radamaensis Donohoo & Gosliner sp. nov.
https://zoobank.org/9879B020-0D6B-40F4-A120-FFBF321919A0
(Fig. 17h, 19h, 24f and 27)

Halgerda toliara? Gaggeri (2006). *Halgerda* sp. 2 Gosliner et al. (2008): 182, bottom photograph. *Halgerda* sp. 9 Gosliner et al. (2015): 191, top right photograph. *Halgerda* sp. 16 Gosliner et al. (2018): 113, top right photograph.

Material examined: Holotype: One specimen, CASIZ 173456, dissected, 12 mm preserved/alive, type locality: Nosy Kalakajaro (13° 58′ 22.0″ S 47° 41′ 45.8″ E), Iles Radama, Madagascar, 15–17 m depth, 17 October 2005, collected by T.M. Gosliner. Paratype: One specimen, CASIZ 234753, 16 mm preserved/alive, type locality: Nosy Kalakajaro (13° 58′ 22.0″ S 47° 41′ 45.8″ E), Iles Radama, Madagascar, 15–17 m depth, 17 October 2005, collected by T.M. Gosliner.

Type locality: Nosy Kalakajaro, Iles Radama, Madagascar.

Etymology: The name *radamaensis* refers to the type locality Iles Radama or Radama Islands, which is found off the coast of Madagascar.

External anatomy: Preserved animals 12–16 mm in length (Fig. 24f). Body oval, semi-rigid, and gelatinous. Dorsum color translucent white with moderate irregular ridging devoid of tubercles. Small semi-white to translucent white tubercles present offset from mantle edge. Forked wide yellow longitudinal line with thick short offshoots along central ridge begins before rhinophores and terminates anterior to gill sheath. Viscera with purple coloration visible through mantle. Thin white marginal band present along mantle edge. Mantle underside translucent white. Gill surrounds elevated anus with six unipinnate branchial leaves. Gill coloration translucent white with rachis and top two-thirds of branchial leaves black. Gill pocket smooth with similar dorsum coloration. Opaque white glands present within branchial leaves. Rhinophores tapered, perfoliate, black pigment present e club and with black pigment extending downward on top of rhinophore stalk. lub base and 14–16 black lamellae. Rhinophoral sheath smooth, translucent white. Foot is broad, anteriorly notched, translucent white and extends beyond mantle. Oral tentacles digitiform.

Internal anatomy (Figs. 17h, 19h and 27a–d): Buccal mass (Fig. 17h) unpigmented. Buccal bulb 1.5 × longer than short, anteriorly narrowed oral tube. Radular sac thin, elongated, and unpigmented. Labial cuticle smooth. Radula composed of smooth hamate teeth with no denticles (Fig. 27a). Radular formula 32 × 29.0.29 in the holotype CASIZ 173456. Inner 15 lateral teeth (Fig. 27b) small, broad-based with short stalks and quickly curved, elongated thick cusps. Middle lateral teeth (Fig. 27c) larger, thicker, and more elongated than inner laterals with rounded tips. Outer lateral teeth (Fig. 27d) are slightly larger and thicker than middle laterals. Outermost four teeth gradually reduce in size with outer three teeth fimbriate.

Reproductive system (Fig. 19h): Triaulic. Thin, elongate preampullary duct expands into thicker ampulla, then gradually narrows into postampullary duct which splits into vas deferens and oviduct. Vas deferens gradually expands into wide, elongate, and looped granular prostate which narrows abruptly into thin, elongate ejaculatory portion. Ejaculatory portion abruptly narrows into large, wide, curved penis which shares common genital atrium with smaller, similarly elongate vagina. Narrow, elongate vagina gradually narrows and enters medium-sized irregularly shaped bursa copulatrix. Semi-thin, elongate duct connects bursa to small irregularly oblong shaped receptaculum seminis. Very thin, short uterine duct connects near receptaculum base and enters medium sized, irregularly rounded female gland mass.

Geographical distribution: Known from Iles Radama, Madagascar (present study) and Nosy Be, Madagascar (Gaggeri 2006). Specimens attributed from Mayotte Island, Comoros Archipelago (Gosliner et al. 2008, 2015, 2018) represent *H. pattiae* sp. nov.

Ecology: Found on reef faces between 6–19 m.

Remarks: Molecular sequencing of both the holotype (CASIZ 173456) and paratype (CASIZ 234753) of *Halgerda radamaensis* sp. nov. was unsuccessful due to prior fixation in formalin; however, the morphological characteristics are distinct enough to distinguish *H. radamaensis* sp. nov. from similar species of *Halgerda*. *Halgerda radamaensis* sp. nov. is morphologically similar to *H. pattiae* sp. nov. (Fig. 24d) and *H. meringuecitrea* (Fig. 24e) and morphological comparisons between the three are made below. Externally, the dorsum coloration of all three species is translucent white with a thin, white marginal band; however, there are distinct patterns and colorations in the ridging and tubercless within each species. In *H. radamaensis* sp. nov., the moderately pronounced ridging is colorless except for a forked, wide, bright yellow longitudinal line with short offshoots present down the central ridging. There are small semi-white to translucent white submarginal tubercles alongside the ridging and offset from the marginal band along the mantle edge. In contrast, the ridging in *H. meringuecitrea* is less pronounced and more irregular with yellow-orange coloration

and there are no tubercles present along the ridging or the edge of the mantle. *Halgerda pattiae* sp. nov. also has less pronounced ridging with vibrant, yellow or white tubercles and a wide, yellow longitudinal line down the central ridging. The rest of the ridging may have yellow coloration that gradually lightens towards the edge of the mantle, but there are always numerous small semi-opaque white tubercles along the lighter parts of the ridging and the edge of the mantle. In *H. radamaensis* sp. nov., the yellow terminates anteriorly to the gill cavity while in *H. pattiae* sp. nov., the central yellow line encircles the gill. The rhinophores are similar between the three species (translucent white with dark brown/black lamellae) but in *H. radamaensis* sp. nov., the black extends below the rhinophore club with some black extending onto the apical portion of the stalk, whereas in *H. meringuecitrea* and *H. pattiae* sp. nov., the black pigment is confined to the rhinophoral club and does not extend on to the stalk. The gill plume varies slightly between species. In *H. radamaensis* sp. nov., the branchial leaves are unipinnate and translucent white with the rachis and top two-thirds of the branchial leaves black. The branchial leaves in *H. meringuecitrea* are similarly patterned, but with dark brown coloration and occasionally bipinnate rachises. In *H. pattiae* sp. nov., the branchial leaves are also unipinnate, but with white coloration and translucent white rachis with a dark brown dorsal stripe.

Internally, the radular teeth and reproductive systems noticeably vary between the three species. In *H. radamaensis* sp. nov., there are 15 small inner lateral teeth with short stalks and quickly curved, elongated thick cusps. The middle and outer lateral teeth are thicker and more elongated, but the outermost four teeth are reduced with outer three teeth also fimbriate. In contrast, *H. meringuecitrea* has 13–14 inner lateral teeth with a similar thickness, but less elongated and with more abruptly curved cusps; while the outermost two to three teeth are reduced in size with a slightly pointed hook (Tibiriçá et al. 2018, Fig. 16b–d). In *H. pattiae* sp. nov., the 16 inner small lateral teeth are also elongated, but thinner with a gentle curve and narrow, pointed cusps; while the outermost two to three teeth are similarly reduced and fimbriate. The reproductive system of *H. radamaensis* sp. nov. is composed of an elongate ampulla; a large, wide, curved penis and a smaller, more elongate vagina; a medium-sized irregularly rounded bursa copulatrix; and a smaller, irregularly oblong receptaculum seminis. *Halgerda meringuecitrea* has a similarly elongate ampulla, but the penis is more elongate and narrower, the vagina is muscular, and the bursa copulatrix and the receptaculum seminis are also much smaller and more rounded (Tibiriçá et al. 2018, Fig. 14c). *Halgerda pattiae* sp. nov. has a similarly large penis, medium-sized bursa copulatrix, and small receptaculum seminis; however, the ampulla is much shorter and wider, the receptaculum more oblong shaped, and the muscular vagina wider than the non-muscular one seen in *H. radamaensis* sp. nov. Based on the unique internal and external characteristics including dorsum morphology and coloration and the presence of an elongated, non-muscular vagina, *H. radamaensis* sp. nov. is a distinct species from *H. meringuecitrea* and *H. pattiae* sp. nov., despite the lack of molecular data for the species. *Halgerda radamaensis* sp. nov. is likely a member of the same clade as *H. meringuecitrea* and *H. pattiae* sp. nov., based on the morphology described. This clade already demonstrates strong regional endemism in the western Indian Ocean with corresponding morphological and molecular divergence. It is highly likely that *H. radamaensis* sp. nov. shows a similar pattern of divergence and that the morphological differences noted above are significant and support the distinctness of this species. We have been trying to obtain additional material from Madagascar since this material was collected in 2005, but have been unsuccessful and feel it is necessary to describe this species based on its unique morphological features.

Discussion

This study produced an updated phylogenetic analysis of the genus *Halgerda* and revealed unexpected diversity in the central and western Pacific Ocean and the western Indian Ocean, including the Red Sea. By combining morphological data with molecular data from two mitochondrial and two nuclear genes, we have uncovered two new species in the Red Sea, four new species in the western Indian Ocean, one new species in Japan, and seven new species in the Indo-Pacific including New Caledonia, French Polynesia, and the Verde Island Passage. We also synonymized *H. elegans* with *H. willeyi*, provided a juvenile description for the previously described *H. dalanghita*, and established a new mesophotic clade. This study brings the total number of described *Halgerda* species from 42 to 55, making *Halgerda* one of the most diverse genera in Discodorididae.

Placement in Discodorididae Despite the numerous morphological studies on *Halgerda*, the position and sister taxon of *Halgerda* within Discodorididae varies from study to study. *Halgerda* has been previously suggested as the sister taxon of *Asteronotus* after a morphological study of caryophyllidia-bearing dorids, and a morphological review of cryptobranch dorids showed that they shared several characteristics including a rigid body, dorsum ridging, and a well-differentiated prostate (Valdés and Gosliner 2001; Valdés 2002). This relationship was later supported in two morphological phylogenies focused on *Halgerda* (Fahey and Gosliner 1999b, 2001a) as well as the first molecular phylogeny (Fahey 2003). It should be noted that in the first molecular phylogeny, Fahey (2003) sequenced only one mitochondrial gene (COI), utilized only one additional

species of Discodorididae for outgroup comparisons, and was focused predominately on species from the Pacific. In 2017, *Discodoris*, rather than *Asteronotus*, was suggested as the sister taxon of *Halgerda* during a four gene molecular phylogenetic study of Doridina; however, that study used limited representation from each family (including one specimen of *Halgerda* and one specimen of *Asteronotus*) to evaluate an entire suborder (Hallas et al. 2017). Tibiriçá et al. (2018) expanded upon the first *Halgerda* molecular phylogeny by sequencing COI and two additional genes (16S and H3) from specimens of *Halgerda* across the Pacific Ocean and the western Indian Ocean. Their phylogeny suggests that *Paradoris* Bergh, 1884 or *Peltodoris* Bergh, 1880b is the sister taxon of *Halgerda*; however, it is unclear which genus is more closely related (Tibiriçá et al. 2018). In our study, we expanded the outgroup to include 16 different genera from Discodorididae including the previously suggested genera *Asteronotus*, *Discodoris*, *Paradoris*, and *Peltodoris*; however, we are still unable to establish a clear sister taxon for *Halgerda*. We suggest a more comprehensive review of the entire family is needed to better understand the relationships between Discodorid genera and establish a sister taxon for *Halgerda*.

Species delimitation Specimens thought to be previously undescribed species of *Halgerda* (i.e., *Halgerda* sp. 3 and *Halgerda* sp. 4; Gosliner et al. 2018) are shown in our molecular phylogeny to be juveniles of the newly described *H. mango* sp. nov. and the previously described *H. dalanghita*, respectively. Externally, these juvenile specimens share only a few obvious morphological characteristics with their adult counterparts; however, closer inspection of the radula and reproductive systems reveals limited differences in the internal juvenile and adult anatomy. This noticeable difference in coloration and patterning between juveniles and adults can also be found in other species of nudibranchs. For example, in *Jorunna rubescens* (Bergh, 1876), a second species of Discodorididae, the adults are white with brown lines and yellow spots; however, the juveniles are more translucent white with opaque white lines (Gosliner et al. 2015, 2018). In the chromodorid *Goniobranchus charlottae* (Schrödl, 1999), the adults and juveniles share a similar reddish-brown coloration; however, the juveniles have large areas of cream-white coloration and a light blue submarginal band. In the adults, the white areas are much smaller and more scattered; there are also small red spots scattered along the dorsum, and the light blue submarginal band is also broken apart into small light blue spots (Schrödl 1999; Gosliner et al. 2015, 2018). Some nudibranch juveniles (e.g., *Phestilla melanobrachia* Bergh, 1874) may change their coloration depending on available food or host regardless of the parent's original color (Yiu et al. 2021).

Occasionally, juveniles may be described as a new species. For example, our molecular phylogeny reveals that specimens matching Bergh's original description of *H. elegans* from 1905 are in fact juveniles of the adult species *H. willeyi* described by Eliot in 1904. Genetic differences in the mitochondrial COI gene between specimens representing these two morphologies and a second adult morphology described in this study ranges between 0.3 and 1.8% (Supplementary Table S3); however, all three morphologies share a suite of internal and external characteristics (see remarks section of *H. willeyi*). We have also determined that specimens formerly identified as *H. willeyi* from the Red Sea and Okinawa, Japan, are actually two new species of *Halgerda*. Both *H. willeyi* and the new species, *H. paulayi* sp. nov. and *H. labyrinthus* sp. nov., are found in separate subclades within our molecular phylogeny and have a strong genetic divergence of 9.5–11.4% between all three species. The morphological differences between these three species are detailed in their respective remark sections. Furthermore, we suggest that *H. willeyi* may very well suffer from the "catch-all problem" given that *H. willeyi*, *H. paulayi* sp. nov., and *H. labyrinthus* sp. nov. share a wide morphological description built around the dorsum coloration and patterning of the pronounced tubercles and lined ridging. All these species highlight the importance of utilizing molecular data in coordination with morphological data to prevent either the over-description of new species solely based on a "novel" or "unique" morphological characteristic (i.e., the novelty problem/splitting) or the lack of new descriptions due to over-grouping based on a universal morphological characteristic or wide morphological description (i.e., the catch-all problem/grouping) (Rudman 1984, 1987; Dayrat and Gosliner 2005; Johnson and Gosliner 2012).

Mesophotic species A new mesophotic clade has been identified within *Halgerda* and includes the following species: *H. scripta* sp. nov., *H. mesophotica* sp. nov., *H. profunda* sp. nov., *H. takipsilim* sp. nov., and *H. okinawa*. Within this clade, *H. mesophotica* sp. nov., *H. profunda* sp. nov., and *H. takipsilim* sp. nov. form a species complex with low genetic diversity (0.9–1.5%); however, the morphological internal and external differences detailed in the remarks section of *H. takipsilim* sp. nov. support the distinctness of each species within *Halgerda*. This new clade is predominantly found in the Philippines and the temperate Central Pacific including Japan; however, all five species within this clade have a similar depth profile (50–90 m). They also have shared morphological characteristics such as large secondary branchial leaves, a thin colored mantle band, numerous inner radular teeth, and a partially covered bursa copulatrix that set them apart from species found in the deep sea. Similarly patterned species of *Halgerda* found in the deep sea between 90 and 400 + m in depth including *Halgerda abyssicola* Fahey &

Gosliner, 2000; *Halgerda azteca* Fahey & Gosliner, 2000; *Halgerda fibra* Fahey & Gosliner, 2000; and *Halgerda orstomi* Fahey & Gosliner, 2000 generally have fewer small inner radular teeth (apart from *H. orstomi*) and occasional denticulation along the outermost radular teeth. The reproductive system of these species includes a large, bulbous vagina that may be glandular or have a proximal sphincter connecting to the bursa copulatrix and a very small, rounded receptaculum seminis. The dorsum coloration and patterning of the deep-sea species noticeably vary from the mesophotic species. In the deep-sea species, there is thick, dark ridging with dark spots, perpendicular dark lines along the dorsum edge, pronounced tubercles, and a similar gill pattern (Fahey and Gosliner 2000). To date, there is no molecular sequencing for any of the previously mentioned deep-sea species due to a lack of collecting and suitable preservation for sequencing; however, we have sequenced other species of *Halgerda* found at similar depths including *H. brunneomaculata*, *H. carlsoni*, and *H. dalanghita*. These three species are found in different clades within our molecular phylogeny and exhibit numerous morphological differences between each other, the previously mentioned deep-sea species, and the newly established mesophotic species. Further collection and sequencing of *H. abyssicola*, *H. azteca*, *H. fibra*, and *H. orstomi* may expand the mesophotic clade identified here, or it may reveal an entirely new and separate clade within *Halgerda*.

Species complexes In 2018, Tibiriçá et al. described two species complexes within *Halgerda*: the *H. carlsoni* complex predominately from the central and western Pacific and the *H. wasinensis* complex from the western Indian Ocean. Here, we provide clarification on the lack of genetic differences between two species in the *H. carlsoni* clade (*H. okinawa* and *H. malesso*) previously identified in Tibiriçá et al. 2018 and provide additional insight into the *H. wasinensis* clade. During their three gene phylogenetic analysis, Tibiriçá et al. used the original 599 bp mitochondrial COI sequences from Fahey (2003), which included a specimen of *H. okinawa* from Japan and a specimen of *H. malesso* from Guam. The results of their molecular phylogeny and species delimitation analyses revealed no genetic differences between these two specimens ($p = 0\%$). As such, Tibiriçá et al. (2018) then question whether *H. malesso* and *H. okinawa* are one extremely variable species or if there was a lack of genetic diversity between the two species. For our study, we successfully resequenced several of the original Fahey (2003) samples including the specimens of *H. okinawa* and *H. malesso*. Our COI sequences were longer (~658 bp); however, our *H. malesso* resequence was 100% identical to Fahey's original sequence and exhibited very little genetic difference with an additional specimen of *H. malesso* (UF 289547) also from Guam. The resequencing of the *H. okinawa* specimen reveals a strong genetic difference of 12.6% in the COI gene between *H. okinawa* and *H. malesso* suggesting that *H. okinawa* is no longer a part of the *H. carlsoni* species complex. Instead, *H. okinawa* is found nested within a new mesophotic clade described in this study. It is likely that Fahey's original *H. okinawa* sequence was an exact duplication of the *H. malesso* sequence and possibly a duplication error during the initial PCR, sequencing, or the submission to Genbank. Sequencing of three additional genes for both *H. okinawa* and *H. malesso* also supports the separation between these two species. Therefore, it is unlikely that *H. malesso* and *H. okinawa* are a single variable species given the strong genetic separation and lack of morphological similarities.

In our species delimitation analyses, the *H. wasinensis* complex identified in Tibiriçá et al. 2018 is partitioned into either four distinct groups (COI ABGD), partially split into two groups (16S ABGD, GYMC), or part of one large taxonomic unit (COI ASAP, 16S ASAP, bPTP) with other species including *H. anosy* sp. nov., *H.* cf. *formosa*, and *H. dichromis* (Fig. 2). The COI ABGD and 16S ABGD analyses successfully recover *H.* aff. *wasinensis* separately from *H. wasinensis*. Futhermore, in the COI ABGD, *H. wasinensis* is partitioned into three taxonomic units, while the COI and 16S ASAP and bPTP analyses group *H. wasinensis* with other members of the clade. The COI ABGD partitions do exhibit some geographical signal as the largest partition is composed of eight specimens from Mozambique, followed by two specimens from Zanzibar and a lone specimen (MB28-004972) from Zavora, Mozambique. The COI intraspecific variation within the *H. wasinensis* studied here ranges between 0.0 and 1.7%, which overlaps slightly with the 1.5–2.8% divergence between *H. wasinensis* and *H.* aff. *wasinensis* (Supplementary Table S4). The over-partitioning of *H. wasinensis* may be attributed to the low genetic diversity within the entire subclade. For instance, the maximum divergence within this subclade is only 3.3% between *H. anosy* sp. nov. and *H.* cf. *formosa* (Table 3). Overlap between intraspecific and interspecific variation may impact DNA barcoding in recently diverged species (Meier et al. 2008; Hubert and Hanner 2015; Tibiriçá et al. 2018); however, hidden diversity may cause an under or overestimation in species richness and may lead the "barcode gap" to be an artifact of limited sampling (Jörger et al. 2012). Further geographical sampling for both *H. wasinensis* and *H.* aff. *wasinensis* in coordination with next-generation sequencing and extensive morphological study may provide clarification for both the *H. wasinensis* and the *H. carlsoni* species complexes.

Continued exploration and discovery of other members of *Halgerda* not already sequenced may help to provide additional deep node support and potentially provide better resolution for the entire genus of *Halgerda* within Discodorididae.

Supplementary Information The online version contains supplementary material available at https://doi.org/10.1007/s12526-022-01334-9.

Acknowledgements This work was facilitated by several individuals who helped collect specimens available for this study. We are especially grateful to A. Alejandrino, A. Anker, L. Becking, R.F. Bolland, P. Bouchet, V. Bonito, G. Calado, Y. Camacho, L. Cervera, R. Delonghery, A. Devilliers, J. Earle, N. Evans, S. Fahey, J. Goodheart, A. Hermosillo, J.F. Hervé, E. Jessup, R. Johnson, M.A. Malaquias, M.C. Malay, S. McKeon, S. van der Meij, F. Michonneau, M. Miller, B. Moore, J. Moore, P.L. Norby, N. Okamota, P. Paleracio, G. Paulayi, D. Pence, C. Pittman, M. Poddubetskaia, M. Pola, A. Principe, R. Pyle, J. Reis, L. Rocha, T. Schils, B. Sellick, B. Shepherd, V. Smith, J. Templado, A. Valdés, R. Whitton, L. Witzel, D. Uyeno, C. Zakroff, the Papua New Guinea Expedition, the South Madagascar Expedition, and the Verde Island Passage Team.

This collaborative research involved the following partners in the Philippines: former Secretary of Agriculture Proceso J. Alcala; former Philippine Consul General Marciano Paynor and the Consular staff in San Francisco; former Bureau of Fisheries and Aquatic Resources (BFAR) Director Attorney Asis G. Perez; BFAR colleagues, especially Attorney Analiza Vitug, Ludivina Labe; National Fisheries and Research Development Institute (NFRDI) colleagues, especially Director Drusila Bayate and November Romena; U.S. Embassy staff, especially Heath Bailey, Richard Bakewell and Maria Theresa N. Villa; staff of the Department of Foreign Affairs; University of the Philippines (UP) administrators and colleagues including UP President Alfredo Pascual, Vice President Giselle Concepción, Dr Annette Meñez; the staff of the National Museum of the Philippines, especially Dr Jeremy Barns, Anna Labrador and Marivene Manuel Santos. We also thank Jessie de los Reyes, Marites Pastorfide, Sol Solleza, Boy Venus, Joy Napeñas, Peri Paleracio, Alexis Principe, the staff of Atlantis Dive Resort Puerto Galera (especially Gordon Strahan, Andy Pope, Marco Inocencio, Stephen Lamont and P. J Aristorenas), the staff of Lago de Oro Beach Club and Protacio Guest House, May Pagsinohin, Susan Po-Rufino, Ipat Luna, Enrique Nuñez, Jen Edrial, Anne Hazel Javier, Jay-o Castillo, Arvel Malubag and Mary Lou Salcedo. Lastly, our sincere thanks are extended to our fellow Academy and Filipino teammates on the expeditions. All the specimens from the Philippines were collected under our Gratuitous Permits (FBP-0041-10, GP-0059-11, GP-0077-14, GP-0085-15, GP-0112-16, GP-0112-17, GP-0159-18) from the shallow waters of the municipalities of Mabini, Tingloy, Calatagan, Romblon and Puerto Galera. This is part of the joint Department of Agriculture-NFRDI-California Academy of Sciences Memorandum of Agreement for the ongoing implementation of the National Science Foundation-funded biodiversity expedition in the Verde Island Passage. The specimens were collected in accordance with the terms and conditions of the gratuitous permit and under the supervision of our partners from BFAR Fisheries Regulatory and Quarantine Division and NFRDI.

Material for some species studied here were kindly supported by Dr Philippe Bouchet and supported by the Muséum National d'Histoire Naturelle, Paris. Specifically, The Madang expedition specimens were obtained during the 'Our Planet Reviewed' Papua Niugini expedition organized by Muséum National d'Histoire Naturelle (MNHN), Pro Natura International (PNI), Institut de Recherche pour le Développement (IRD) and University of Papua New Guinea (UPNG), Principal Investigators Philippe Bouchet, Claude Payri and Sarah Samadi. The organizers acknowledge funding from the Total Foundation, Prince Albert II of Monaco Foundation, Fondation EDF, Stavros Niarchos Foundation and Entrepose Contracting and in-kind support from the Divine Word University (DWU). The expedition operated under a permit delivered by the Papua New Guinea Department of Environment and Conservation. Material from Zanzibar was collected in collaboration with the Zanzibar Department of Fisheries Development under a permit authorized by the department. The kind assistance of Dr Mohammed S. Mohammed and his staff support is gratefully acknowledged. Material from Saudi Arabia was supported by funding from the King Abdullah University for Science and Technology and we are extremely grateful to Dr. Mike Berumen and the staff at KAUST.

Field work in South Africa was supported privately by Brian Sellick.

We acknowledge and thank the support of San Francisco State University for supporting this project, which is a part of Samantha Donohoo's master's thesis research. We would also like to thank our lab mates in the Gosliner Slug Lab and the staff in the Department of Invertebrate Zoology and the Center for Comparative Genomics at the California Academy of Sciences for all their help. We also appreciate the feedback we received from two anonymous reviewers and the editors at Marine Biodiversity that improved this manuscript.

Funding This work was also generously supported by a National Science Foundation grant, DEB 12576304 to T.M.G, Richard Mooi, Luis Rocha and Gary Williams to inventory the biodiversity of the Verde Island Passage and NSF 1856407 to Terrence Gosliner, which supported much of Samantha Donohoo's research. Fieldwork was also supported by the California Academy of Sciences Hope for Reefs initiative.

All the specimens from the Philippines were collected under our Gratuitous Permits (FBP-0041–10, GP-0059–11, GP-0077–14, GP-0085–15, GP-0112–16, GP-0112–17, GP-0159–18) from the shallow waters of the municipalities of Mabini, Tingloy, Calatagan, Romblon, and Puerto Galera. The Papua New Guinea research operated under a permit delivered by the Papua New Guinea Department of Environment and Conservation. Material from Zanzibar was collected in collaboration with the Zanzibar Department of Fisheries Development under a permit authorized by the department. Field work in South Africa was by permits RES2020/06 and RES2021-63 from the South African Department of the Environment and the Department of Forestry, Fisheries and the Environment. Permits for research in Saudi Arabia were granted by King Abdullah University for Science and Technology.

Declarations

Conflict of interest The authors declare no competing interests.

Ethical approval No animal testing was performed during this study.

Sampling and field studies All necessary permits for sampling and observational field studies have been obtained by the authors from the competent authorities and are mentioned in the acknowledgements, if applicable. The study is compliant with CBD and Nagoya protocols.

Data availability The genome sequence data that support the findings of this study are available at GenBank (https://www.ncbi.nlm.nih.gov/) under the following accession numbers: MW220875–MW220954; OM780016–OM780018; MW220114–MW220194; MW223019–MW223087; and MW414939–MW415018.

Author contribution TMG worked on the conceptualization, collected specimens, contributed to resources, and performed funding acquisition. SAD, SGV, and JMH performed lab work. SAD wrote the original draft, performed formal analysis, and worked on visualization of the final figures. SAD, JMH, and TMG reviewed and edited the final manuscript.

References

Abraham PS (1877) Revision of the anthobranchiate nudibranchiate Mollusca, with descriptions or notices of forty-one hitherto undescribed species. Proc Zool Soc Lond 196–269, pls. 27–30

Alfaro ME, Zoller S, Lutzoni F (2003) Bayes or bootstrap? a simulation study comparing the performance of bayesian markov chain

monte carlo sampling and bootstrapping in assessing phylogenetic confidence. Mol Biol Evol 20:255–266. https://doi.org/10.1093/molbev/msg028
Allan JK (1932) Australian Nudibranchs Aust Zool 7(2):87–105
Bas J (2022) Genus *Halgerda*. iNaturalist. https://www.inaturalist.org/observations/138572706. Accessed 23 October 2022
Bergh R (1874) Neue Nacktschnecken der Südsee, malacologische Untersuchungen II. J Mus Godeffroy 2(6):91–116 ([1–26], pls 1–4)
Bergh R (1876) Malacologische Untersuchungen. In: C. Semper C (Ed), Reisen im Archipel der Philippinen von Dr. Carl Gottfried Semper. Zweiter Theil. Wissenschaftliche Resultate, Band 2, Theil 2, Heft 10. C. W. Kreidel, Wiesbaden, pp 377–427, pls 49–53
Bergh R (1877) Malacologische Untersuchungen. In: C. Semper C (Ed), Reisen im Archipel der Philippinen, Zweiter Theil, Wissenschaftliche Resultate, Band 2, Theil 2, Heft 10. C. W. Kreidel, Wiesbaden, pp 495–546
Bergh R (1878) Malacologische Untersuchungen. In: C. Semper C (Ed), Reisen im Archipel der Philippinen. Zweiter Theil. Wissenschaftliche Resultate. Band 2, Theil 2, Heft 13 & 14. 2 Hälfte. C. W. Wiesbaden, pp. 547–601 & 603–645
Bergh R (1879) Neue Chromodoriden Malakozoologische Blätter Neue Folge 1:87–116
Bergh R (1880a) Beiträge zur Kenntniss der japanischen nudibranchien. I. Verhandlungen Der Koniglich-Kaiserlichen Zoologisch-Botanischen Gesellschaft in Wien 30:155–200
Bergh R (1880b) Malacologische Untersuchungen. In: C. Semper C (Ed), Reisen im Archipel der Philippinen, Zweiter Theil, Wissenschaftliche Resultate, Theil 4, Heft 2. C. W. Kreidel, Wiesbaden, pp 1–78, pls. A–F
Bergh R (1889) Malacologische Untersuchungen. In: C. Semper C (Ed), Reisen im Archipel der Philippinen. Zweiter Theil. Wissenschaftliche Resultate. Band 2, Theil 3, Heft 16. 2 Hälfte. C. W. Wiesbaden, pp 815–872
Bergh R (1891) Die cryptobranchiaten Dorididen. Zoologische Jahrbücher, Abteilung Für Systematik, Geographie Und Biologie Der Tiere 6:103–144
Bergh R (1905) Die Opisthobranchiata der Siboga-Expedition. Monographie 50. E.J. Brill, Leiden, pp 1–248, pls. 1–20. https://doi.org/10.5962/bhl.title.11223
Bertsch H, Johnson S (1982) Three new species of dorid nudibranchs (Gastropoda: Opisthobranchia) from the Hawaiian Islands. Veliger 24(3):208–218
Camacho-Garcia YE, Gosliner TM (2008) Nudibranch dorids from the Pacific coast of Costa Rica with the descriptions of a new species. Bull Mar Sci 83(2):367–389
Carlson CH, Hoff PJ (1993) Three new *Halgerda* species (Doridoidea: Nudibrancha: Opisthobranchia) from Guam. Veliger 36(1):16–26
Carlson CH, Hoff PJ (2000) Three new Pacific species of *Halgerda* (Opisthobranchia: Nudibranchia: Doridoidea). Veliger 43(2):154–163
Chan JM, Gosliner TM (2007) Preliminary phylogeny of *Thordisa* (Nudibranchia: Discodorididae) with descriptions of five new species. Veliger 48(4):284–308
Coleman N (2001) 1001 Nudibranchs: catalogue of indo-pacific sea Slugs. Neville Coleman's Underwater Geographic, Australia
Colgan DJ, McLauchlan A, Wilson GDF, Livingston SP, Edgecombe GD, Macaranas J, Cassis G, Gray MR (1998) Histone H3 and U2 snRNA DNA sequences and arthropod molecular evolution. Aust J Zool 46(5):419–437.https://doi.org/10.1071/ZO98048
Cooper JG (1863) Some new genera and species of California Mollusca. Proc Calif Acad Sci 1(2):202–207
Cuvier G (1817) Le règne animal distribué d'après son organisation. In: Contenant Les Reptiles, Les Poissons, Les Mollusques, Les Annélides. Tome 2. Deterville, Paris, pp 351–508, pl. XVIII
Dayrat B, Gosliner TM (2005) Species names and metaphyly: a case study in Discodorididae (Mollusca, Gastropoda, Euthyneura, Nudibranchia, Doridina). Zool Scr 34(2):199–224. https://doi.org/10.1111/j.1463-6409.2005.00178.x
Dayrat B, Tillier A, Lecointre G, Tillier S (2001) New clades of euthyneuran gastropods (Mollusca) from 28S rRNA sequences. Mol Phylogenet Evol 19:225–235.https://doi.org/10.1006/mpev.2001.0926
Debelius H (1996) Nudibranchs and sea snails: Indo-Pacific field guide. IKAN-Unterwasserarchiv, Frankfurt, pp 1–324
Debelius H, Kuiter RH (2007) Nudibranchs of the world. IKAN-Unterwasserarchiv, Frankfurt, pp 1–360
Donohoo SA, Gosliner TM (2020) A tale of two genera: the revival of *Hoplodoris* (Nudibranchia: Discodorididae) with the description of new species of *Hoplodoris* and *Asteronotus*. Zootaxa 4890(1):1–37. https://doi.org/10.11646/zootaxa.4890.1.1
Drummond AJ, Rambaut A (2007) BEAST: Bayesian evolutionary analysis by sampling trees. BMC Evol Biol 7(1):214. https://doi.org/10.1186/1471-2148-7-214
Drummond AJ, Suchard MA, Xie D, Rambaut A (2012) Bayesian phylogenetics with BEAUti and the BEAST 1.7. Mol Phylogenet Evol 29:1969–1973. https://doi.org/10.1093/molbev/mss075
Eales NB (1938) A systematic and anatomical account of the Opisthobranchia. Sci Rep John Murray Expedition 1933–34 5(4):77–122
Ehrenberg CG (1828–1831) Symbolae physicae animalia evertebrata exclusis insectis. Series prima cum tabularum decade prima continent animalia Africana et Asiatica. Decas Prima. In: F.G. Hemprich & C.G. Ehrenberg (Eds.), Symbolae physicae, seu Icones adhue ineditae corporum naturalium novorum aut minus cognitorum, quae ex itineribus per Libyam, Aegyptum, Nubiam, Dengalam, Syriam, Arabiam et Habessiniam Pars Zoologica, 4. Berlin, Officina Academica. pls. 1–2 (1828), text (1831)
Eliot CNE (1904) On some nudibranchs from east Africa and Zanzibar. Part III. Doridiidae Cryptobranchiatae. I Proc Zool Soc Lond 2:354–385
Fahey SJ (2003) Phylogeny of *Halgerda* (Mollusca: Gastropoda) based on combined analysis of mitochondrial CO1 and morphology. Invertebr Syst 17:617–624. https://doi.org/10.1071/IS02048
Fahey SJ, Carroll AR (2007) Natural products isolated from species of *Halgerda* Bergh, 1880 (Mollusca: Nudibranchia) and their ecological and evolutionary implications. J Chem Ecol 33:1226–1234. https://doi.org/10.1007/s10886-007-9288-z
Fahey SJ, Gosliner TM (1999a) Description of three new species of *Halgerda* from the western Indian Ocean with a redescription of *Halgerda formosa* Bergh, 1880. Proc Calif Acad Sci (4) 51(8):365–383
Fahey SJ, Gosliner TM (1999b) Preliminary phylogeny of *Halgerda* (Nudibranchia: Halgerdidae) from the tropical Indo-Pacific, with descriptions of three new species. Proc Calif Acad Sci (4) 51(11):425–448
Fahey SJ, Gosliner TM (2000) New records of *Halgerda* Bergh, 1880 (Opisthobranchia, Nudibranchia) from the deep western Pacific Ocean, with descriptions of four new species. Zoosystema 22(3):471–498
Fahey SJ, Gosliner TM (2001a) The phylogeny of Halgerda (Opisthobranchia, Nudibranchia) with the description of a new species from Okinawa. Zool Scr 30(3):199–213
Fahey SJ, Gosliner TM (2001b) On the genus *Halgerda* (Nudibranchia: Halgerdidae) from Western Australia with descriptions of four new species. Boll Malacol 37(5–8):55–76
Fahey SJ, Gosliner TM (2003) Mistaken identities: on the Discodorididae genera *Hoplodoris* Bergh, 1880 and *Carminodoris* Bergh, 1889 (Opisthobranchia, Nudibranchia). Proc Calif Acad Sci (4) 54(10):169–208
Fahey SJ, Healy JM (2003) Sperm ultrastructure in the nudibranch genus *Halgerda* with reference to other Discodorididae and to Chromodorididae (Mollusca : Opisthobranchia). J Morphol 257:9–21. https://doi.org/10.1002/jmor.10086

Folmer O, Hoeh WR, Black MB, Vrijenhoek RC (1994) Conserved primers for PCR amplification of mitochondrial DNA from different invertebrate phyla. Mol Mar Biol Biotechnol 3:294–299
Fujisawa T, Barraclough TG (2013) Delimiting species using single-locus data and the generalized mixed yule coalescent approach: a revised method and evaluation on simulated data sets. Syst Biol 62:707–724. https://doi.org/10.1093/sysbio/syt033
García-Méndez K, Padula V, Valdés Á (2022) Integrative systematics of the genus *Dondice* Marcus, 1958 (Gastropoda, Nudibranchia, Myrrhinidae) in the Western Atlantic. Mar Biodivers 52(5):1–46. https://doi.org/10.1007/s12526-022-01273-5
Gaggeri U (2006) *Halgerda toliara*? from Nosy Be, Madagacar. [Message in] Sea Slug Forum. Australian Museum, Sydney. http://www.seaslugforum.net/find/19007. Accessed 23 October 2022
Giribet G, Okusu A, Lindgren AR, Huff SW, Schrödl M, Nishiguchi MK (2006) Evidence for a clade composed of molluscs with serially repeated structures: monoplacophorans are related to chitons. Proc Natl Acad Sci USA 103(20):7723–7728. https://doi.org/10.1073/pnas.0602578103
Göbbeler K, Klussmann-Kolb A (2010) Out of Antarctica? –new insights into the phylogeny and biogeography of the Pleurobranchomorpha (Mollusca, Gastropoda). Mol Phylogenet Evol 55(3):996–1007. https://doi.org/10.1016/j.ympev.2009.11.027
Gosliner TM (1987) Nudibranchs of Southern Africa. Sea Challengers, Monterey, pp 1–136
Gosliner TM, Behrens DW, Williams GC (1996) Coral reef animals of the Indo-Pacific. Sea Challengers, Monterey, pp 1–314
Gosliner TM, Fahey SJ (1998) Description of a new species of *Halgerda* from the Indo-Pacific with a redescription of *Halgerda elegans* Bergh. Proc Calif Acad Sci 50(15):347–359
Gosliner TM, Behrens DW, Valdés Á (2008) Indo-Pacific nudibranchs and sea slugs: a field guide to the world's most diverse fauna. Sea Challengers, Gig Harbor pp 1–426
Gosliner TM, Behrens D, Valdés Á (2015) Indo-Pacific nudibranchs and sea slugs: a field guide to the world's most diverse fauna. New World Publications, Inc., Jacksonville, pp 1–408
Gosliner TM, Valdés Á, Behrens DW (2018) Indo-Pacific nudibranchs and sea slugs: a field guide to the world's most diverse fauna. New World Publications, Inc., Jacksonville, pp 1–451
QGIS.org (2022) QGIS Geographic Information System. QGIS Association. Available from http://www.qgis.org. Accessed 11 Mar 2022
Hallas JM, Gosliner TM (2015) Family matters: the first molecular phylogeny of the Onchidoridae Gray, 1827 (Mollusca, Gastropoda, Nudibranchia). Mol Phylogenet Evol 88:16–27. https://doi.org/10.1016/j.ympev.2015.03.015
Hallas JM, Chichvarkhin A, Gosliner TM (2017) Aligning evidence: concerns regarding multiple sequence alignments in estimating the phylogeny of the Nudibranchia suborder Doridina. R Soc Open Sci 4(10):171095. https://doi.org/10.1098/rsos.171095
van Hasselt JC (1824) Extrait d'une lettre du Dr. J.C. van Hasselt au Prof. Van Swinderen, sur mollusques de Java, le 25 mai 1823 (I). Bull Sci Nat Geol 3:237–245
Hervé JF (2010) Guide des Nudibranches de Nouvelle-Calédonie et autres Opisthobranches. Editions Catherine Ledru, Nouméa, pp 1–401
Hubert N, Hanner R (2015) DNA barcoding, species delineation and taxonomy: a historical perspective. DNA Barcodes 3(1). https://doi.org/10.1515/dna-2015-0006
Humann P, Deloach N (2010) Reef creature identification: tropical Pacific. New World Publications, Jacksonville, pp 1–233
Johnson S, Boucher LM (1983) Notes on some opisthobranchs (Mollusca: Gastropoda) from the Marshall Islands, including 57 new records. Pac Sci 37(3):251–291
Johnson RF, Gosliner TM (2012) Traditional taxonomic groupings mask evolutionary history: a molecular phylogeny and new classification of the chromodorid nudibranchs. PLoS ONE 7(4):e33479. https://doi.org/10.1371/journal.pone.0033479
Jörger KM, Norenburg JL, Wilson NG, Schrödl M (2012) Barcoding against a paradox? Combined molecular species delineations reveal multiple cryptic lineages in elusive meiofaunal sea slugs. BMC Evol Biol 12(1):1–18. https://doi.org/10.1186/1471-2148-12-245
Katoh K, Asimenos G, Toh H (2009) Multiple alignment of DNA sequences with MAFFT. Methods Mol Biol 537:39–64. https://doi.org/10.1007/978-1-59745-251-9_3
Kay EA, Young DK (1969) The Doridacea (Opisthobranchia; Mollusca) of the Hawaiian Islands. Pac Sci 23:172–231
Kearse M, Moir R, Wilson A, Stones-Havas S, Cheung M, Sturrock S, Buxton S, Cooper A, Markowitz S, Duran C, Thierer T, Ashton B, Meintjes P, Drummond A (2012) Geneious basic: an integrated and extendable desktop software platform for the organization and analysis of sequence data. Bioinformatics 28:1647–1649. https://doi.org/10.1093/bioinformatics/bts199
Keiu S (2000) Opisthobranchs of Izu Peninsula. TBS-Britannica, Toyko, pp 1–178
Kekkonen M, Mutanen M, Kaila L, Nieminen M, Hebert PD (2015) Delineating species with DNA barcodes: a case of taxon dependent method performance in moths. PLoS ONE 10(4):e0122481. https://doi.org/10.1371/journal.pone.0122481
Lanfear R, Frandsen PB, Wright AM, Calcott ST, B, (2016) PartitionFinder 2: new methods for selecting partitioned models of evolution for molecular and morphological phylogenetic analyses. Mol Biol Evol 34(3):772–773. https://doi.org/10.1093/molbev/msw260
Lindsay T, Kelly J, Chichvarkhin A, Craig S, Kajihara H, Mackie J, Valdés Á (2016) Changing spots: pseudocryptic speciation in the North Pacific dorid nudibranch *Diaulula sandiegensis* (Cooper, 1863)(Gastropoda: Heterobranchia). J Molluscan Stud 82(4):564–574. https://doi.org/10.1093/mollus/eyw026
Maddison WP, Maddison DR (2018) Mesquite: a modular system for evolutionary analysis. Available from http://mesquiteproject.org/mesquiteArchives/mesquite1.02/mesquite/download/MesquiteManual.pdf. Accessed 11 Mar 2022
Marcus Er (1955) Opisthobranchia from Brazil. Bol Fac Filos Ciênc Let Univ São Paulo, Zool 20:89–261, pls. 1–30. https://doi.org/10.11606/issn.2526-3382.bffclzoologia.1955.120213
Marcus Er (1958) On western Atlantic opisthobranchiate gastropods. Am Mus Novit 1906:1–82
MacFarland FM (1905) A preliminary account of the Dorididae of Monterey Bay, California. Proc Biol Soc Wash 18:35–54
Meier R, Zhang G, Ali F (2008) The use of mean instead of smallest interspecific distances exaggerates the size of the "barcoding gap" and leads to misidentification. Syst Biol 57(5):809–813. https://doi.org/10.1080/10635150802406343
MolluscaBase (2021) MolluscaBase. *Halgerda* Bergh, 1880. Available from https://molluscabase.org/aphia.php?p=taxdetails&id=205320. Accessed 11 Mar 2022
Nakano R (2004) Opisthobranchs of Japan Islands. Rutles, Tokyo, pp 1–303
Neuhaus J, Rauch C, Bakken T, Picton B, Pola M, Malaquias MAE (2021) The genus *Jorunna* (Nudibranchia: Discodorididae) in Europe: a new species and a possible case of incipient speciation. J Molluscan Stud 87(4):eyab028. https://doi.org/10.1093/mollus/eyab028
Ong E, Hallas JM, Gosliner TM (2017) Like a bat out of heaven: the phylogeny and diversity of the bat-winged slugs (Heterobranchia: Gastropteridae). Zool J Linnean Soc 180(4):755–789. https://doi.org/10.1093/zoolinnean/zlw018
Ono A (1999) Opisthobranchs of Kerama Islands. TBS-Britannica & Co., Japan, pp 1–184
Ono A (2004) Opisthobranchs of Ryukyu Islands. Rutles, Tokyo, pp 1–304

Palumbi SR, Martin AP, Romano S, McMillan WO, Stice L, Grabowski G (1991) The simple fool's guide to PCR. University of Hawaii, Honolulu, Department of Zoology

Platt AR, Woodhall RW, George AL (2007) Improved DNA sequencing quality and efficiency using an optimized fast cycle sequencing protocol. Biotechniques 43:58–62. https://doi.org/10.2144/000112499

Poddubetskaia M (2003) *Halgerda toliara*? from Mayotte. [Message in] Sea Slug Forum. Australian Museum, Sydney. http://www.seaslugforum.net/find/9550. Accessed 23 October 2022

Poddubetskaia M (2004) *Halgerda cf. toliara* from Mayotte. [Message in] Sea Slug Forum. Australian Museum, Sydney. http://www.seaslugforum.net/find/11745. Accessed 23 October 2022

Pola M, Gosliner TM (2010) The first molecular phylogeny of cladobranchian opisthobranchs (Mollusca, Gastropoda, Nudibranchia). Mol Phylogenet Evol 56(3):931–941. https://doi.org/10.1016/j.ympev.2010.05.003

Pons J, Barraclough TG, Gomez-Zurita J, Cardoso A, Duran P, Hazell S, Kamoun S, Sumlin WD, Vogler AP (2006) Sequence-based species delimitation for the DNA taxonomy of undescribed insects. Syst Biol 55:595–609. https://doi.org/10.1080/10635150600852011

Puillandre N, Lambert A, Brouillet S, Achaz G (2012) ABGD, Automatic Barcode Gap Discovery for primary species delimitation. Mol Ecol 21:1864–1877. https://doi.org/10.1111/j.1365-294X.2011.05239.x

Puillandre N, Brouillet S, Achaz G (2021) ASAP: assemble species by automatic partitioning. Mol Ecol Resour 21(2):609–620. https://doi.org/10.1111/1755-0998.13281

Rambaut A (2018). FigTree v1.4.4. http://tree.bio.ed.ac.uk/software/figtree/ . Accessed 11 Mar 2022

Ronquist F, Huelsenbeck JP (2003) MrBayes 3: Bayesian phylogenetic inference under mixed models. Bioinformatics 19:1572–1574. https://doi.org/10.1093/bioinformatics/btg180

Rudman WB (1984) The Chromodorididae (Opisthobranchia: Mollusca) of the Indo-West Pacific: a review of the genera. Zool J Linn Soc 81:115–273. https://doi.org/10.1111/j.1096-3642.1984.tb01174.x

Rudman WB (1987) The Chromodorididae (Opisthobranchia: Mollusca) of the Indo-West Pacific: *Chromodoris epicuria*, *C. aureopurpurea*, *C. annulata*, *C. coi* and *Risbecia tryoni* colour groups. Zool J Linn Soc 90:305–407. https://doi.org/10.1111/j.1096-3642.1987.tb01357.x

Rudman WB (1978) The dorid opisthobranch genera *Halgerda* Bergh and *Sclerodoris* Eliot from the Indo-West. Zool J Linnean Soc 62:59–88. https://doi.org/10.1111/j.1096-3642.1978.tb00523.x

Rudman WB (2001) Feb 6. Comment on *Halgerda willeyi*? from the Adriatic by Tom Turk. [Message in] Sea Slug Forum. Australian Museum, Sydney. http://www.seaslugforum.net/find/3301. Accessed 23 Oct 2022

Schrödl M (1999) *Glossodoris charlottae*, a new chromodorid nudibranch from the Red Sea (Gastropoda, Opisthobranchia). Vita Marina 46(3–4):89–94

Sellick B, Gosliner T, Van Heerden I (2020) Nudibranchs and sea slugs of the Aliwal Shoal. LT Printers, Pietermaritzburg, pp 1–60

Stamatakis A (2014) RAxML version 8: a tool for phylogenetic analysis and post-analysis of large phylogenies. Bioinformatics 30:1312–1313. https://doi.org/10.1093/bioinformatics/btu033

Steinberg JE (1963) Notes on the opisthobranchs of the West Coast of North America—III. Further nomenclatorial changes in the order Nudibranchia. Veliger 6:63–67

Stiefel K (2011) Halgerda. Flickr. https://www.flickr.com/photos/pacificklaus/5644883774. Accessed 23 Oct 2022

Stöver BC, Müller KF (2010) TreeGraph 2: Combining and visualizing evidence from different phylogenetic analyses. BMC Bioinform 11:7

Strömvoll J, Jones G (2019) A guide to the sea slugs of the Maputaland Coast. Southern Underwater Research Group, Cape Town, pp 1–103

Talavera G, Castresana J (2007) Improvement of phylogenies after removing divergent and ambiguously aligned blocks from protein sequence alignments. Syst Biol 56:564–577. https://doi.org/10.1080/10635150701472164

Tibiriçá Y, Pola M, Cervera JL (2018) Systematics of the genus *Halgerda* Bergh, 1880 (Heterobranchia : Nudibranchia) of Mozambique with descriptions of six new species. Invertebr Syst 32:1388–1421. https://doi.org/10.1071/IS17095

Turk T (2001) Feb 6. *Halgerda willeyi*? from the Adriatic. [Message in] Sea Slug Forum. Australian Museum, Sydney. http://www.seaslugforum.net/find/3301. Accessed 23 Oct 2022

Valdés Á, Gosliner TM (2001) Systematics and phylogeny of the caryophyllidia-bearing dorids (Mollusca, Nudibranchia). Zool J Linn Soc 133(2):103–198. https://doi.org/10.1111/j.1096-3642.2001.tb00689.x

Valdés A (2002) A phylogenetic analysis and systematic revision of the cryptobranch dorids (Mollusca, Nudibranchia, Anthobranchia). Zool J Linn Soc 136:535–636. https://doi.org/10.1046/j.1096-3642.2002.00039.x

Vayssière AJBM (1912) Recherches zoologiques et anatomiques sur les Opisthobranches de la Mer Rouge et du Golfe d'Aden. Pt. 2. Ann Fac Sci Marseille 20:5–157

Willan RC, Brodie GD (1989) The nudibranch *Halgerda aurantiomaculata* (Allan, 1932)(Doridoidea: Dorididae) in Fijian waters. Veliger 32(1):69–80

Yiu SKF, Chung SSW, Qiu JW (2021) New observations on the corallivorous nudibranch *Phestilla melanobrachia*: morphology, dietary spectrum and early development. J Molluscan Stud 87(4):eyab034. https://doi.org/10.1093/mollus/eyab034

Yonow N (2008) Sea slugs of the Red Sea. Pensoft Publishers, Sofia, pp 1–304

Yonow N, Anderson RC, Buttress SG (2002) Opisthobranch molluscs from the Chagos Archipelago, Central Indian Ocean. J Nat Hist 36:831–882. https://doi.org/10.1080/00222930110039161

Zhang J, Kapli P, Pavlidis P, Stamatakis A (2013) A general species delimitation method with applications to phylogenetic placements. Bioinformatics 29(22):2869–2876. https://doi.org/10.1093/bioinformatics/btt499